

HIGH THROUGHPUT MASS SPECTROMETRY FOR MICROBIAL IDENTIFICATION

A Dissertation
Presented to
The Academic Faculty

by

Carrie Y. Pierce

In Partial Fulfillment
of the Requirements for the Degree
Doctor of Philosophy in the
School of Chemistry & Biochemistry

Georgia Institute of Technology

May 2011

HIGH THROUGHPUT MASS SPECTROMETRY FOR MICROBIAL IDENTIFICATION

Approved by:

Dr. Facundo M. Fernández, Advisor
School of Chemistry & Biochemistry
Georgia Institute of Technology

Dr. Lawrence A. Bottomley
School of Chemistry & Biochemistry
Georgia Institute of Technology

Dr. Christine K. Payne
School of Chemistry & Biochemistry
Georgia Institute of Technology

Dr. John R. Barr
NCEH/Division of Laboratory Sciences
*Centers for Disease Control and
Prevention*

Dr. Jiri Janata
School of Chemistry & Biochemistry
Georgia Institute of Technology

Dr. Alfred H. Merrill
School of Biology
Georgia Institute of Technology

Date Approved: March 29th, 2011

Excessive reservations and paralyzing despondency have not helped the sciences to advance nor are they helping them to advance, but a healthy optimism that cheerfully searches for new ways to understand, as it is convinced that it will be possible to find them.

— Dr. Alois Alzheimer¹

To get something you never had you have to do something you never did.

This is dedicated to...

The memory of my mother, Deborah Joyce, who lived her life for her children and husband and loved unconditionally, my father, Kenn, for teaching me, by example, perseverance and what really matters in life, my husband and twin flame, Jason Daniel, without whom I would not be whole; who has always been my rock and foundation and without him none of this would be possible, and my children, Jostlyn Ansley and Ryan Ariston, for showing me how to live, laugh, love, and play and who unknowingly encourage me to strive to be the woman I want to be

Thank you for your unconditional love, support and faith.

ACKNOWLEDGEMENTS

First and foremost, I would like to express my sincere appreciation and thanks to my advisor, Dr. Facundo M. Fernández, His guidance, support, patience, and enthusiasm has made this long journey possible. His mentorship has enabled me to grow as a scientist and it has been a privilege for me to have had the opportunity of working under his supervision and learn from his experience. I would also like to express my earnest gratitude and utmost respect to Dr. John R. Barr, who has allowed me to pursue my educational dreams while working under his supervision and whose expertise challenges me to advance the sciences. I am indebted to both Dr. Fernández and Dr. Barr and appreciate their dedication and commitment towards my success and for accommodating my personal extraordinary circumstances during the tenure of my graduate student life. I would also like to express sincere thanks to Dr. Jiri Janata, Dr. Larry Bottomley, Dr. Christine Payne, and Dr. Al Merrill for their advisement and for serving on my committee.

I would like to thank my undergraduate professors at the Georgia Institute of Technology for their help building my foundation in chemistry. I would like to especially thank my colleague, Dr. Jon Rees for his guidance, tolerance, and understanding. I would also like to thank Dr. Joanne Mei, Dr. David Collard, Dr. Tracie Williams, Dr. Adrian Woolfitt, and Dr. Hercules Moura for their continued support through the years and Dr. Cameron Tyson for facilitating my graduate experience. I am also appreciative of the collaborations provided by Dr. Edward Shaw, Dr. Herbert Thompson, Dr. Robert Massung, and Mrs. Rachael Priestly. I want to especially thank Ms. Rachael Trimpert

Schmidt for her friendship over the past years, my Georgia Tech group members, past and present, and the CDC colleagues who gave insightful discussions and friendships.

Finally, I will like to remember my mother, Deborah Young, and my father, Kenneth Young, for their unconditional love and support whose contribution to my life is beyond my writing limit, and my brother Chase Young. Most importantly, I would like to remember my best friend and husband, Jason Pierce, for his unwavering love, devotion, support, understanding, and especially patience that has enabled me to reach this major milestone in my life. I would also like to give heartfelt thanks to my beautiful children, Jostlyn Ansley and Ryan Ariston, for sacrificing “mommy time” during this doctoral experience.

TABLE OF CONTENTS

ACKNOWLEDGEMENTS	v
LIST OF TABLES	xi
LIST OF FIGURES	xii
LIST OF SYMBOLS	xvi
LIST OF ABBREVIATIONS	xvii
SUMMARY	xxi
CHAPTER 1. OVERVIEW	1
1.1. ABSTRACT.....	1
1.2. PATHOGENIC BACTERIA	1
1.2.1. History of bacteria and natural infection.....	1
1.2.2. Overview of bacteria as bioweapons.....	4
1.2.3. Coxiella burnetii.....	6
1.2.4. Staphylococcus aureus	7
1.2.5. Bacteriophage.....	8
1.3. EXISTING METHODOLOGIES FOR BACTERIAL DETECTION	9
1.3.1. Traditional methods	9
1.3.2. Serological methods.....	10
1.3.3. Molecular methods.....	11
1.3.4. Proteomic methods.....	13
1.3.5. Other methods	13
1.4. MASS SPECTROMETRY AND MICROBIAL IDENTIFICATION	14
1.4.1. Mass spectrometry	14
1.4.2. MS-based proteomics and microbial identification	15

1.4.3. MALDI-TOF MS	18
1.4.4. DART-TOF MS	21
1.4.5. LC-ESI-MS/MS	22
1.4.6. Data analysis	28
CHAPTER 2. AMBIENT GENERATION OF FATTY ACID METHYL ESTER PROFILES FROM BACTERIAL WHOLE CELLS BY DIRECT ANALYSIS IN REAL TIME (DART) MASS SPECTROMETRY	31
2.1. ABSTRACT.....	31
2.2. INTRODUCTION	31
2.2.1. Ambient mass spectrometry	31
2.2.2. FAMEs methodology	32
2.3. EXPERIMENTAL.....	33
2.4. RESULTS AND DISCUSSION	35
2.5. CONCLUSIONS.....	42
CHAPTER 3. STRAIN AND PHASE IDENTIFICATION OF THE U.S. CATEGORY B AGENT COXIELLA BURNETII BY MATRIX-ASSISTED LASER DESORPTION/IONIZATION TIME-OF-FLIGHT MASS SPECTROMETRY AND MULTIVARIATE PATTERN RECOGNITION.....	43
3.1. ABSTRACT.....	43
3.2. INTRODUCTION	44
3.2.1. C. burnetii: Facts and existing methodologies	44
3.2.2. Mass spectrometry and microorganism identification	45
3.3. EXPERIMENTAL.....	49
3.3.1. Background of different strains.....	49
3.3.2. Microorganism propagation and cell culture	50
3.3.3. Sample preparation.....	50
3.3.4. MALDI-TOF MS analysis	51

3.3.5. Data preprocessing and multivariate analysis	52
3.4. RESULTS AND DISCUSSION	54
3.4.1. Characteristics of MALDI-TOF MS mass spectra of different <i>C. burnetii</i> strains.....	54
3.4.2. Partial least squares modeling of <i>C. burnetii</i> MALDI-TOF MS data at the strain level (Model I)	58
3.4.3. Partial least squares modeling of <i>C. burnetii</i> MALDI-TOF MS data at the phase level (Model II).....	65
3.5. CONCLUSIONS.....	70
CHAPTER 4. RAPID DETECTION OF STAPHYLOCOCCUS AUREUS USING ¹⁵N-LABELED BACTERIOPHAGE AMPLIFICATION COUPLED WITH MATRIX-ASSISTED LASER DESORPTION/IONIZATION TIME-OF-FLIGHT MASS SPECTROMETRY	72
4.1. ABSTRACT.....	72
4.2. INTRODUCTION	73
4.3. EXPERIMENTAL.....	76
4.3.1. <i>S. aureus</i> and bacteriophage 53.....	76
4.3.2. ¹⁵ N Bacteriophage 53 infection/amplification.....	77
4.3.3. Bioluminescence-based detection assay	78
4.3.4. Tryptic digest of bacteriophage 53.....	79
4.3.5. Nano-LC-MS/MS.....	79
4.3.6. Database Searching and Protein ID Validation.....	80
4.3.7. MALDI-TOF MS analysis	81
4.4. RESULTS AND DISCUSSION	82
4.5. CONCLUSIONS.....	91
CHAPTER 5. VIABLE STAPHYLOCOCCUS AUREUS QUANTITATION USING ¹⁵N METABOLICALLY-LABELED BACTERIOPHAGE AMPLIFICATION COUPLED WITH A MULTIPLE REACTION MONITORING PROTEOMICS WORKFLOW	93

5.1. ABSTRACT.....	93
5.2. INTRODUCTION	94
5.3. EXPERIMENTAL.....	97
5.3.1. <i>S. aureus</i> and bacteriophage 53.....	97
5.3.2. Biosynthetic production of ¹⁵ N <i>S. aureus</i> and ¹⁵ N bacteriophage 53.....	98
5.3.3. Nano-LC-MS/MS.....	99
5.3.4. Protein identification and target peptide determination	100
5.3.5. Preparation of <i>S. aureus</i> working stock and standard solutions.....	101
5.3.6. ¹⁵ N bacteriophage 53 infection/amplification procedures	102
5.3.7. Rapid enzymatic digestion procedure	102
5.3.8. LC-MS/MS Instrumentation and methodology	103
5.4. RESULTS AND DISCUSSION	105
5.5. CONCLUSIONS.....	119
CHAPTER 6. CONCLUSIONS AND OUTLOOK	122
6.1. ABSTRACT.....	122
6.2. MASS SPECTROMETRY FOR CLINICAL DIAGNOSTICS	122
6.3. PROPOSED FUTURE DIRECTIONS.....	128
6.3.1. <i>C. burnetii</i> analysis and strain-level discrimination by MS	128
6.3.2. <i>S. aureus</i> detection and quantitation by MS.....	129
REFERENCES.....	132
LIST OF PUBLICATIONS	162
VITA.....	163

LIST OF TABLES

Table 2-1 Comparison of bacterial fatty acid profiles and corresponding relative abundances for <i>E. coli</i> , <i>S. pyogenes</i> , and <i>C. burnetii</i> (Nine Mile I strain).....	38
Table 3-1 Mass spectral peaks in the range of 1-6 kDa for <i>C. burnetii</i> (species-selective spectral signals common to all <i>C. burnetii</i> strains).....	55
Table 3-2 Mass spectral peaks in the range of 1-6 kDa for <i>C. burnetii</i> ^a (strain-specific spectral signals unique to all <i>C. burnetii</i> strains)	56
Table 3-3 Intra-well variability and mean peak intensities observed in <i>C. burnetii</i> MALDI-MS spectral data. Four composite spectra (n = 4) were acquired per well. Each composite spectrum was the sum of 2500 laser shots.....	57
Table 3-4 Inter-well (n = 3 wells) and inter-day variability in MALDI-MS data. The spectrum from each well was obtained by averaging four composite mass spectra.	58
Table 5-1 Target Staphylococcal bacteriophage 53 capsid protein peptide sequences and their corresponding ¹⁵ N metabolically labeled counterparts. The unique peptide sequences were chosen to identify the 35.0 kDa (¹⁴ N) and 35.5 kDa (¹⁵ N) capsid protein from Staphylococcal bacteriophage 53. MS/MS = mass spectrometry/mass spectrometry.....	107
Table 5-2 Precision and accuracy of <i>S. aureus</i> quantitative measurements. Three technical replicates were performed for n = 5 identical samples at two concentration levels. Std. dev. = standard deviation; %RSD = % relative standard deviation.....	117
Table 5-3 Verification of completeness of digestion for the SIAQSIEK, LGVILPVTK, and LIYGIPQLIEYK quantitative peptide transitions. For ¹⁵ N PAD MS measurements, 5.0x10 ⁵ CFU mL ⁻¹ of spiked <i>S. aureus</i> was subjected to phage amplification, tryptic digest, and LC-MS/MS analysis. Triplicate results for each preparation are shown and intra-peptide and inter-peptide means (CFU mL ⁻¹ tested), standard deviations, and percent relative standard deviations (%RSDs) for n = 3 sample preparations is reported. Std. dev. = standard deviation; %RSD = % relative standard deviation.	119

LIST OF FIGURES

Figure 2-1 (a) Reconstructed ion chronograms for <i>E. coli</i> . (b) Reconstructed ion chronograms for <i>S. pyogenes</i> . Ions shown have a relative intensity of > 5%.....	36
Figure 2-2 Eighteen minute-long isothermal (200 °C) DART-TOF MS run showing repeat signals produced by 4μL of an <i>E.coli</i> suspension manually deposited at the bottom of a glass capillary, and placed in front of the ion source via a mechanical sample holder. The peak marked with an asterisk was produced by a faulty injection. A glass capillary wetted with PEG was manually inserted in front of the mass spectrometer inlet for a few seconds after each bacterial suspension was probed.....	37
Figure 2-3 Positive ion mass spectrum of (a) <i>E. coli</i> (Gram negative) and (b) <i>S. pyogenes</i> (Gram positive) acquired by direct DART-TOF MS analysis after <i>in-situ</i> thermal hydrolysis/methylation of the bacterial membrane fatty acids to generate the corresponding FAMES.....	39
Figure 2-4 Positive ion mass spectrum of <i>C. burnetii</i> Nine Mile I (Gram negative) acquired by DART-TOF MS analysis of <i>in-situ</i> thermal hydrolysis/methylation ionization of the bacterial membrane fatty acids to generate the corresponding FAMES.....	41
Figure 2-5 Positive ion mass spectrum of (a) <i>C. burnetii</i> Nine Mile II (Gram negative) and (b) <i>C. burnetii</i> RSA 514 (Gram negative) acquired by DART-TOF MS analysis of <i>in-situ</i> thermal hydrolysis/methylation ionization of the bacterial membrane fatty acids to generate the corresponding fatty acid methyl esters (FAMES).	41
Figure 3-1 Average MALDI-TOF MS spectra of purified <i>C. burnetii</i> cultures by strain for day one. Intensity was normalized to the base peak at $m/z = 2951$	55
Figure 3-2 PCA scores plot for MALDI-TOF MS <i>C. burnetii</i> data. The symbol labels are as follows: I=Nine Mile I, M=M 44, A=Australian QD, K-P=KAV/PAV, H=Henzerling, O=Ohio.	59
Figure 3-3 Root mean squared error of crossvalidation (RMSECV) as a function of the number of LVs added to the PLS-DA Model I (strain level model). Leave-one-out crossvalidation was used. The optimum number of LVs chosen was 8.	60

Figure 3-4 Y-predicted value as a function of sample number for six <i>C.burnetii</i> strain classes. The filled circular symbols correspond to objects used as unknowns in the test set. Test set objects have been marked with its own class label to demonstrate the PLS-DA model's accuracy to discriminate at the strain level (I=Nine Mile I, M=M44, A=Australian QD, K-P=KAV/PAV, H=Henzerling, O=Ohio). All other objects were used as part of the training set. The dashed red line represents the classification decision threshold. Unknown samples falling above this threshold have a statistically-significant probability of belonging to the same class as the corresponding training objects.....	62
Figure 3-5 Preprocessed (normalized, smoothed, denoised, binarized and averaged) mass spectral data used for building PLS-DA Model I (strain level). The data shown corresponds to the Nine Mile I strain samples.	64
Figure 3-6 Root mean squared error of crossvalidation (RMSECV) as a function of the number of LVs added to the PLS-DA Model II (phase level model). Leave-one-out crossvalidation was used. The optimum number of LVs chosen was 4.	65
Figure 3-7 Y-predicted value as a function of sample number for different <i>C. burnetii</i> antigenic phases. The filled circular symbols correspond to objects used as unknowns in the test set. Unknown samples falling above the decision threshold have a statistically-significant probability of belonging to class I (phase I), whereas objects below the line, most probably belong to class II (phase II). The symbol labels are as follows: I=Nine Mile I, M=M44, A=Australian QD, K-P=KAV/PAV, H=Henzerling, O=Ohio.	66
Figure 3-8 Scores plot (LV 2 vs. LV 4) for PLS-DA Model II (phase level model). The symbol labels are as follows: I=Nine Mile I, M=M44, A=Australian QD, K-P=KAV/PAV, H=Henzerling, O=Ohio. The explained Y-variance for each latent variable is expressed between parentheses.	67
Figure 3-9 Loadings for latent variable 2 (top) and 4 (bottom) in PLS-DA Model II. The highlighted mass-to-charge regions correspond to: A=1286-1300, B=1450-1532, C=3564-3644, D=5439-5488, E=5488-5566.....	68
Figure 3-10 Detail of the mass spectral region between m/z 5420 and 5560. The spectra shown correspond to the first day of experiments.....	69
Figure 4-1 MALDI-TOF MS spectra of capsid protein peaks for (a) ¹⁴ N cultured bacteriophage 53 and (b) ¹⁵ N cultured bacteriophage 53 as the 35.04 and 35.46 kDa biomarkers, respectively, approach the instrument's detection limit. Samples were spotted in triplicate, and each mass spectrum corresponds to 6000 accumulated laser shots. Data were acquired in the 25,000 to 40,000 m/z range.....	83

Figure 4-2 MALDI-TOF mass spectra acquired at various time points during conventional ^{14}N *in vitro* phage infection of *S. aureus* performed at 37 °C; (a) 90-, (b) 120-, (c) 150-, (d) 180-, (e) 210-, (f) 240-min infection time. Initial *S. aureus* bacterial concentrations and initial ^{14}N phage concentrations were 6.7×10^7 CFU mL^{-1} and 1.0×10^6 PFU mL^{-1} , respectively. 85

Figure 4-3 Phage-mediated bioluminescent detection of *S. aureus*. Bioluminescence (RLU) was measured over time following addition of bacteriophage. A fixed *S. aureus* concentration of 6.7×10^7 CFU mL^{-1} was used for all samples. The black solid line corresponds to the *S. aureus* phage-free control. Data were acquired in triplicate and the mean values are plotted. (a) Signal response times for ^{14}N and ^{15}N bacteriophage at a fixed concentration of 8.0×10^7 PFU mL^{-1} . (b) Average relative bioluminescence as a function of time showing dose-dependent detection. Samples were labeled A through D, with the corresponding light emission profiles similarly labeled in the graph. Bacteriophage 53 concentrations were A) 8.0×10^4 PFU mL^{-1} ; B) 8.0×10^5 PFU mL^{-1} ; C) 8.0×10^6 PFU mL^{-1} ; D) 8.0×10^7 PFU mL^{-1} . To establish the onset of phage amplification in luminescence experiments via an objective metric, a sample was deemed as having bacteriophage amplification if the point-by-point second derivative ratios of the phage-containing vs. control curves were greater than or equal to 3. *S. aureus* samples infected with higher phage concentrations, bacteriophage amplification is detected well before the onset of bacteriophage amplification in *S. aureus* samples with lower bacteriophage concentrations. As phage concentration was increased from 10^4 to 10^7 PFU mL^{-1} , response times needed to observe an increase in RLUs decreased. Ranging from the highest concentration of bacteriophage to the lowest, the times from infection to initiation of bacteriophage amplification were 81.5 min, 141.5 min, 161.5 min, and 251.5 min, respectively. 87

Figure 4-4 MALDI-TOF mass spectra acquired at various time points during ^{15}N *in vitro* phage infection of *S. aureus* performed at 37 °C; (a) 0-, (initial infection); (b) 30-, (c) 60-, (d) 90-, (e) 120-, (f) 150-min infection time. Initial *S. aureus* bacterial concentrations and initial ^{15}N phage concentrations were 6.7×10^7 CFU mL^{-1} and 2.0×10^8 PFU mL^{-1} , respectively. 89

Figure 4-5 Resulting MALDI mass spectra acquired from analysis of ^{15}N bacteriophage amplified media. Samples were prepared as serial dilutions of *S. aureus* culture in TSB with a bacteriophage concentration of 2.0×10^8 PFU mL^{-1} . Spectral peaks have been normalized to the base peak in each spectrum, and spectra have been overlaid for comparative purposes. (a) 6.7×10^7 CFU mL^{-1} ; (b) 6.7×10^6 CFU mL^{-1} ; (c) 6.7×10^5 CFU mL^{-1} ; (d) 6.7×10^4 CFU mL^{-1} 90

Figure 5-1 Schematic of the alternate column regeneration configuration for chromatographic separation prior to mass spectrometric detection. 105

Figure 5-2 Amino acid sequence of the major capsid head protein of interest present in Staphylococcal bacteriophage 53. The sequence coverage (47%) is highlighted and the three target peptides used for quantitation of *S. aureus* are indicated in bold red font. The sequence (gi | 66395381) was obtained from the National Center for Biotechnology Information database. 106

Figure 5-3 Liquid chromatography tandem mass spectrometry (LC-MS/MS) extracted ion chromatograms of target ^{14}N transitions (quantitative and confirmation) monitored for peptides from a major capsid head protein unique to bacteriophage 53. A stock solution with 5.0×10^5 PFU mL^{-1} concentration of ^{14}N phage was analyzed to determine the instrument's sensitivity for the target peptides (no phage amplification). The chromatograms demonstrate a typical response as the ^{14}N phage concentration approaches the instrument's limit of detection. Data were acquired on a Thermo Scientific TSQ Vantage. 108

Figure 5-4 Calibration curve generated for two-fold serial dilutions of the ^{14}N wild type bacteriophage stock solution without amplification or ^{15}N label. The observed area counts for the SIAQSIEK quantitative MRM transition were plotted against expected ^{14}N phage concentration (PFU mL^{-1}). The resulting calibration curve for the SIAQSIEK quantitative peptide was linear (0.99) in the 5.0×10^5 PFU mL^{-1} to 3.2×10^7 PFU mL^{-1} range. 109

Figure 5-5 Liquid chromatography tandem mass spectrometry (LC-MS/MS) extracted ion chromatograms of the quantitative transitions monitored. The chromatograms show a standard solution (2.0×10^5 CFU mL^{-1}) a) $t = 0$ h; prior to the phage amplification event and b) $t = 2$ h; the end point of the infection. The $t = 0$ h and $t = 2$ h chromatograms are displayed on identical scales based on ion counts. 111

Figure 5-6 Plot showing the probability $P(n)$ of bacteria cells being infected by n phage using equation 1, a bacteriophage concentration of 1.0×10^9 PFU mL^{-1} , and a multiplicity of infection (MOI) of $2.77 \geq 95\%$ of all bacteria will have at least one infectious phage attached for a sample of *S. aureus* at a concentration of 3.6×10^8 CFU mL^{-1} 112

Figure 5-7 Calibration curves generated for *S. aureus* quantitation. Triplicate instrument runs were performed for each standard and the mean area ratios (unlabeled phage/ ^{15}N phage) for each quantitative peptide transition were plotted against expected *S. aureus* concentration. Calibration curves for $n = 5$ days were compared to evaluate reproducibility. The resulting calibration curves for SIAQSIEK, LGVILPVTk, and LIYGIPQLIEYK were linear (0.98-0.99) in the 5.0×10^4 CFU mL^{-1} to 2.0×10^6 mL^{-1} range. 116

LIST OF SYMBOLS

Da	Dalton
h	hour
i.d.	Internal Diameter
kDa	kiloDalton
mmu	Millimass Unit
m/z	mass-to-charge ratio
OD	Optical Density
ppm	Parts-Per-Million
RLU	Relative Light Unit
T	Absolute temperature
t	Time
v/v	volume/volume ratio

LIST OF ABBREVIATIONS

ACN	Acetonitrile
AP	Atmospheric pressure
APCI	Atmospheric pressure chemical ionization
ATCC	American Type Culture Collection
BSL	Biosafety Level
BWC	Biological Weapons Convention
CA	Collisional activation
<i>C. burnetii</i>	<i>Coxiella burnetii</i>
CDC	Centers for Disease Control and Prevention
CFU mL ⁻¹	Cell Forming Units per Milliliter
CHCA	α -cyano-4-hydroxycinnamic acid
CI	Chemical Ionization
CID	Collision Induced Dissociation
CV	Coefficient of Variation
Da	Dalton
DART	Direct Analysis in Real Time
DESI	Desorption Electrospray Ionization
DHB	5-dihydroxybenzoic acid
DL	Detection Limit
DNA	Deoxyribonucleic acid
DOD	Department of Defense

<i>E. coli</i>	<i>Escherichia coli</i>
EI	Electron Ionization
ELISA	Enzyme-linked immunosorbent assay
ESI	Electrospray Ionization
FA	Formic Acid
FAB	Fast Atom Bombardment
FAME	Fatty Acid Methyl Ester
FBI	Federal Bureau of Investigation
FDA	Food and Drug Administration
FTIR	Fourier Transform Infrared Spectroscopy
FT-MS	Fourier Transform Mass Spectrometry
GC	Gas Chromatography
HPLC	High Performance Liquid Chromatography
IFA	Indirect Fluorescence Antibody Assay
ISTD	Internal Standard
LC	Liquid Chromatography
LD ₅₀	Lethal Dose 50%
LPS	Lipopolysaccharide
LV	Latent Variable
MALDI	Matrix-Assisted Laser Desorption/Ionization
MRI	Magnetic Resonance Imaging
MRM	Multiple Reaction Monitoring
MS	Mass Spectrometry

MS/MS	Tandem Mass Spectrometry
NCBI	National Center for Biotechnology Information
NM I	<i>C. burnetii</i> Nine Mile phase I
NM II	<i>C. burnetii</i> Nine Mile phase II
PAD	Phage Amplification Detection
PAGE	Polyacrylamide Gel Electrophoresis
PARAFAC	Parallel Factor Analysis
PCA	Principal Components Analysis
PCR	Polymerase Chain Reaction
PEG	Polyethylene Glycol
PFGE	Pulsed Field Gel Electrophoresis
PFU mL ⁻¹	Plaque Forming Units per Milliliter
PLS	Partial Least Squares
PLS-DA	Partial Least Squares-Discriminant Analysis
PTFE	Polytetrafluoroethylene
Py-MS	Pyrolysis Mass Spectrometry
Q	Quadrupole
Q-q-Q	Triple Quadrupole
Q fever	Query fever
Q-q-TOF	Quadrupole Time-of-Flight
RFLP	Restriction Fragment Length Polymorphism
R-LPS	Rough-type Lipopolysaccharide
RLU	Relative Light Unit

RMSECV	Root Mean Square Error of Crossvalidation
RNA	Ribonucleic acid
RSD	Relative Standard Deviation
<i>S. aureus</i>	<i>Staphylococcus aureus</i>
<i>S. pyogenes</i>	<i>Streptococcus pyogenes</i>
SA	Sinnapinic acid
S-LPS	Smooth Lipopolysaccharide
S/N	Signal-to-Noise Ratio
TFA	Trifluoroacetic acid
THB	Todd Hewitt broth
TIC	Total Ion Chromatogram
TOF	Time-of-Flight
TSB	Tryptic Soy Broth
UK	United Kingdom
US	United States of America
USAMRIID	United States Army Medical Research Institute for Infectious Diseases
USSR	Union of Soviet Socialist Republics
UV	Ultraviolet
WWI	World War I
WWII	World War II

SUMMARY

Bacteria cause significant morbidity and mortality throughout the world, including deadly diseases such as tuberculosis, meningitis, cholera, and pneumonia. Timely and accurate bacterial identification is critical in areas such as clinical diagnostics, environmental monitoring, food safety, water and air quality assessment, and identification of biological threat agents². At present, there is an established need for high throughput, sensitive, selective, and rapid methods for the detection of pathogenic bacteria, as existing methods, while nominally effective, have failed to sufficiently reduce the massive impact of bacterial contamination and infection. The work presented in this thesis focuses on addressing this need and augmenting conventional microorganism research through development of mass spectrometry (MS)-based proteomic applications. MS, a well established tool for addressing biological problems, offers a broad range of laboratory procedures that can be used for taxonomic classification and identification of microorganisms^{3, 4}. These methods provide a powerful complement to many of the widely used molecular biology approaches and play critical functions in various fields of science. While implementation of modern biomolecule-identifying instrumentation, such as MS, has long been postulated to have a role in the microbiology laboratory, it has yet to be accepted on a large scale. Described in this document are MS methods that erect strong foundations on which new bacterial diagnostics may be based. A general introduction on key aspects of this work is presented in Chapter 1, where different approaches for detection of pathogenic bacteria are reviewed, and an overview regarding MS and microbial identification is provided. Chapter 2 presents the first implementation

of microbial identification via rapid, open air Direct Analysis in Real Time MS (DART MS) to generate ions directly from microbial samples, including the disease-causing bacteria, *Coxiella burnetii*, *Streptococcus pyogenes*, and *Escherichia coli*. Chapter 3 expands on whole cell *C. burnetii* MS analysis and presents a rapid differentiation method to the strain-level for *C. burnetii* using mass profiling/fingerprinting matrix-assisted laser desorption/ionization time-of-flight (MALDI-TOF) MS and multivariate pattern recognition. Chapter 4 presents a unique “top-down” proteomics approach using ¹⁵N-labeled bacteriophage amplification coupled with MALDI-TOF MS as a detector for the rapid and selective identification of *Staphylococcus aureus*. Chapter 5 extends the idea of using isotopically labeled bacteriophage amplification by implementing a “bottom-up” proteomics approach that not only identifies *S. aureus* in a sample, but also quantifies the bacterial concentration in the sample using liquid chromatography-electrospray ionization tandem mass spectrometry (LC-ESI/MS/MS) as a detector. In conclusion, Chapter 6, summarizes and contextualizes the work presented in this dissertation, and outlines how future research can build upon the experimentation detailed in this document.

CHAPTER 1. OVERVIEW

1.1. Abstract

Microorganism detection methods should offer high sensitivity, specificity, and reproducibility, and be rapid and robust with minimal to no sample preparation. They should be widely applicable with low cost-per-sample. Fulfilling these criteria is challenging, and the work described herein attempts to address potential avenues towards these goals. This chapter briefly highlights the history of bacteria and infection, describes bacteria as bioweapons, and presents overviews of what is known about the disease-causing organisms *C. burnetii* and *S. aureus*. Also, current microbial detection methodologies are reviewed, and microorganism differentiation by MS is presented. In addition, an introduction to matrix-assisted laser desorption/ionization time-of flight mass spectrometry (MALDI-TOF MS), direct analysis in real time mass spectrometry (DART-TOF MS), and liquid chromatography tandem mass spectrometry (LC-MS/MS) as they relate to microorganism identification, is provided.

1.2. Pathogenic Bacteria

1.2.1. History of bacteria and natural infection

Bacteria existed long before humans evolved, and bacterial disease most likely co-evolved with each species that involuntarily hosts them. Historically, some of the best-known infectious bacterial diseases having inflicted our ancestors are bubonic plague (*Yersinia pestis*), tuberculosis (mycobacteria), syphilis (*Treponema pallidum*), cholera (*Vibrio cholera*), typhoid (*Salmonella typhi*), typhus (Rickettsiae), and rheumatic fever

(Group A Streptococci). However, for the longest time the cause of infectious diseases was unknown, leading to devastating outcomes and limited prevention and treatment.

Pioneers of microbial discovery can be traced to Girolamo Fracastoro, a colleague of Copernicus, who wrote in 1546 that infection or contagion passes from one to another via direct contact, through the air, or by contact with contaminate articles, in very small imperceptible particles, which he called seeds of disease^{5, 6}. In the 17th century, Antonie van Leeuwenhoek observed Fracastoro's speculative particles with a hand-held microscope and his research was among the first observations on living bacteria ever recorded⁷. In 1796 Edward Jenner was recognized for performing the world's first vaccination⁸, laying the foundation for modern vaccinology⁹. Rudolph Virchow, an experimental biologist, is credited for multiple important discoveries including his scientific contribution to cell theory and his book *Cellular Pathology*, published in 1858, that allowed pathologic histology to become widely studied. Through the mid to late 19th century, Louis Pasteur's research led to remarkable breakthroughs in the causes and preventions of diseases. His greatest achievements included establishing the germ theory of disease, creating the first anthrax and rabies vaccinations, inventing pasteurization, and recognizing that emergent growth of bacteria is due to biogenesis rather than spontaneous generation⁷. However, it was not until Robert Koch's work in the 1880's that the actual pathogen was discovered. Koch is best known for isolating *Bacillus anthracis*, *Tuberculosis bacillus*, and *Vibrio cholera*, cultivating pure cultures of bacteria on solid media and formulating Koch's postulates, which must be satisfied before it is accepted that particular bacteria cause particular disease¹⁰. As Pasteur and Koch's scientific contributions revolutionized work in infectious diseases, they are often considered the

founders of microbiology. Following their work, the last two decades of the 19th century saw phenomenal developments in which a plethora of pathogenic bacteria were discovered⁶. Thus, with the beginning of microbiology, bacterial pathogens became apparent, acceptance of the microbe theory of disease began to be accepted, and the importance of bacterial detection became paramount for diagnosis.

With the benefits of today's scientific knowledge, powerful tools are available to advance microbial discovery, progress research, and develop and implement prevention and treatment strategies. One obvious example is the successful implementation of immunizations. Vaccine development and distribution is a high-ranking achievement of the past century. Many devastating infectious diseases such as measles, pertussis, smallpox, polio, diphtheria, and rubella that have haunted years past, have now been contained due to safe, effective, and affordable vaccines¹¹ and prior to new vaccine development, the disease-causing organisms must be identified and characterized. Still, infectious diseases are not something of the past and vaccines for many emerging and reemerging diseases remain elusive. In the past three decades alone, major etiological agents and infectious diseases, such as the Ebola virus, *Legionella pneumophila*, Prion disease, Hepatitis C, Human Immunodeficiency Virus (HIV), *Helicobacter pylori*, Hantavirus, and numerous antibiotic-resistant bacteria, have emerged. The increasing ease and affordability of cross-continent air travel contributes to the emergence and reemergence of diseases once thought eradicated in parts of the world¹², and global-scale mobility of people is believed to facilitate transmission of infectious diseases on an international level¹³. Additionally, bacterial contamination of food and water supplies is a long-standing problem around the globe¹⁴, and is a major cause of morbidity and

mortality worldwide¹⁵. In the United States (US), bacterial infections are a leading cause of death in children and the elderly¹⁶ and hospital-acquired and health care-acquired infections affect more than 2 million patients, cost \$4.5 billion, and contribute to 88,000 deaths in hospitals annually^{17, 18}. Thus, combating microbial infections requires a solid understanding of the nature of the disease, its origin, and its treatment. Perhaps more importantly is that the causative infectious agent must be identified. These concerns emphasize the importance of preserving public health through disease control and the continued need of rapid microorganism identification and differentiation tools to support this initiative.

1.2.2. Overview of bacteria as bioweapons

While the overwhelming majority of infectious diseases are a result of natural causes, pathogens can also be used as lethal bioweapons and this threat must be considered. In the US, bioagents are separated into three categories depending on how easily they can be spread and the severity of illness or death they cause. Category A agents (e.g. anthrax (*Bacillus anthracis*), botulism (*Clostridium botulinum* toxin), and tularemia (*Francisella tularensis*)) are given the high priority. Category B agents (e.g. ricin toxin, (*Ricinus communis*), Q fever (Q fever) (*C. burnetii*), and typhus fever (*Rickettsia prowazekii*)) are given the second-highest priority, and category C agents, which include emerging infectious pathogens that could be engineered for mass dissemination, are given the third highest priority¹⁹.

Generally speaking, bioterrorism refers to the use of pathogens or toxins derived from living organisms as a means of perpetrating an attack²⁰ with a clear motive to

produce a political or social statement. Historically, known or alleged use of biological weapons include, smallpox (England), anthrax (Germany, USSR, Zimbabwe), glanders (Germany, USSR), tularemia (USSR), T2 mycotoxins (US, USSR), enteric pathogens (Japan), and plague (Japan)²¹. During the 20th century alone, historical records clearly show a series of offensive biological weapons programs maintained by major nations such as Germany, France, the UK, the US, the USSR, and Iraq²². However, in 1972 the Biological Weapons Convention (BWC), ratified by more than 100 nations, prohibited the development, production, stockpiling, and transfer of biological agents for use as weapons²³. Despite this peaceful schedule, many experts believe that several signatory countries may be violating the convention's terms by developing secret offensive biological weapons programs. Notable post-Convention biological attacks include the 1978 assassination of Bulgarian dissident Georgii Markov after exposure to a ricin-containing dart distributed by a USSR or Bulgarian secret service agent, the 1984 *Salmonella* bacteria attack in Oregon by the Rajneeshee cult, the early 1990s anthrax and botulinum toxin dissemination attempts in Japan by the Aum Shinrikyo cult, and the 2003 ricin dissemination plots in Europe by al-Qaeda members. Additionally, the recent US anthrax attacks of 2001, involving the deliberate release of anthrax spores to government officials and media personnel, prompted a national investigation that confirmed 22 cases of anthrax; five of which were fatal. These were the first bioterrorism-related cases of anthrax in the US, and are currently considered the worst biological attack in US history²⁴.

Response efforts to a bioterrorism attack are in many ways the same as response efforts to naturally-occurring outbreaks of communicable diseases. Both situations

require early identification of ill or exposed individuals, rapid implementation of preventive therapy, special infection control considerations, and collaboration and communication with the public health system²⁵. Proper preparedness is therefore critical and at all levels, it is of immense importance to have methods in place for characterization and identification of microorganisms.

1.2.3. Coxiella burnetii

C. burnetii is an obligate intracellular gram negative bacterium that produces the debilitating zoonotic disease Q fever. The bacterium is highly resistant to desiccation and other environmental stresses and may remain viable for extended periods of time²⁶. *C. burnetii* is given a second highest priority ranking among US bioagents, classifying it as a category B bioterrorism agent due to its high infectivity. Human Q fever is an airborne infection with an inhalational LD₅₀ of a single organism, potentially making it the most infectious organism known to man. Historically *C. burnetii* has been weaponized by both the US and USSR and Q fever epidemics have been documented during WWI and WWII. Further, since 2003, over 200 cases of Q fever have surfaced in US military personnel stationed overseas. At present, The Netherlands is suffering from the largest Q fever epidemic ever reported globally. Since its first emergence in 2007, over 4000 confirmed cases of Q fever have been reported, and efforts are still underway to try to contain the outbreak. The infectivity of *C. burnetii* is dependent on the virulence of the organism, with phase I strains capable of infection (virulent) and phase II strains being non-infectious (avirulent). Previous studies have demonstrated that phase variation is related to truncation of the lipopolysaccharide (LPS) moieties on the cell surface. Although

several early studies suggested that the truncation of LPS was due to genomic deletions that eliminated several of the genes involved in LPS biosynthesis, the examination of additional phase II variants has shown that these large deletions are not always present²⁷.

In addition to phase variation, certain *C. burnetii* strains have been associated with either acute or chronic infections. Acute infections manifest themselves as a flu-like, febrile illness that is often characterized as a fever of unknown origin with atypical pneumonia or hepatitis. Chronic Q fever infection is manifested most often by endocarditis and involves damage to the aortic and mitral valves²⁶. Different plasmids are found in the chronic and acute strains and previous studies have suggested that these plasmids and the proteins they encode are responsible for the variable disease manifestations of the acute and chronic strains²⁸. Because the consequences of false negative or false positive *C. burnetii* detection could be disastrous in terms of human morbidity and mortality as well as financial cost, effective *C. burnetii* identification methods are highly desirable.

1.2.4. *Staphylococcus aureus*

S. aureus is a gram positive facultative anaerobic bacteria. It is a versatile pathogenic bacterium²⁹ and an important human pathogen³⁰. *S. aureus* is responsible for a significant number of healthcare-associated infections³¹ and is the leading cause of community-acquired infections³²⁻³⁴. The bacterium causes a broad spectrum of infections ranging from acute to chronic disease^{35,36}, is a common etiological agent of opportunistic infections, and can be life-threatening in immunocompromised patients. Many strains of *S. aureus* have remarkable environmental stability and can be resistant to many

disinfectants and antiseptics. Transmission usually occurs via pus from infected wounds, skin to skin contact, or through contact with infected materials such as towels or bed linens. Methicillin-resistant forms of *S. aureus* (MRSA) were first reported in the 1960s³⁷. Today, an increasing prevalence of *S. aureus* strains that are resistant to antibiotics is emerging. These strains pose an even greater threat to the general public and are a public health priority worldwide³⁸. Early diagnosis is central for infection control and may lead to decreased morbidity and mortality, reduced transmission, shortened hospital stays, and lower hospitalization costs^{39, 40}. These issues indicate the importance of the development and improvement of diagnostic methods that allow rapid identification and quantification of this bacterium³¹.

1.2.5. Bacteriophage

Bacteriophages (phages) are viruses that infect bacteria. They are common in all natural environments and are directly related to the variety of species of bacteria present. Bacteriophages are estimated to be the most widely distributed and diverse entities in the biosphere and can be found in all reservoirs populated by bacterial hosts. Phages were discovered independently by the British microbiologist Felix Twort and the French-Canadian Felix d'Herelle in 1915 and 1917⁴¹. Bacteriophages, literally meaning to eat bacteria, were first named by d'Herelle upon observing these small particles devouring bacteria and destroying cultures. Prior to the introduction of antibiotics in the 1940's, phage therapeutics were implemented worldwide as anti-bacterial agents⁴², and continue to be used as an alternative to antibiotics for treatment of bacterial infections in the former U.S.S.R. and Eastern Europe⁴³. The phage replication cycle, consisting of

adsorption, penetration, maturation, release, reinfection, is only initiated when bacteriophage interact with specific bacterial hosts. This phage-host specificity has had considerable success for identification of numerous bacteria including *Bacillus* species⁴⁴⁻⁴⁶, *Listeria* species^{47, 48}, *Salmonella* species⁴⁹⁻⁵¹, *Streptococcus pyogenes*, *S. aureus*^{52, 53}, and continues to be explored as an alternative strategy for bacterial identification.

1.3. Existing Methodologies for Bacterial Detection

Although bacteria can be classified into a large number of groups or subgroups based on cell structure, cellular metabolism or differences in cellular components, the fundamental terms used for bacterial identification are the *genus* and *species*. When clinically relevant, serotypes, genotypes, or some other subgroup may be used for classification. A species is essentially a collection of strains while a strain is defined as a population of organisms that descends from a single organism or pure culture isolate that can be characterized by at least one diagnostic phenotypic trait⁵⁴. Numerous methods have been developed for the identification of genera, species, and subgroups of bacteria however, none have yet achieved all the advantages of specificity, speed, accuracy and low cost, with no serious drawbacks³.

1.3.1. Traditional methods

In practice, conventional methods that rely on phenotypic identification of microorganisms using culture, staining, and biochemical methods still play a dominant role in diagnostic laboratories⁵⁵, however these methods can show considerable variability due to environmental changes such as culture, subculture, or storage

conditions⁵⁵. The most widely used methods are plate culture-based, however, these methods can be time-consuming (1-5 days) and quite laborious⁵⁶. Differential staining techniques (Gram stain, acid-fast, endospore) have value for subjective observation of bacterial morphology; however, pure cultures are often needed for observation. Additionally, while staining techniques can complement analyses, the cells of many bacteria usually resemble others and additional biochemical tests are needed for confident identification³. A broad range of biochemical tests are available as well as selective media and chemotaxonomic methods, however because the time required to grow pure cultures delays identification, serological and molecular methods, that can potentially bypass this step, are often employed³.

1.3.2. Serological methods

Serological methods are immunoanalytical techniques that involve antigen-antibody reactions. Antibodies targeted to a specific pathogen are most often selectively tagged with labels and are primarily detected via optical and fluorescence detection techniques. Both monoclonal and polyclonal antibodies can be utilized and depending on the antigen, specificity of the antibody, and the serological test utilized, detection of genera, species, and serotypes of bacteria is achievable³. Antibody-based methods are used in a variety of clinical applications however enzyme-linked-immunoassays (ELISA) and immunofluorescence assays (IFA) are the most common serological methods routinely used for identifying clinically relevant bacteria. ELISAs are sensitive, rapid, and simple techniques that involve at least one specific antibody interaction with its antigen. Traditionally, an ELISA's end-point of analysis produced an observable color change to indicate the presence of antigen however, newer fluorogenic,

electrochemiluminescent techniques have been introduced to produce quantifiable signals. IFAs achieve sensitive detection by use of antibody-bound fluorophores for antigen binding, and detection is primarily via epifluorescence microscopy or flow cytometry. Immunomagnetic separation (IMS) techniques allow isolation and concentration of the bacterial sample via magnetic beads coupled to the antibodies. The antibody-bound affinity device is recovered with a magnet and the target sample is recovered for subsequent identification. Recently described immunoanalytical bacterial detection methods include the use of quantum dots (QDs)^{57, 58}, immunoliposomes^{59,60}, fluorescent bioconjugated silica nanoparticles⁶¹, and fluorescent protein-labeled bacteriophage^{62, 63}. These newer labeling techniques have been shown to provide highly amplified and reproducible signals and can be found in an increasing number of biological applications. Immuno-biosensors have been explored^{64, 65,66, 67,68} that can offer rapid and simplistic measurements but these methods often have insufficient sensitivity and limited detection capabilities. Overall, immunoaffinity techniques offer sensitive and rapid measurements but the accuracy is dependent on the specificity of the antibody selected. While these methods are efficient, high false positive rates and cross-reactivity are a concern, especially when mixed bacterial populations are present.

1.3.3. Molecular methods

The recent genomic revolution has produced a vast array of molecular biology tools for microorganism discrimination. These nucleic acid based methods offer selectivity derived from the genetic characteristics of a pathogen's genome, which remains largely stable over time and is resistant to environmental changes. Molecular

methods are based on amplification (polymerase chain reaction) or probe-based (nucleic acid hybridization, microarrays) techniques that detect particular genes that are specific to bacteria. Nucleic acid hybridization uses oligonucleotide DNA or RNA probes to form hybrid complexes (DNA-DNA, DNA-RNA, RNA-RNA) with similar, complementary sequences. Oligonucleotide probes are labeled by color, radioactivity, fluorescence or chemiluminescence, and enable detection at the strain level in a matter of hours. Polymerase chain reaction (PCR), one of the most sensitive techniques for rapid bacterial identification³, relies on primer sequences designed to facilitate bacterial identification at any level of specificity: strain, species or genus. DNA amplification using PCR provides a means of producing large quantities of DNA from a relatively small number of organisms, directly from clinical samples or from small amounts of cultured bacterial cells, thus improving the sensitivity and decreasing the time required for identification⁶⁹. While PCR remains one of the most important and widely adopted techniques for rapid microorganism identification, existing limitations include inability to distinguish dead bacteria from live cells, ambiguity of test results that need culture confirmation, cost, and the fairly advanced technical skills required. Microarrays are promising alternative technology that offers versatility, rapidity, and simultaneous identification of diverse bacteria on a single slide. Specific bacterial detection in complex matrices is achieved if a fluorescent-labeled DNA probe derived from the sample of interest hybridizes with the DNA on the array chip^{70, 71}. Hundreds or thousands of genes can be fixed onto a substrate, allowing for multiple bacteria detection. However, inherent complexity and relative expense currently limit its practical use as a standard clinical application.

1.3.4. Proteomic methods

In parallel with advances in genomics, the on-going proteomics revolution has made available additional tools for microbial discovery⁷² and has shifted traditional techniques for bacterial identification and classification². Proteomics, the large-scale analysis and investigation of proteins, is primarily mass spectrometric and bioinformatics-based and allows interrogation of biomolecules produced by an organism. These biomolecules correspond to peptides, proteins, or any relevant organic molecule that can be used to facilitate identification, differentiation, and characterization of a particular microorganism. This multifaceted approach has been shown to be rapid, sometimes high-throughput, and produce unprecedented levels of discrimination among strains of bacteria². Further, integration of genomic and proteomic data can offer more comprehensive information and provide insight into complex biological processes. These advantages enhance bacterial identification capabilities across multiple fields and allow for rapid and reliable methods for the characterization of disease-causing organisms and for forensic microbial identification.

1.3.5. Other methods

Bacteriophage amplification for bacterial detection is an alternative approach to conventional methods⁷³⁻⁷⁵ that is based on the interaction of phages with their host bacteria. This interaction and subsequent detection relies on the ability of bacteriophage to specifically infect viable host bacteria cells. Following infection, the phage multiply within the bacterial cell, enzymatically disrupt the cell wall of the host bacteria, and release new progeny phage particles that are used for indirect detection of the bacteria of interest⁷⁶. The potential benefits of microorganism identification mediated by phage

amplification is enhanced sensitivity, and faster, more accurate, and more reproducible results.

Alternative technologies that fall outside of mainstream bacterial detection methodologies and the scope of this chapter, include phage typing⁷⁷, tissue culture⁷⁸, capillary electrophoresis⁷⁹, infrared spectroscopy⁸⁰, Fourier transform infrared (FTIR) spectroscopy⁸¹, polyacrylamide gel electrophoresis (PAGE)⁸², amplified ribosomal DNA restriction analysis (ARDRA)⁸³, and pulsed-field gel electrophoresis (PFGE)^{3, 84}.

1.4. Mass Spectrometry and microbial identification

1.4.1. Mass spectrometry

Mass spectrometry (MS) is an analytical technique first used in 1897 by J.J. Thomson to provide information on the chemical composition of a sample based on the mass-to-charge ratio (m/z) of its ionized components. A mass spectrometer has three essential modules: an ion source, which transforms the neutral molecules in the sample into ionized species; an analyzer, which sorts the ions by their masses using electric and/or magnetic fields; and a detector, which measures the value of some indicator quantity (arrival time, mirror current, direct ionic current) and thus provides data for indirectly calculating the abundances of respective ions. The mass analyzer is the central component of the technology and key parameters include resolution, mass accuracy, sensitivity and speed to produce information-rich mass spectra⁸⁵. There are four classical types of analyzers used for biological mass spectrometric applications: ion trap (IT), time-of-flight (TOF), quadrupole (Q), and Fourier transform ion-cyclotron resonance (FT-ICR). They are different in design and performance, each having their own strengths

and weaknesses, and can function as stand-alone devices or can be coupled in tandem to create hybrid instrumentation that maximizes the advantages of each⁸⁵.

Electrospray ionization (ESI) and matrix-assisted laser desorption ionization (MALDI) are currently the two most commonly used ionization techniques used to volatilize and ionize samples for mass spectrometric analysis^{86, 87}, while various ambient ionization techniques have recently been introduced⁸⁸⁻⁹¹. A more detailed description of MALDI-TOF MS, direct analysis in real time (DART)-TOF MS, and LC-ESI/MS/MS, and their pertinence to microbial identification and characterization are provided below.

1.4.2. MS-based proteomics and microbial identification

Proteomics plays a central role in the discovery of disease biomarkers and microbial targets, and MS is the principal methodology for proteomics. The use of MS for characterization of bacteria was investigated by Anhalt & Fenselau as early as 1975⁹². Today, it is well defined that biomolecules from different microorganisms can be vaporized, directly ionized, and introduced into a mass spectrometer⁸⁶. These biomolecules can then be identified by their structures such that taxonomic distinctions are made based on unique signatures, intact biomarkers, and fragmentation patterns. In general, microorganism differentiation by MS identifies cells or cellular components present in a particular sample through peaks of interest that are observed in a mass spectrum. Proteins are the most abundant and reliable components for detection and characterization of microorganisms but in addition to proteins other biological markers, including DNA, RNA, oligosaccharides, phospholipids, and fatty acid methyl esters can be used for detection. It has been shown by numerous researchers that mass spectral

information with sufficient specificity can be obtained to allow identification of microorganisms from different genera, different species, and from different strains within the same species⁹³⁻⁹⁷. MS-based proteomics is wide-ranging with recent approaches in microbial identification falling into two broad classes; (1) mass profiling techniques and (2) sequencing-based techniques.

Mass profiling uses entire mass spectral regions and provides signatures, patterns, or fingerprints for unique identification^{98, 99}. MALDI-TOF MS is at the core of recent developments in mass profiling⁷² where taxonomic distinctions are made based on characteristic mass spectral ‘fingerprints’, not individual MS peaks. Identification is based upon the complex patterns observed, and the characteristic nature of bacterial mass spectra where emphasis is placed on spectral reproducibility and the presence or absence of peaks in a designated spectral region, rather than peak identities. To eliminate subjectivity in comparing spectra visually, multivariate algorithms^{100,101, 102} are commonly used for spectral interpretation. These algorithms facilitate microorganism characterization by comparing and estimating similarities between acquired and reference spectra and allow experimentally-acquired spectra to be matched against previously-constructed libraries containing known spectra. Mass profiling has shown to be a very popular approach for rapid analysis of microbials¹⁰³⁻¹⁰⁷ and are advantageous when complete protein sequence information is not available because no knowledge of the type of biomarker ions is needed, however in the presence of mixed organisms populations these methods have been shown to have limitations¹⁰⁸. Additionally, generated spectra can be influenced by many experimental factors making data interpretation difficult. Mass profiling methods must give careful attention to standardization of experimental

details such that reproducible spectra are obtained, and can be accurately compared to reference spectral libraries. If this necessary requirement is fulfilled, quality spectral data with high reproducibility is feasible⁶⁹.

Confident identification of microorganisms through protein sequencing techniques is performed by analyzing individual peaks in a mass spectrum, determining the sequence of a partial protein or peptide fragment that corresponds to the peak(s) of interest, and identifying the microorganism from the expressed protein sequence information¹⁰⁹⁻¹¹⁴. This approach often includes purification and separation procedures, protease digestion of proteins and peptide ion fragmentation techniques. The experimentally observed intact masses and MS-induced fragments are compared using databases that contain stored data of calculated peptide masses that are predicted from the amino acid sequences and are derived from the originating protein. MALDI-TOF MS, ESI-MS, and the commercial introduction of tandem mass spectrometers have been central for protein sequencing analyses. Protein sequencing techniques can be further grouped into two major types of approaches for biomarker discovery: 1) Top-down proteomics involves isolating native proteins directly from samples and generating intact protein ions for MS analysis. Biomarker identification and selection is then derived from the undigested native proteins of interest. Top-down proteomics is advantageous in that it allows potential access to complete protein sequences and can elucidate posttranslational modifications, however analysis requires ultrahigh resolution instrumentation, spectral interpretation is complex and purified or partially purified samples are generally needed. 2) Bottom-up proteomics involves enzymatic digestion of samples, liquid chromatography-based peptide separations, and tandem mass spectrometric (MS/MS)

analysis for identification and quantitation. Bottom-up MS-based proteomics is the most mature of the sequencing techniques, and some of the most widely used workflows include peptide mass mapping^{115, 116}, *de novo* sequencing¹¹⁷, peptide sequence tagging¹¹⁸, and “shotgun” techniques^{119, 120}. Bottom-up techniques are advantageous in that they enable the analysis of complex samples and can be quantitative, but are limited in their speed, and in that only partial sequence coverage is obtained, which may not be sufficient to identify protein isoforms or types and locations of posttranslational modifications.

1.4.3. MALDI-TOF MS

The work of Karas and Hillenkamp and Tanaka in demonstrating the ability of matrix-assisted laser desorption/ionization (MALDI) to generate high m/z ions for the analysis of biomolecules^{87, 121-123} played a pivotal role in biomolecule characterization by extending the range of molecular weights and sample types that could be investigated. Today, MALDI is widely used for mass spectrometric analysis of large, nonvolatile biomolecules, including peptides, proteins, oligonucleotides, and oligosaccharides, thus enabling applications in a wide range of scientific fields¹²⁴. MALDI is a soft ionization technique where analyte desorption and ionization is triggered by a UV laser beam that is fired onto the sample that is co-crystallized in a matrix compound. This matrix serves to absorb the laser energy, mitigating fragmentation and facilitating vaporization/ionization of the analyte¹²¹. MALDI is primarily coupled to TOF mass analyzers due to its pulsed nature. MALDI's soft ionization transforms neutral proteins and other cellular components present in samples into intact charged ions, and then pulses these ions into the ion optics of the TOF mass spectrometer. The ions are then accelerated by strong

electric fields into the flight tube of the instrument with the ion's flight time inside the mass analyzer dependent on its mass and charge. All ions start out with approximately the same kinetic energy thus, smaller ions will have a higher velocity and shorter flight times than larger ions. MALDI-TOF MS does not involve a chromatographic separation, and ions are generally singly charged, resulting in easier-to-interpret spectra that are acquired in seconds over a broad mass range. MALDI-TOF MS has extensively been used for analyzing a variety of biomolecules^{55, 69, 125, 126} and its ability to produce information rich mass spectra in a theoretical unlimited mass range make it extremely popular for direct whole-cell and isolated intact protein analysis by top-down approaches. Additionally, MALDI's speed, sensitivity, tolerance to contaminants, and broadband capability¹⁰⁸ make it attractive for analyzing microorganism-containing samples via mass profiling in that it can be used to produce a "snapshot" of proteins and other cellular components present in whole cell microorganisms^{108, 116, 127}. MALDI-TOF MS has resulted in powerful yet easy to use instrumentation that has been utilized to detect viruses¹²⁸⁻¹³⁰, fungi¹³¹⁻¹³³, and bacteria^{69, 94, 108}. In 1996, Holland and colleagues published the first article on rapid identification of whole cell bacteria via MALDI-TOF spectral patterns⁹⁵ and since this time MALDI analysis of bacteria has been extensively used to rapidly identify and differentiate bacteria at the genus, species, subtype, and strain levels^{69, 106, 108, 134-136}. MALDI-TOF MS is an attractive identification tool for bacteria because of the ease of sample preparation that accompanies the technique, as bacteria can be applied directly to the sample plate with little to no sample clean up¹³⁷. Additionally, MALDI-TOF MS's relatively high tolerance to salts and buffers, that are often found in bacterial culture media¹³³, help simplify sample preparation protocols prior to analysis.

Further, MALDI analysis can be easily automated, allowing high sample throughput when analyzing numerous samples. The work detailed in Chapter 3 of this thesis discusses a new method for direct whole-cell bacterial detection of *C. burnetii* to the strain-level by MALDI-TOF mass profiling and statistical analysis.

While MALDI-TOF MS can be a powerful tool for direct bacterial detection, there are drawbacks that currently limit its widespread use. Current bacterial detection limits are relatively high for real world scenarios and are not particularly competitive with PCR and immunodiagnosics¹³⁸. For this reason, much emphasis has been placed on sample preparations techniques to produce sensitive MALDI-TOF MS methods for microorganisms identification. In particular, a heavy reliance is placed on traditional culture to isolate and amplify bacterium, which limits rapid detection in a true sense⁶⁹. Mixed populations of microorganisms are often present, which can necessitate incorporation of a purification step to isolate or separate the targeted bacterium, which further extends analysis times¹⁰⁸. Finally, accurate peptide and protein analysis requires sample-to-sample comparison; however it has been found that day-to-day and culture-to-culture reproducibility of MALDI-TOF mass spectra of bacteria can be low and because MALDI mass peaks are typically of protein origin, factors that change protein expression such as growth time, growth temperature, and growth media can significantly alter MALDI mass spectra^{139, 140}. For these reasons, alternative MALDI-TOF MS techniques have been introduced for the analysis of bacteria. One such technique that addresses these limitations utilizes phage amplification detection (PAD) MALDI-TOF MS for indirect bacterial detection. PAD MALDI-TOF MS was first introduced by Madonna and coworkers to imply the presence of bacteria in samples and address the problem of

sensitivity for bacterial detection¹⁴¹. This work was expanded on by Rees and coworkers¹⁴⁰ to overcome issues associated with diverse bacterial communities by using PAD MALDI-TOF MS to simultaneously detect bacteria in mixed bacterial populations. In Chapter 4, the use of isotopically ¹⁵N-labeled PAD coupled with MALDI-TOF MS will be used to overcome some of the existing limitations associated with both direct bacterial detection via MALDI-TOF MS and with existing PAD MALDI-TOF MS approaches. This ¹⁵N PAD MALDI-TOF MS method offers enhanced specificity, improved sensitivity, simplified mass spectral interpretation, protein expression variation elimination, and reduction in total analysis times.

1.4.4. DART-TOF MS

Direct analysis in real time (DART) ionization, introduced by Cody et al. in 2005⁸⁸, is a recently introduced ambient ionization technique that has gained a significant amount of popularity¹⁴²⁻¹⁴⁷. DART ionization allows for the direct analysis of sample surfaces of any size, shape texture/morphology by creating ions in the open air and quickly probing intact solid samples in their native state. Mass spectra are produced in less than a second without the need for sample preparation or chromatographic separation. In conventional mass spectrometric experiments, the sample is generally dissolved prior to analysis. However, DART eliminates the requirement for samples to be dissolved prior to being ionized, which greatly increases the scope of sample types amenable to MS analysis. DART-TOF MS uses an ionizing beam of heated metastable helium atoms to ionize atmospheric water and generate water clusters which in turn ionize the sample in the gas stream and produce mass spectra that are relatively clean and

simple¹⁴⁸. DART-TOF MS has demonstrated success in a broad range of analytical applications including chemical warfare agents, amino acids, peptides, drugs of abuse, explosives, pharmaceuticals, and oligosaccharides⁸⁸. Since its inception, DART-TOF MS has also had proven success in numerous protocols for biological analyte identification¹⁴⁹⁻¹⁵³. Due to the limited molecular weight range of analytes that can be transformed into the gaseous phase following thermal desorption¹⁵⁴, DART is relatively limited in mass range (up to ~800 Da), and its ability to monitor high m/z peptides and partial protein sequences for microbial identification is constrained. Alternative detection strategies that can be used for microbial identification that monitor low to mid-mass range analytes include lipid analysis, activity assays. Recently, Bevilacqua and colleagues were able to circumvent this low-mass limitation by developing a biotoxin activity assay to detect the protein toxin ricin¹⁵⁵. The work detailed in Chapter 2 of this thesis expands the analytical toolbox for microbial analysis by presenting a new approach for direct whole-cell bacterial detection to the strain-level by fatty acid methyl ester (FAME) DART-TOF mass profiling.

1.4.5. LC-ESI-MS/MS

The concept of electrospray ionization (ESI) was introduced by Chapman^{156, 157} in the late 1930's and was later demonstrated in 1968 by Dole¹⁵⁸. The first reported coupling of liquid chromatography (LC) to MS for the analysis of biomolecules was reported by Horning in 1974 through an atmospheric pressure chemical ionization (APCI) interface^{159, 160}, but the final breakthrough that enabled the effective coupling of LC to MS for widespread routine application occurred in 1988 when Fenn and coworkers¹⁶¹⁻¹⁶³ and Aleksandrov and coworkers¹⁶⁴⁻¹⁶⁶ demonstrated the ESI-MS

interface. This research demonstrated ESI-MS analyses of peptides and proteins up to 40 kDa¹⁶⁷ in molecular weight (later extended to 180 kDa the following year⁸⁶) and was a major breakthrough that led to an explosion in popularity of the electrospray technique. In conventional ESI, the first step involves the transformation of a sample solution into a charged aerosol. This aerosol undergoes desolvation as droplets migrate against a countercurrent flow of N₂ into the high-vacuum regions of a mass spectrometer. The charged aerosol is generated by application of a potential either to the exterior of a conductive capillary, or directly to a solution via a conductive liquid-liquid junction. This potential induces charge separation in the solution and causes charge to build up and migrate to the tip of the capillary, forming a Taylor cone and causing the ejection of charged droplets¹⁶⁸. Since the electrospray ionization process requires thorough solvent evaporation, typical ESI solutions are prepared by mixing a volatile organic solvent with water. Small amounts (0.002%-0.1% v/v) of a weak organic acid, typically formic, trifluoroacetic, or acetic acid, are added to the solution to facilitate formation of positively charged ions and to increase the conductivity of the solution¹⁶⁹. The charged aerosol generated by the Taylor cone is then directed into the mass spectrometer through an orifice or heated capillary. Electrospray sources are typically operated with flow rates ranging between 0.1 - 1.0 mL/min however, they can also be operated with much lower flow rates. By decreasing the inner diameter of the conductive capillary used in the ESI source, flow rates as low as μ L to nL/min can successfully be employed. Micro- and nano-ESI generate much smaller initial droplets; resulting in improved ionization efficiency due to the smaller initial droplet population, improved desolvation, increased

tolerance to sample contamination, reduction in adduct formation¹⁶⁹⁻¹⁷¹, and improved sensitivity¹⁷².

ESI is similar in character to MALDI in relative softness, but generates more multiply charged ions, and is currently used as an alternative means for biological analysis. Interfacing separation techniques, such as LC, with ESI-MS improves overall response, allows sequential analyte elution from the column for detection of more components, and simultaneously reducing ion suppression since fewer components are present during ionization¹⁷³. This in turn offers better run-to-run reproducibility, increased sensitivity, and increased spectral quality. Therefore, while chromatography adds to the time required for data acquisition and analysis times are greater than those seen with MALDI approaches, spectral output is of higher quality¹⁷³.

ESI coupled to tandem mass spectrometers are routinely used for analyses. Tandem mass spectrometry (MS/MS) is beneficial in that the mass selection stages remove chemical background and other unwanted interferents, and provides high structural selectivity and increased signal-to-noise ratio¹⁷⁴. Tandem instruments consist of multiple stages of mass analysis separation. This mass selection can be accomplished with a single mass spectrometer with MS steps separated in time (tandem-in-time) or with separate mass spectrometers with the MS steps separated in space (tandem-in-space). In either case, each mass stage is separated by a region where selected masses are activated in some way that causes the formation of fragment ions. There are four main types of MS/MS modes (precursor ion scan, product ion scan, neutral loss scan, selected/multiple reaction monitoring). A quantitative MS/MS approach based on multiple reaction monitoring MS/MS (MRM MS) will be presented in Chapter 5, thus

this MS/MS mode will be discussed in further detail. In MRM, the first mass selection stage selects a single (precursor) mass that is characteristic of a given analyte. Following selection, the mass-selected ions pass through an activation region where the precursor ions are dissociated and produce smaller fragment (product) ions. These fragment ions are usually produced through collision-induced dissociation (CID) or collisional activation (CA). Following dissociation, the second stage of mass selection is used to filter and separate selected product ions according to mass and the resulting MS/MS spectrum consists of only product ions from the selected precursor.

ESI is most often coupled to ion traps, triple quadrupole (Q-q-Q), and quadrupole-time-of-flight (QqTOF) MS/MS instruments. Ion trap analyzers for tandem-in-time analysis are robust, sensitive, and relatively inexpensive, but have relatively low mass accuracy and resolution when compared to other types of instruments. QqTOF hybrid platforms select ions of a particular m/z in the first mass analyzer (Q), fragment ions in a collision cell (q), and analyze the fragmented ions in the TOF analyzer. This hybrid platform offers high sensitivity, resolution and high mass accuracy. Similarly, Q-q-Q-derived technologies consist of three quadrupole mass spectrometers in series where Q_1 and Q_3 perform mass filtering functions while the middle q_2 quadrupole is employed as the collision cell.

The LC-ESI-MS/MS instrumental platform has led to significant improvements in types and complexity of samples that can be analyzed, sensitivity of detection, and amount of structural information that can be obtained¹⁷⁵. Recently, LC-ESI-MS/MS has had success for detection of diverse biomolecules, including phospholipids¹⁷⁶, glycolipids¹⁷⁷, carbohydrates¹⁷⁸, proteins¹⁷⁹⁻¹⁸¹, and peptides¹⁸²⁻¹⁸⁴. For these reasons,

LC-ESI-MS/MS is becoming increasingly popular for MS-based microbial biomarker discovery and bacterial identification^{116, 185}. Despite the complexity of bacteria, LC-ESI-MS/MS analyses of whole cell or crude cell extracts can produce reproducible measurements without the need for rigorous sample clean-up. LC-ESI-MS/MS is also capable of detecting targeted bacteria in mixed samples² while simultaneously yielding increased detection sensitivity. Lipids, carbohydrates, proteins, and nucleic acids are among the top choices for bacterial characterization by MS; however compared to other cellular components, proteins make up over 50% of a bacteria's dry cell weight, therefore they have greater potential to yield unique biomarkers for microbial characterizations¹⁷². Multiply charged protein and peptide ions are easily produced by ESI because they have possess multiple sites where protonation or deprotonation can occur. This is advantageous in that high molecular weight analytes can be detected at low m/z values, where mass analyzers and detectors perform at their best. Because MS peptide fragmentation is not random, but follows defined pathways, the first stage of an MRM experiment selects the m/z of the intact precursor peptide ions, while the second stage, following collisional activation, monitors one or more specific fragments from the primary amino acid sequence of the target. The highly specific MRM-based data generated is then used to determine the amino acid composition of specific peptides of interest to reveal the identity of the microorganism. This has significantly increased the accuracy of protein identification compared with microbial identification using only molecular weight information from a single MALDI-TOF MS analysis².

Until about a decade ago, proteomics was largely a qualitative discipline; today, quantitative strategies have become widely used¹⁸⁶. While MS has long been used in a

quantitative manner in the small molecule field¹⁸⁷, the field of quantitative mass-spectrometry-based proteomics is currently under fast development¹⁸⁶. LC-ESI-MS/MS is playing an integral role in this process with both label-free and stable isotope MS approaches available for accurate quantification of analyte concentration. Label-free quantitation compares ion intensities of identical peptides or the number of acquired spectra for each protein. Stable isotope quantitation is based on the fact that a labeled species differs from the unlabeled one in terms of its mass but exhibits almost identical chemical properties such as ion yields and retention times. Stable isotope labels can be introduced chemically, enzymatically, and metabolically. The latter is introduced to the whole cell or organism through the growth medium. In the field of proteomics, ¹⁵N-labeling was first used to study bacteria in 1999¹⁸⁸ and quantitative protein analysis based on metabolic labeling has since been applied in various applications¹⁸⁹⁻¹⁹². Chapter 5 of this thesis presents a stable isotope labeling method using quantitative LC-ESI-MS/MS mass-spectrometry-based proteomics to quantify *S. aureus*. In this novel technique, a metabolically labeled ¹⁵N reference bacteriophage is utilized as both the input phage and as the internal standard for quantitation. Quantitation of the *S. aureus* samples was achieved by comparing peak areas of targeted peptides from the metabolically labeled ¹⁵N reference bacteriophage internal standard with that of the wild-type ¹⁴N peptide fragments that were produced by phage amplification and subsequent digestion when the host bacteria was present.

1.4.6. Data analysis

Regardless of the experimental approach selected, the amount of data generated and collected from MS-based work is significant. The simplest form of mass profiling data analysis is by visual determination of replicate mass spectra of the same microorganism and comparison of spectra from different microorganisms¹¹⁶. This necessarily requires that either some masses are unique for a given bacterium relative to a set of different bacterial mass spectra, the intensity distribution is distinctly different for the same set of masses between different bacterial mass spectra¹¹⁶, or both. Chapter 2 of this thesis presents generated FAME profiles from whole-cell bacteria via DART-TOF MS that display markedly different spectra in terms of both mass and intensity that allow differentiation to the strain level by visual analysis alone. However, visually inspecting and manually processing acquired data is time and labor intensive, and can be inefficient and inconsistent. Alternatively, diverse data analysis methods to analyze MS-data, including protein/peptide occurrence, abundance, identity, sequence, structure, properties, and interactions, have been developed¹⁹³. A variety of data analysis methods specific to MALDI MS are also available, such as cross-correlation¹⁰⁰, automated mass extraction¹⁹⁴, and cluster analysis^{101, 195}, to transform spectral data into meaningful information for microorganism differentiation. Chapter 3 of this thesis presents a whole-cell *C. burnetii* MALDI fingerprinting technique that utilizes a multivariate pattern recognition algorithm to interpret mass spectral data. Multivariate pattern recognition allows mass spectral data interpretation calculated from individual experimental variables or measurements on a magnitude that is impossible to achieve by human discernment alone¹⁹⁶. In this work, MALDI bacterial protein mass patterns were processed using multivariate pattern

recognition method based on partial least squares-discriminant analysis (PLS-DA) for accurate discrimination of *C. burnetii* to the strain level⁹⁹, which will be discussed in further detail in Chapter 3.

Public genomic databases and internet-accessible protein sequence databases are widely available for protein characterization by MS. The most commonly used databases are the National Center for Biotechnology Information's (NCBI) Entrez Protein database, the NCBI Reference Sequence (RefSeq) database, and UniProt (consisting of Swiss-Prot and its supplement TrEMBL). Various databases searching methods, which make use of partial protein sequences derived from MS techniques, allow limited sequence information to be searched against existing protein databases, and a number of different algorithms that compare mass spectra against comprehensive protein sequence databases exists. In order to accurately identify a particular microorganism via bioinformatics-based approaches, the genome of the microorganism must be fully sequenced to ensure the proteome database is complete, and thus contains the proteins for the 'unknown' microorganism. In 2011, 1457 fully sequenced microbial genomes were available, together with 3911 prokaryotic genome-sequencing projects 'in progress'¹⁹⁷, providing an unprecedented resource for microbial proteomics studies. While fully sequenced genomes were not available for the *C. burnetii* strain-level MS applications, the work presented in Chapters 4 and 5 was dependent on unambiguous protein biomarker determination by matching the experimentally-determined protein against the predicted protein sequence available from online protein sequence databases. MALDI-TOF MS and LC-MS/MS data was analyzed, database searching of the MS/MS spectra was utilized, sequence

information from protein databases was extracted, and MS/MS-based peptide and protein identification was algorithmically validated for successful microorganism identification.

CHAPTER 2. AMBIENT GENERATION OF FATTY ACID METHYL ESTER PROFILES FROM BACTERIAL WHOLE CELLS BY DIRECT ANALYSIS IN REAL TIME (DART) MASS SPECTROMETRY

2.1. Abstract

This chapter describes the first implementation of DART-TOF MS) used for the rapid and direct detection of fatty acid methyl esters (FAMES) produced from whole bacterial cells. A detailed description of the bacterial sample preparation procedures and instrumental set-up, including the DART ion source and TOF MS detection parameters, is provided. Preliminary data collected from *E. coli*, *S. pyogenes*, and *C. burnetii* is also presented.

2.2. Introduction

2.2.1. Ambient mass spectrometry

MS is a well established tool for addressing biological problems. Through the work of Fenselau's, it has been shown that the application of MS to biomarker discovery for microbial identification offers a powerful complement to traditional microbiological approaches¹⁹⁸. In the last decade, a wide variety of desorption/ionization methods for MS has been developed and subsequently applied to microbial identification problems¹⁰⁸. Recently, several new high throughput “ambient” ionization methods that operate in open air have been reported¹⁹⁹. Two of the most studied ambient ionization methods have been desorption electrospray ionization (DESI)⁸⁹ and DART⁸⁸.

Takáts et al. were the first to recognize the potential of these ambient ionization methods for microorganism identification, showing DESI mass spectra of freshly harvested, untreated *Escherichia coli* and *Pseudomonas aeruginosa* samples deposited on PTFE²⁰⁰. However, the potential of other ambient ionization methods, such as DART, for generating ions from microbial samples has not yet been reported. This chapter describes the first results on the generation of fatty acid methyl ester ions from whole bacterial suspensions by DART, and their identification by accurate-mass orthogonal TOF MS.

DART is conducted in open air, allowing for the rapid, non-contact analysis of solid, liquid, and gaseous materials without sample preparation⁸⁸. The DART process begins with a He stream that supports a point-to-plane glow discharge. A series of processes within this discharge (electron-impact, ion-electron recombination) produce metastable He atoms (He*, 19.8 eV), which are carried downstream by the gas. Immediately after the region where the discharge takes place, the gas stream is heated to temperatures that can be varied from 150 to 450 °C. Although the DART ionization mechanisms are not yet fully understood, it has been proposed that, upon exiting the ion source, He* atoms induce Penning ionization of atmospheric water, generating protonated water clusters⁸⁸. Gaseous analytes vaporized from the solid or liquid sample react with these clusters, forming protonated adduct ions. A more detailed discussion of DART ionization can be found elsewhere^{88, 201, 202}.

2.2.2. FAMES methodology

As recently described by Fox⁷², one of the “gold standard” methods routinely used in the field of clinical bacterial identification is based on the determination of

microbial fatty acid methyl ester (FAME) composition after culture, which forms the basis of the commercial Sherlock® microbial identification system (MIDI, Inc., Newark, DE). FAME composition analysis starts with saponification of the lipidic material in bacterial cells, followed by fatty acid methylation, and gas chromatographic analysis with flame ionization or mass spectrometric detection. Sample preparation for this method takes several hours, and each chromatographic run can take 20 to 30 min⁷².

Alternative approaches to FAME composition that avoid the chromatographic separation step have also been reported. For example, Xu *et al.* described a method that relies on *in situ* lipid hydrolysis and methylation of bacterial samples to generate FAMEs, followed by chemical ionization (CI) MS²⁰³. As CI occurs by proton transfer, it has the advantage of reducing the amount of internal energy deposited on the generated ions, thus significantly reducing FAME ion fragmentation. For most analytes, DART ionization has also been found to occur by proton transfer, as in CI. In addition, it was observed that DART sensitivity is particularly good for volatile or semi-volatile molecules, such as FAMEs. Due to these concurrent features, it seems logical to investigate the feasibility of producing FAME ions by DART. The successful demonstration of the generation of FAME ions from bacterial whole cells via DART constitutes the first step that could lead, in the future, to the successful development of new approaches for high throughput microbial identification in a variety of biological, foodstuff, and water samples in open air, with minimum sample preparation.

2.3. Experimental

FAMEs were generated from whole cell bacterial suspensions (*Streptococcus pyogenes* ATCC 700294; 10^7 CFU μL^{-1} ; *E. coli* ATCC 25922; 10^7 CFU μL^{-1} ; γ -irradiated

C. burnetii; 10^8 CFU μL^{-1}). *S. pyogenes* and *E. coli* were cultured by inoculation in tubes containing 30 mL of Todd Hewitt broth (THB). After incubation at 37 °C for 18-24 h, cells were washed three times with 10 mL of TRIS-sucrose buffer (0.01 M TRIS, 0.025 M sucrose, pH 7.0) by centrifugation under refrigeration (4-10 °C). Cells were then suspended in 500 μL of ultrapure water, and kept at -80 °C. All *C. burnetii* strains were cultured in identical conditions as described previously¹³⁴. Aqueous bacterial suspensions were diluted 1:1 (v/v) with a 0.27 M solution of tetramethylammonium hydroxide (TMAH) (+99%, Aldrich, Milwaukee, WI) to produce thermal hydrolysis and methylation of bacterial lipids. The DART source was interfaced to a JMS-100TLC (AccuTOF™) orthogonal time-of-flight mass spectrometer (JEOL, USA, Inc., Peabody, MA) operated in positive-ion mode. Helium gas (7.0 L min^{-1}) was introduced into the DART glow discharge chamber where a needle electrode was held at -3000 V. This discharge is physically detached from the open-air ionization region where the sample is placed by two small cylindrical chambers, each ending in a DC-biased electrode. The first electrode was held at 300 V and the exit electrode at 150 V. The gas flow and electrode potentials have a broad operating maximum and many combinations of settings presented similar sensitivities. The DART ion source was positioned in front of the mass spectrometer inlet orifice. The inlet orifice voltage was 54 V vs. ground. The distance between the DART ion source exit, and the spectrometer inlet was 20 mm. A sliding arm was used to assure reproducible sample positioning within the DART ionizing stream. An alligator clip secured to this arm was used to hold a 1.5 o.d. x 90 mm long glass capillary tube in the vertical position. A 4 μL aliquot of the whole bacterial cell suspension mixed with TMAH was deposited directly with a micropipette to the bottom of the capillary

tube. The capillary was positioned so that, after sliding the sample holder arm, the bottom of the tube came in contact with the DART He stream directly in front of the spectrometer inlet orifice. Clean, unused, capillary tubes were used each time. The DART ion source was heated following a rapid temperature gradient. The initial temperature was set at 150 °C, and data acquisition began at $t = 0$ min. Data were acquired for 1 min for background correction purposes. At $t = 1$ min the sliding sample holder was quickly shifted, placing the capillary (with the sample on its surface) in front of the spectrometer inlet. The temperature controller was simultaneously switched to ramp to 500 °C in 3 min. Spectral data were acquired until the total ion signal intensity completely decreased to background levels at $t = 7$ min. The sample was then removed from the ionization region. At $t = 8$ min a separate capillary tube loaded with neat poly(ethylene glycol) (PEG, average molecular weight 600) was briefly (1-2 s) introduced into the He stream to obtain a reference mass spectrum for TOF accurate mass measurements. Data acquisition was stopped at $t = 9$ min. The fatty acids investigated ranged from C8:1 ($C_n:x$, n = number of carbons and x = number of unsaturations) to C24:0. Spectra were acquired every 250 ms in the 150 to 600 u mass range.

2.4. Results and Discussion

Figure 2-1a and 2-1b show the *E. coli* and *S. pyogenes* reconstructed ion “chronograms” obtained by DART-TOF MS. It can be seen that when the DART temperature is ramped, discrimination in the temporal domain occurs. Identical FAMES show different time evolution profiles for different bacterial samples, possibly due to structural differences of the bacterial membranes probed. These differences are probably

caused by differences in the hydrolysis and desorption rates. In both cases the C8:0 FAME is desorbed earlier in the temperature gradient, but with a different peak shape for each sample.

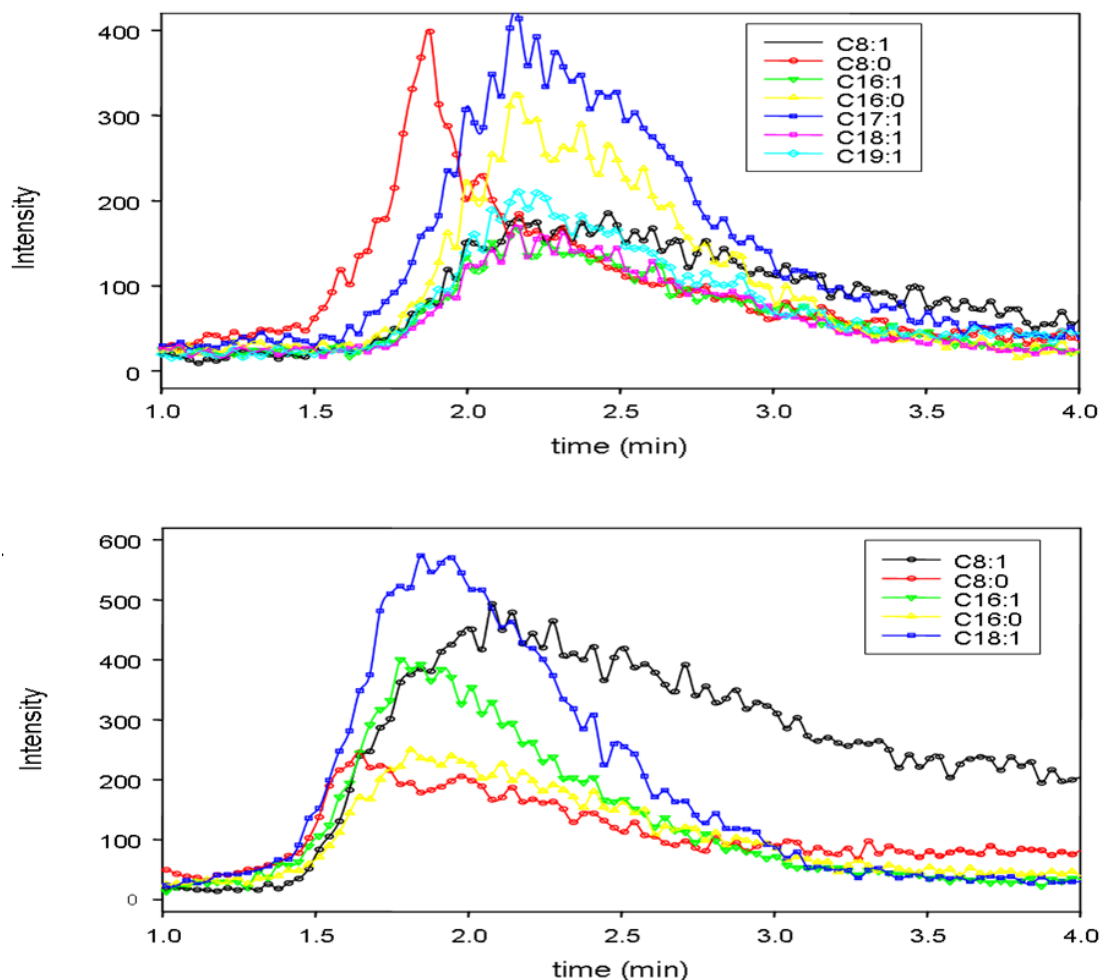


Figure 2-1 (a) Reconstructed ion chromatograms for *E. coli*. (b) Reconstructed ion chromatograms for *S. pyogenes*. Ions shown have a relative intensity of > 5%.

With this approach, the analysis time was 9 min, however the relevant FAME data is produced in the first 3-4 min, indicating the procedure could be further optimized. DART FAME analysis was also possible at a constant temperature of 200 °C in about 30s per sample, but temporal signal discrimination was lost in this mode (Figure 2-2).

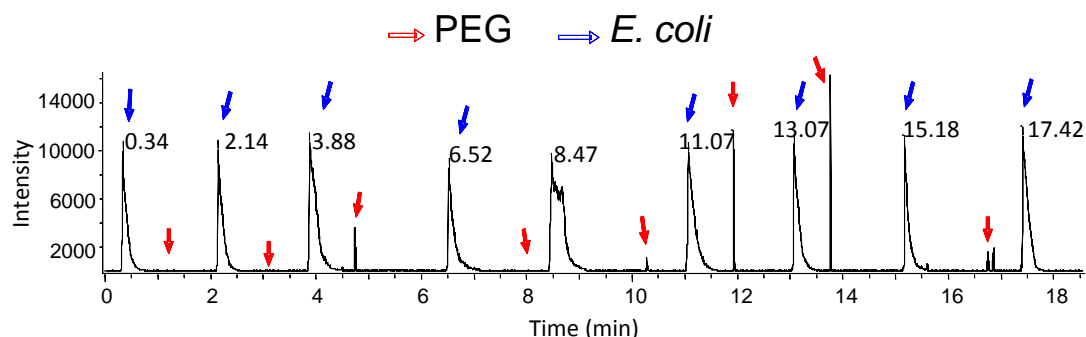


Figure 2-2 Eighteen minute-long isothermal (200 °C) DART-TOF MS run showing repeat signals produced by 4 μ L of an *E.coli* suspension manually deposited at the bottom of a glass capillary, and placed in front of the ion source via a mechanical sample holder. The peak marked with an asterisk was produced by a faulty injection. A glass capillary wetted with PEG was manually inserted in front of the mass spectrometer inlet for a few seconds after each bacterial suspension was probed.

Table 2-1 shows the types of ions identified by accurate mass measurements, their theoretical m/z , and their relative abundance for *E. coli*, and *S. pyogenes* samples. Spectral data for *C. burnetii*, which is discussed later in the context of these particular research interests, is also presented. Peaks were assigned with an average mass accuracy of 6 mmu. No attempt was made to identify FAME peaks with m/z lower than 150 or above 400 because bacterial FAME MS analysis is generally restricted to this m/z range. From these profiles, mass spectra were then obtained by averaging multiple scans within a 10 s window at the maximum of the total ion chromatogram.

Table 2-1 Comparison of bacterial fatty acid profiles and corresponding relative abundances for *E. coli*, *S. pyogenes*, and *C. burnetii* (Nine Mile I strain).

Fatty acid	Theoretical m/z	Abundance (mass [mmu])		
		<i>E. coli</i>	<i>S. pyogenes</i>	<i>C. burnetii</i>
C8:1	157.1229	5.2 [6]	14.3 [8]	-
C8:0	159.1385	8.0 [12]	10.6 [4]	2.8 [12]
C9:1	171.1385	2.3 [10]	2.1 [6]	6.4 [1]
C9:0	173.1542	4.9 [9]	-	10.9 [6]
C10:1	185.1542	2.8 [3]	3.5 [10]	-
C10:0	187.1698	3.9 [8]	-	9.2 [5]
C11:1	199.1698	-	4.4 [11]	6.0 [13]
C11:0	201.1855	3.0 [9]	-	9.5 [13]
C12:1	213.1855	2.5 [4]	1.8 [12]	4.5 [2]
C12:0	215.2011	2.9 [5]	-	-
C13:0	229.2168	-	-	6.7 [8]
C14:1	241.2168	1.3 [6]	1.6 [7]	-
C14:0	243.2324	3.5 [2]	-	8.4 [6]
C15:1	255.2324	-	-	3.2 [2]
C15:0	257.2481	4.1 [4]	-	26.0 [6]
C16:1	269.2481	10.6 [5]	24.0 [3]	10.3 [2]
C16:0	271.2637	17.6 [4]	19.1 [2]	20.1 [2]
C17:1 ^a	283.2637	21.7 [4]	-	6.3 [1]
C17:0	285.2794	-	-	28.1 [2]
C18:2	295.2637	0.5 [9]	3.4 [5]	-
C18:1	297.2794	6.9 [6]	31.8 [2]	12.8 [4]
C19:1 ^a	311.2950	12.9 [6]	-	4.1 [13]
C20:2	323.2950	-	-	2.1 [8]

^aCyclopropyl fatty acids are common constituents of bacterial lipids.

CycloC17:0 and cycloC19:0 accurate masses are identical to that of the monoenoic fatty acids C17:1 and C19:1, respectively.

Figure 2-3a illustrates DART-TOF mass spectrum for *E. coli*. For this bacterium, it has been reported that C14:0 (myristic acid), C16:0 (palmitic acid), C16:1 (palmitoleic acid), C17:1/cycloC17:0, C18:1 (oleic acid), and C19:1/cycloC19:0 account for over 98% of total fatty acid components²⁰³. The experimental spectrum in Figure 2-3a shows that these fatty acids were all detectable as protonated methyl esters, with C17:1/cycloC17:0 being the most abundant. The protonated fatty acids methyl esters of C16:1, C16:0, and C18:1 dominated the spectra for *S. pyogenes*, with C18:1 having the highest intensity

(Fig 2-3b). C9:0, C10:0, C11:0, C12:0, C14:0, C15:0, C17:1/cycloC17:0, and C19:1/cycloC19:0 were found to be present in *E. coli* only, while C11:1 was uniquely detected in *S. pyogenes*. C17:1/cycloC17:0 and C19:1/cycloC19:0 were found in *E. coli* at relatively high abundances but were not detected in the *S. pyogenes* spectrum, in agreement with the membrane characteristics of Gram negative bacteria²⁰³. Some FAME ions were also common to *E. coli*, and *S. pyogenes*, however clear differences existed in the relative abundances of these ions in the respective mass spectra.

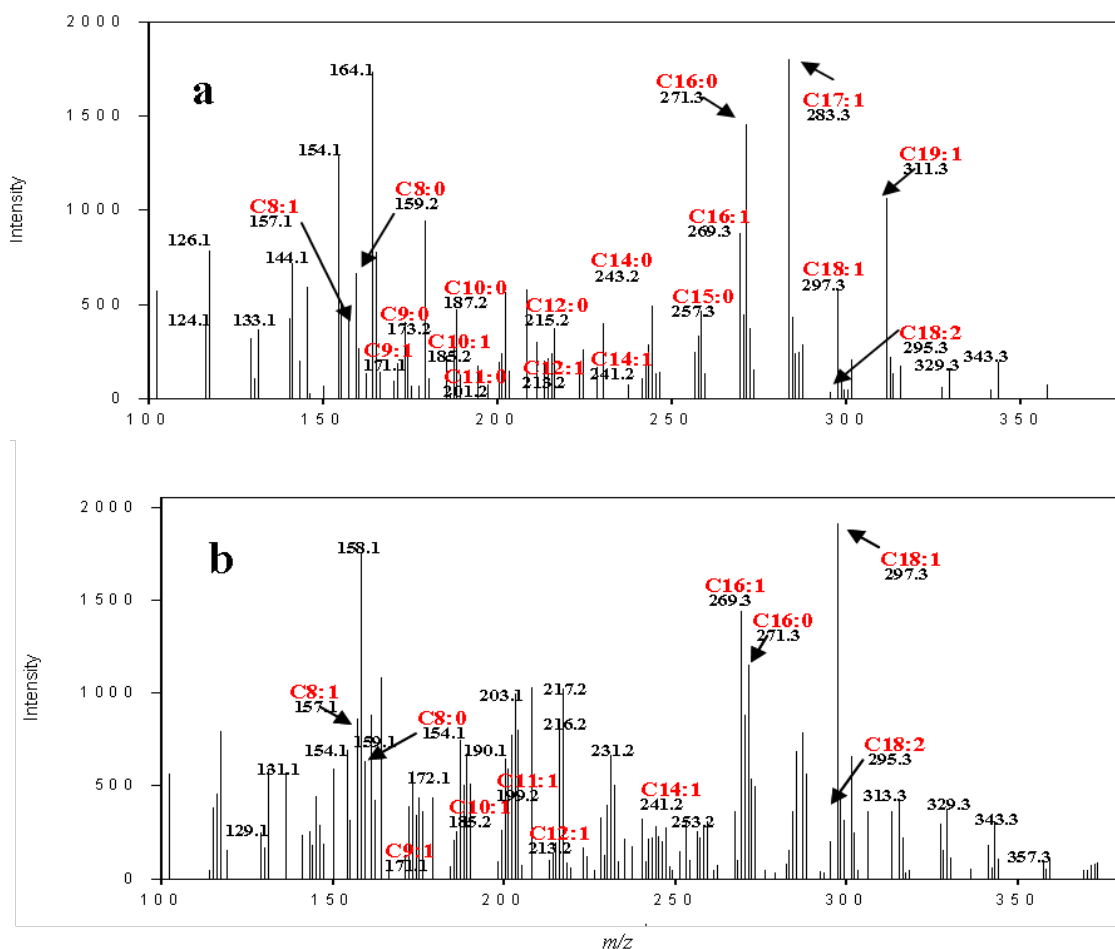


Figure 2-3 Positive ion mass spectrum of (a) *E. coli* (Gram negative) and (b) *S. pyogenes* (Gram positive) acquired by direct DART-TOF MS analysis after *in-situ* thermal hydrolysis/methylation of the bacterial membrane fatty acids to generate the corresponding FAMEs.

Differences among samples were thus observed in the spectral, temporal and intensity domains. The FAME spectra obtained by DART-TOF MS were not identical to the ones obtained by CI-based methods²⁰³. However, these differences are to be expected, as differences in sample growth conditions, or in the ion yields or ion transmission of the different instruments used could affect the observed FAME ion intensities²⁰². Notwithstanding these differences, these findings indicate that it is possible to generate FAME ions from bacterial samples by DART.

In order to further investigate the types of ions observed from different bacterial samples, three strains of *C. burnetii*, were investigated by the DART-TOF MS approach. Figure 2-4 shows the *C. burnetii* (Nine Mile I strain) FAME mass spectrum obtained by DART-TOF MS. Several FAMES were identified, with C9:0, C12:0, C15:1, C15:0, C16:0, and C17:0 being the most abundant; and C15:0 alone accounting for over 38% of the total signal intensity. C15:1, C17:0, C19:0, C21:1, C21:0, C24:1, and C24:0 were found to be unique to *C. burnetii* Nine Mile I when compared to *E. coli* and *S. pyogenes* (Table 2-1), exhibiting a distinct mass spectrum (Figure 2-4). DART-TOF mass spectra for two other *C. burnetii* strains (Nine Mile II and RSA 514) (Figure 2-5), show marked spectral difference with the Nine Mile I strain.

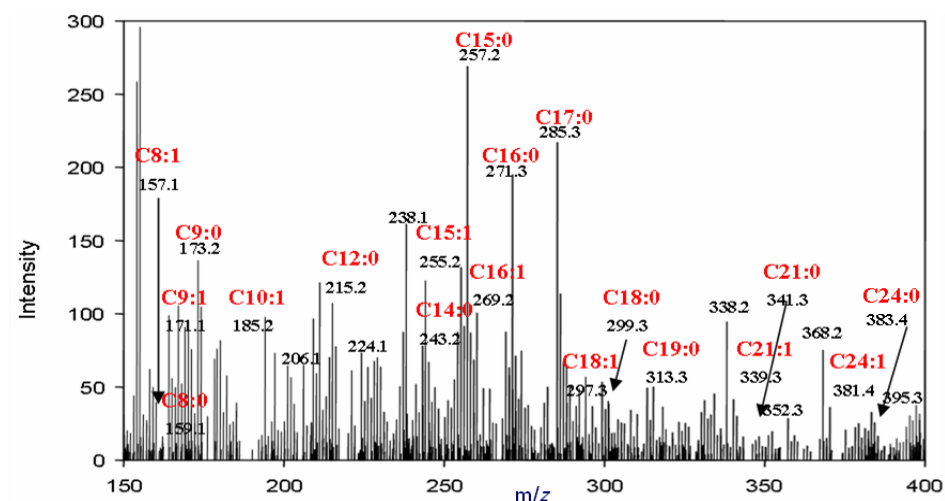


Figure 2-4 Positive ion mass spectrum of *C. burnetii* Nine Mile I (Gram negative) acquired by DART-TOF MS analysis of *in-situ* thermal hydrolysis/methylation ionization of the bacterial membrane fatty acids to generate the corresponding FAMES.

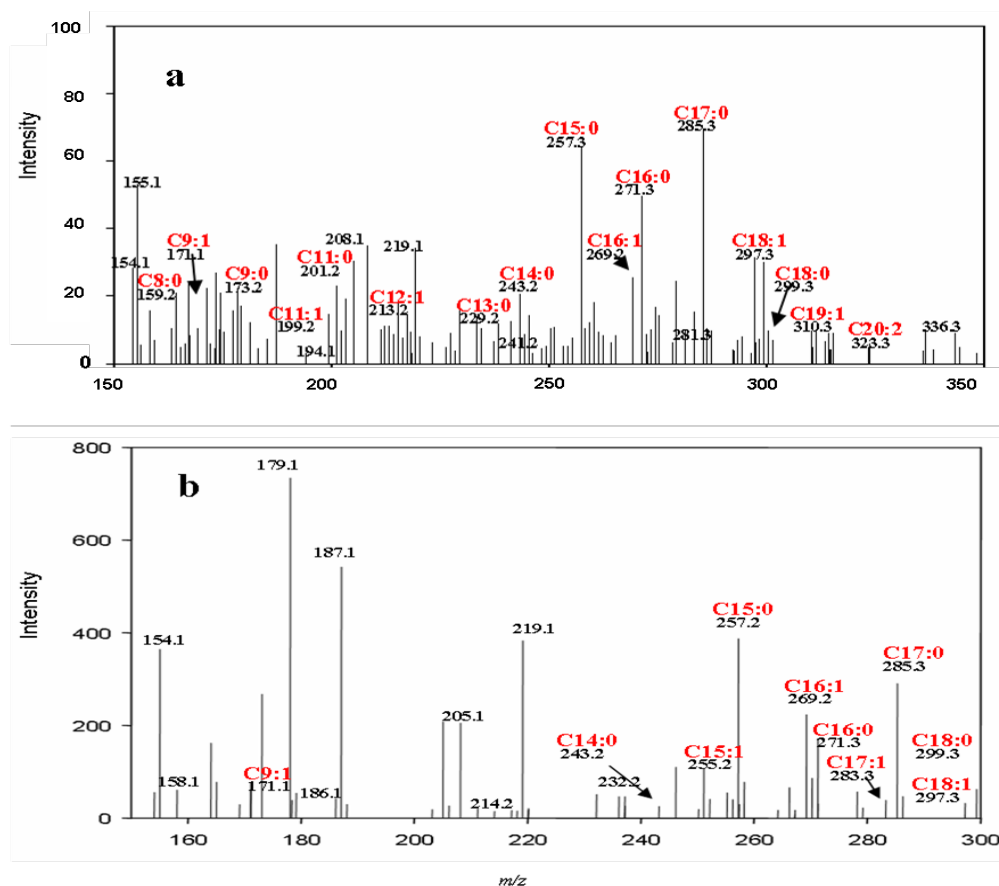


Figure 2-5 Positive ion mass spectrum of (a) *C. burnetii* Nine Mile II (Gram negative) and (b) *C. burnetii* RSA 514 (Gram negative) acquired by DART-TOF MS analysis of *in-situ* thermal hydrolysis/methylation ionization of the bacterial membrane fatty acids to generate the corresponding fatty acid methyl esters (FAMES).

2.5. Conclusions

In conclusion, the results show that DART-TOF MS can successfully produce unique fatty acid methyl ester mass spectra from various bacterial samples. The method is fast and operates in open air, opening the possibility of investigating the presence of microorganisms on other types of surfaces. The FAME mass spectra were generated using a simple procedure, which involved co-deposition of intact bacteria and TMAH solution prior to DART-TOF MS analysis. So far, mass spectral analysis has been performed by simple visual inspection in one of the analytical dimensions at a time (i.e. time, m/z , or intensity) but more sophisticated multiway data analysis approaches, such as parallel factor analysis (PARAFAC) could also be applied to this type of data²⁰⁴. Future research will focus on improving sensitivity, studying bacterial mixtures, and the effect of different ionization and culture conditions on the observed mass spectra.

CHAPTER 3. STRAIN AND PHASE IDENTIFICATION OF THE U.S. CATEGORY B AGENT COXIELLA BURNETII BY MATRIX- ASSISTED LASER DESORPTION/IONIZATION TIME-OF-FLIGHT MASS SPECTROMETRY AND MULTIVARIATE PATTERN RECOGNITION

3.1. Abstract

Chapter 2 described initial findings for bacterial characterization, including *C. burnetii* differentiation, and the performance of ambient MS by evaluating bacterial FAMEs profiles. Although these preliminary studies demonstrated the potential of MS for identification of *C. burnetii* and strain-level discrimination, to further demonstrate the capability of mass spectral fingerprinting we investigated additional *C. burnetii* strains by MS and incorporated multivariate pattern recognition. The approach included in Chapter 3 involves the combined use of MALDI-TOF MS and supervised pattern recognition *via* Partial Least Squares-Discriminant Analysis (PLS-DA). *C. burnetii* isolates investigated in this study included the following prototype strains from different geographical and/or historical origins and with different antigenic properties: *Nine Mile I*, *Australian QD*, *M44*, *KAV*, *PAV*, *Henzerling*, and *Ohio*. After culture and purification following standard protocols, linear MALDI-TOF mass spectra of pure bacterial cultures were acquired in positive ion mode. Mass spectral data were normalized, baseline-corrected, denoised, binarized and modeled by PLS-DA under crossvalidation conditions. Robustness with respect to uncontrolled variations in the sample preparation and MALDI analysis

protocol was assessed by repeating the experiment on five different days spanning a period of six months. The method was validated by the prediction of unknown *C. burnetii* samples in an independent test set with 100% sensitivity and specificity for 5 out of 6 strain classes.

3.2. Introduction

3.2.1. *C. burnetii*: Facts and existing methodologies

C. burnetii, the causative agent of Q fever, is an obligate intracellular bacterium and a highly infectious pathogen for humans, usually acquired through contact with animals. It is found in a wide range of mammals including sheep, goats, and cattle and has been found throughout the world, except New Zealand²⁰⁵. In addition to being a threat to public health in its native form, *C. burnetii* is considered a US Category B bioterrorism agent due to its long-term environmental stability, resistance to heat and drying, extremely low infectious dose (ID₅₀ approaching one organism), aerosol infectious route, history of weaponization by various countries, and the ease of producing large quantities of infectious material²⁰⁶.

Although all *C. burnetii* strains described to date belong to the same serotype, many strains do differ in their immunological properties^{207, 208}. *C. burnetii* strains can be divided into two broad antigenic groups: Phase I and Phase II. Phase I is the virulent, highly infectious, natural phase of *C. burnetii* that corresponds to a “smooth” lipopolysaccharide²⁰⁹ (S-LPS) and is found in infected animals and humans, while phase II is the avirulent or less infectious phase of *C. burnetii* that is obtained only after serial passages in tissue or egg culture and corresponds to a “rough-type” LPS (R-LPS)

structure²⁰⁵ as a result of LPS truncation²¹⁰. This phenotype is the only well established trait proven to be associated with virulence. The antigenic differences presented by the two phases are useful for the serological differentiation between acute and chronic Q fever, as the presence of anti-phase II antibodies is indicative of acute Q fever while an increased anti-phase I titer is indicative of a chronic infection²⁰⁵.

Currently, Q fever diagnosis and *C. burnetii* detection are carried out by a number of methods²¹¹. The current diagnostic “gold standard” used for the detection of *C. burnetii* infection is Indirect Fluorescent Antibody (IFA) assay²¹². Other serodiagnostic assays are used less frequently to diagnose acute and chronic Q fever, including complement fixation, ELISA, Western Blotting, microagglutination, and immunohistochemistry²¹³⁻²¹⁶. When *C. burnetii* strain identification is desired, common approaches include PCR and subsequent DNA sequencing, restriction fragment length polymorphism (RFLP) analysis, and phase and plasmid typing. Isolation of the organism is typically performed in tissue culture cells or in embryonated eggs.

3.2.2. Mass spectrometry and microorganism identification

In cases where microorganisms are intentionally used to harm citizens, as in the 2001 *Bacillus anthracis* attack in the US, the development of highly-automatable confirmatory identification methods is desirable, as forensic microbial identification at the strain level is crucial in narrowing down the possible sources of the biological material²¹⁷. In particular, the application of MS to microbial identification and differentiation offers a powerful complement to traditional microbiological approaches, mostly due to its broadband detection capabilities. In this sense, MS provides a potential

advantage when compared to targeted assays that focus on a specific gene within a specific organism such as PCR.

Several reviews^{108, 218, 219}, one feature article²²⁰ and a recent book³ provide an excellent overview of the trends in the field of microorganism identification by MS. As discussed before, the main approaches can be grouped in two broad classes. Proteomic-based methods that employ tandem MS^{110, 221-224}, top-down approaches²²⁵, or accurate mass measurements²²⁶, rely on the identification of microorganism-specific peptide biomarkers. Related methods include the comparison between observed protein masses in the MALDI spectrum and protein databases^{227, 228}, and the identification of PCR amplicons via electrospray MS²²⁹.

The second group of methods relies on mass spectral library building followed by fingerprint matching²³⁰, or pattern recognition techniques. These methods are useful for microorganisms for which complete protein databases are not available, such as for some *C. burnetii* strains. Pattern recognition-based approaches using different analytical techniques such as chemical ionization of fatty acid methyl esters²³¹, ion mobility spectrometry^{232, 233}, secondary-ion mass spectrometry²³⁴ and MALDI MS^{235, 236} have been reported, with MALDI applications being the most popular due to its ability to produce information-rich mass spectra in a mass range of up to several tens of kDa.

MALDI MS in combination with unsupervised pattern recognition algorithms such as Hierarchical Cluster Analysis²³⁷, or Principal Component Analysis (PCA)²³⁸, or supervised algorithms such as Artificial Neural Networks²³⁹ has shown mixed degrees of success for analyzing microbial mass spectral data. Statistical studies of bacterial MALDI MS experiments have provided some insight on the factors reducing the success

of these approaches, showing that, whereas some mass spectral peaks are highly reproducible, and appear consistently, others appear much less reliably^{235, 240}. Two main sources of variability can be identified in microbial MALDI MS experiments. The first originates in changes in culture conditions that produce changes in protein expression levels, altering the intensity and/or occurrence of the observed mass spectral peaks²⁴¹. It is well known that culture conditions have to be kept as constant as possible to ensure reproducibility of the obtained MALDI fingerprints. In cases where culture conditions change, such as if different media batches are used, correction algorithms can be applied to transform the new set of fingerprints²⁴² with varying degrees of success. A second source of variability in the MALDI data originates in the intrinsic reproducibility of the MALDI processes, including variables such as the sample preparation protocol²⁴³, the type and quality of matrix chosen, ionization suppression effects²⁴⁴, mass scale drifts, and the possible impact of automatic data acquisition algorithms. In an effort to standardize the conditions for MALDI bacterial fingerprinting, Wunschel et al. have recently studied the sources of bacterial MALDI mass spectral variability in a comprehensive inter-laboratory study²⁴⁵.

Soft modeling methods that create optimal linear relationships among constructs specified by a conceptual model, such as PCA and PLS, can successfully mitigate the detrimental effects of noisy and highly collinear spectra²⁴⁶, such as those found in bacterial MALDI data. Because PCA relies on the generation of scores on orthogonal principal components²⁴⁷, it attempts to capture the directions of maximum variance, not seeking to capture “among-group” and “within-group” *differences* of the investigated objects²⁴⁸. Soft modeling by PLS-Discriminant Analysis (PLS-DA) is a more recent

supervised pattern recognition approach that attempts to overcome some of the drawbacks observed in PCA^{248, 249}. During PLS-DA the principal components are rotated to generate latent variables (LVs), which maximize the discriminant power between different classes, not the total mass spectral variance as in PCA, and as such, class separation is greatly improved²⁵⁰.

Because PLS-DA is a relatively modern soft modeling approach, it has not been extensively evaluated with MS data. This work presents initial results on the robust identification of purified *C. burnetii* cultures using PLS-DA. First, the occurrence and intensity of different MALDI-TOF mass spectral peaks for whole cell *C. burnetii* suspensions was assessed for experiments performed under seemingly-identical conditions. Secondly, data smoothing, denoising and binarization and PLS-DA multivariate analysis were applied to successfully differentiate seven *C. burnetii* strains in a training set containing spectral data obtained on four different days within a period of six months, despite the intrinsic MALDI variability. In addition, a two-class discrimination of *C. burnetii* phase I strains versus phase II strains was established in order to assess the antigenicity of a given purified culture. All models were validated by classifying unknown *C. burnetii* samples run on a fifth day. To the best of our knowledge, this was the first study on *C. burnetii* strain and phase discrimination using MALDI-TOF MS and PLS-DA pattern recognition.

3.3. Experimental

3.3.1. Background of different strains

Samples of Australian QD, M44, KAV, PAV, Henzerling, and Ohio strains were originally grown at The United States Army Medical Research Institute for Infectious Diseases (USAMRID) (Fort Detrick, MD). *C. burnetii* Nine Mile phase I (NM I) was grown in, and all strain samples were provided by, the Q fever unit of the Centers for Disease Control and Prevention (CDC). *C. burnetii* strains were originally classified as belonging to phase I or phase II based on complement fixation.

The *C. burnetii* NM I strain (RSA493 clone 7), was first isolated in 1935 from a *Dermacentor andersonii* tick, and is a plaque-purified phase I strain and a prototype strain of acute Q fever. To date, NM I is the only strain for which the entire genetic sequence of the NM I chromosome and its plasmid have been determined^{216, 251}. The Henzerling strain (phase I), was isolated in Italy (1945) from a WWII US army infantryman, and is currently used in Australia as a vaccine strain. The Ohio strain (phase I, found in Ohio, US) was first isolated from cow's milk. KAV and PAV strains (1979), both phase I, represent the chronic form of Q fever (QpRS plasmid) and were first isolated from the aortic valves of two separate patients suffering from endocarditis. The Australian QD strain (phase II), was first isolated in Australia from acute human febrile blood. The M44 (phase II) is a variant of the greek "Grita" strain and has been used to develop the attenuated European and Russian vaccines.

3.3.2. Microorganism propagation and cell culture

C. burnetii isolates were propagated in chick embryo yolk sacs and purified by Renografin as previously described¹³⁴. All strains were grown according to the following protocol: embryonated, antibiotic-free, and specific pathogen-free eggs were inoculated with *C. burnetii* at 7 days and incubated for an additional 7-9 days at 37 °C and 98% humidity. The eggs were rocked a minimum of two times per day to increase embryo viability. When candling detected a 50% embryo die-off, the yolk sac of each egg was harvested. Tissue disruption was followed by a series of differential centrifugations,²⁵² Celite absorption, and a final centrifugation through Renografin gradient²⁵³. All of these steps were performed in US biological safety level 3 (BSL3) facilities following strict biosafety protocols. Purified bacteria were enumerated by optical density at 420 nm as previously reported²⁵⁴. Identical cultures were used for every set of experiments performed on different days. In accordance with transfer protocols, and to ensure the safety of investigators using MALDI-TOF MS instrumentation, *C. burnetii* samples were subjected to 2×10^6 rad of gamma radiation before MALDI-TOF MS analysis. This has been shown to completely eliminate *C. burnetii* viability without altering cell-wall morphology or cell-surface antigenic epitopes allowing MALDI-TOF MS data to be later obtained in a non-BSL3 setting²⁵⁵.

3.3.3. Sample preparation

Bacterial suspensions were adjusted to a concentration of 10^{10} organisms μL^{-1} according to the cell count obtained at 420 nm using 50% acetonitrile (ACN) and Milli-Q grade water (Millipore, Billerica, MA) containing 0.1% trifluoroacetic acid (TFA) and

premixed with equal volumes of a saturated (20 mg mL⁻¹) α -cyano-4-hydroxycinnamic acid solution (CHCA; Sigma-Aldrich, St. Louis, MO). MALDI-TOF targets used in this study were 192-well stainless steel plates which were washed with 18 M Ω cm water and allowed to dry at room temperature. When dry, 1.0 μ L of the premixed solution containing the CHCA matrix and the whole bacterial cells was spotted on the plate.

3.3.4. MALDI-TOF MS analysis

Initial mass spectra were acquired in linear and reflectron mode with various matrices as previously described in Shaw et al.¹³⁴. While CHCA, 2,5-dihydroxy benzoic acid (DHB, 1-6 kDa) and sinapic acid (3-25 kDa) were all found to produce optimal spectra in their respective ranges, signal intensities were strongest, and mass spectral peaks were most prominent in the 1-6 kDa range using CHCA, thus this mass range and matrix was selected for marker comparison and PLS-DA modeling applications. Profile mass spectra were acquired on a MALDI-TOF/TOF MS 4700 Proteomics Analyzer (Applied Biosystems, Framlingham, MA) equipped with a diode-pumped Nd:YAG laser (355 nm). Analyses were performed in positive ion mode at an accelerating voltage of 20 kV, and an extraction delay of 2 ns with the data system operating under automatic data acquisition control. The mass scale was calibrated before analysis with peptide/protein calibration mixtures (Applied Biosystems). Profile mass spectra were exported in ASCII format using custom Microsoft Visual Basic for Applications (VBA) macros within the Data ExplorerTM MS software (Applied Biosystems).

3.3.5. Data preprocessing and multivariate analysis

Pure preparations of every individual strain were plated on triplicate target plate wells in order to incorporate into the PLS-DA model the variability innate to MALDI sample preparation and sample analysis, giving a total of 3×7 strains = 21 plate wells analyzed per experiment. This experiment was repeated on 5 separate days to assess the overall method repeatability. A total of 2500 single laser shots were summed into a composite spectrum corresponding to a single x-y position within a well. For each well, four composite spectra with the highest number of ion counts were selected for further analysis. These profile spectra were all preprocessed identically by (a) normalizing to the base peak intensities, (b) applying high-pass filtering to flatten the MALDI baseline signals, (c) smoothing using a two-pass, 21-point Gaussian smooth, (d) denoising²⁵⁶ using a sigma value of 3, and finally, (e) converting to a binary profile format in which any positive intensities were assigned the value of 1. This preprocessing procedure was found to give the best performance and lowest error rates for the statistical algorithms and was an improvement over previous work¹³⁴. After spectral data are binarized, ion abundance information is still preserved within the spectral peak width. A major advantage of this data processing approach is that classical peak detection or peak picking is not required, and that the processed data present less variability than the original MALDI data. The four processed composite spectra from each well were averaged for each of the seven *C. burnetii* strains. Notice that binarization was performed prior to averaging the four composite spectra obtained for each well, in order to capture the MALDI detection variability of each particular mass spectral peak. No further processing was applied to the data. No peak alignment was necessary, as the mass

scale was calibrated prior to each set of measurements (and no significant drifts occurred).

PLS-DA of all spectral data was carried out using MatLab v.7.0 (The MathWorks, Inc., Cambridge, UK) and the PLS Toolbox v.3.5 (Eigenvector Research, Inc., Manson, WA). Complete preprocessed profile mass spectra were used for PLS-DA. Spectra from days 1 to 4 constituted the training set and spectra from a fifth day were used as the test set. In order to ensure a realistic impression of model performance for predicting unknown samples, PLS-DA latent variable decomposition was carried out on the training set using leave-one-out crossvalidation. During crossvalidation, objects were sequentially removed from the training data set and a sub-model based on the remaining objects was used to build a PLS-DA model and predict the left-out objects. Latent variables were chosen at the point where the root mean square error of cross-validation (RMSECV) leveled.

Two different PLS-DA models were created, one for the identification of *C. burnetii* at the strain and one at the phase level. Model I (strain level) was composed of seventy-two runs (training objects) in six strain classes: Class 1: 12 x NM I, Class 2: 12 x Australian QD, Class 3: 12 x M44, Class 4: 12 x Ohio, Class 5: 6 x KAV and 6 x PAV, Class 6: 12 x Henzerling. Model II (phase level) was composed of seventy-two runs in two classes. Class 1 was composed as follows: 48 x phase I objects corresponding to the following strains: NM I (12 objects), Henzerling (12 objects), Ohio (12 objects), KAV (6 objects), PAV (6 objects) and Class 2: 24 x phase II objects: Australian QD (12 objects), M44 (12 objects).

To assist in interpreting the results of the PLS-DA models, an in-house peak detection algorithm was used to extract the most intense peaks from the dataset. This peak list's function was independent of that for model building and was constructed solely for investigative purposes.

3.4. Results and Discussion

3.4.1. Characteristics of MALDI-TOF MS mass spectra of different *C. burnetii* strains

Seven *C. burnetii* strains were analyzed by MALDI-TOF MS and PLS-DA. The 1-6 kDa region showed the mass spectral signals with the best signal-to-noise ratio, and was considered the most appropriate range for attempting to classify this organism. Average MALDI-TOF MS spectra for each of the seven strains collected on day 1 are shown in Figure 3-1.

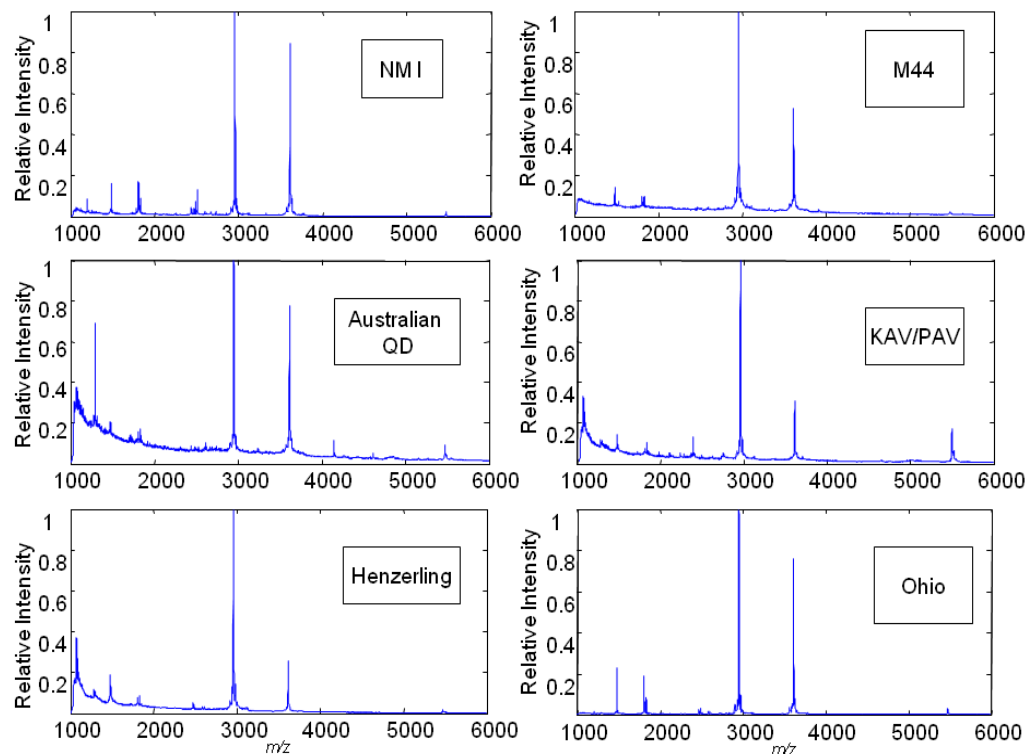


Figure 3-1 Average MALDI-TOF MS spectra of purified *C. burnetii* cultures by strain for day one. Intensity was normalized to the base peak at $m/z = 2951$.

Solely for exploratory purposes, the most intense peaks from each strain were compared using an independent peak detection algorithm. Table 3-1 lists subsets of m/z values that present mass spectral peaks common to the *C. burnetii* species and Table 3-2 lists subsets of m/z values that represent mass spectral peaks that were only observed in a given strain.

Table 3-1 Mass spectral peaks in the range of 1-6 kDa for *C. burnetii* (species-selective spectral signals common to all *C. burnetii* strains)

1829
2951
3612

Table 3-2 Mass spectral peaks in the range of 1-6 kDa for *C. burnetii*^a (strain-specific spectral signals unique to all *C. burnetii* strains)

NMI	1196 (14)
Aus	1292 (30)
KAV/PAV	1348 (7)
KAV/PAV	1362 (9)
KAV/PAV	1372 (7)
KAV/PAV	1385 (5)
M44	1526 (4)
NMI	1780 (8)
NMI	1816 (3)
KAV/PAV	2108 (5)
KAV/PAV	2237 (5)
KAV/PAV	2367 (4)
KAV/PAV	2389 (13)
NMI	2437 (8)
NMI	2504 (27)
NMI	2672 (3)
KAV/PAV	2748 (6)
NMI	3331 (5)
M44	3573 (4)
Aus	4139 (20)
KAV/PAV	5499 (81)
KAV/PAV	5519 (23)
KAV/PAV	5539 (8)

^aMasses are expressed in Da and represent $[M+H]^+$ ions. Signals lower than a cut-off threshold of 3% relative intensity were discarded. Averaged percent relative intensities for days 1-4 are shown in parentheses.

Previous work¹³⁴ reported the presence of NM I biomarkers with m/z of 1829, 2504, 2951, 3612 and 5470. Intense signals at m/z 1829, 2951 and 3612 were common to all *C. burnetii* strains investigated here, whereas the signal at m/z 2504 is only detected for NM I. The signal at m/z 5470 previously detected in NM I¹³⁴ was also detected for the Australian QD, Henzerling, M44 and Ohio strains. No distinct mass spectral features that differentiated the KAV and PAV strains were detected. It is important to note that PLS-DA uses the full mass spectral profile, not a peak list, and thus, no peak picking is necessary prior to modeling.

Reproducibility of MALDI-TOF MS spectra, particularly variations in signal intensity, is an important concern that can adversely affect mass spectral fingerprinting approaches to microbial identification. Tables 3-3 and 3-4 detail the intra- and inter-well variability encountered in *C. burnetii* MALDI-TOF MS data following base peak normalization, and the mean intensity differences observed between the days included in the training set. As can be observed (Table 3-3), intra-well variability can be significant, due to the presence of sample “sweet-spots”, produced during the co-crystallization process with the MALDI matrix. Upon averaging of composite spectra, inter-well variability was considerably reduced (Table 3-4). Although significant inter-day differences in the mean percent relative intensities were still observed after composite spectra averaging, the remaining inter-day mean intensity differences were successfully mitigated after MALDI data denoising and binarization and soft PLS-DA modeling, to the extent of not precluding from correctly classifying *C. burnetii* strains, as discussed below.

Table 3-3 Intra-well variability and mean peak intensities observed in *C. burnetii* MALDI-MS spectral data. Four composite spectra (n=4) were acquired per well. Each composite spectrum was the sum of 2500 laser shots.

		Mean Percent Relative Intensities normalized to <i>m/z</i> 2951 (%CV intra-well)			
		<i>m/z</i> = 1478	<i>m/z</i> = 1808	<i>m/z</i> = 1829	<i>m/z</i> = 3612
Day 1					
n = 4	well 1	48.4 (46.3)	33.7 (11.0)	11.5 (52.0)	86.3 (25.9)
n = 4	well 2	36.8 (29.3)	22.7 (25.5)	10.0 (39.9)	76.0 (21.4)
n = 4	well 3	46.1 (20.9)	24.6 (26.1)	16.2 (19.7)	91.3 (13.4)
Day 2					
n = 4	well 1	13.8 (26.2)	7.2 (32.1)	17.9 (11.7)	69.5 (26.6)
n = 4	well 2	10.3 (25.3)	4.2 (24.0)	16.2 (56.7)	52.7 (10.7)
n = 4	well 3	10.0 (57.7)	5.3 (40.7)	21.8 (11.9)	50.8 (17.4)
Day 3					
n = 4	well 1	13.2 (21.3)	1.0 (N/A)	26.8 (27.4)	48.4 (8.5)
n = 4	well 2	14.3 (4.6)	4.7 (41.8)	19.4 (31.9)	42.3 (9.6)
n = 4	well 3	16.2 (42.4)	4.9 (35.8)	19.6 (15.4)	40.4 (40.0)
Day 4					
n = 4	well 1	62.7 (26.2)	33.2 (10.5)	17.3 (39.7)	74.8 (6.3)
n = 4	well 2	52.6 (11.4)	25.7 (19.6)	11.6 (19.2)	74.5 (12.3)
n = 4	well 3	44.0 (13.6)	22.5 (13.9)	10.5 (38.9)	82.1 (11.7)

Table 3-4 Inter-well (n=3 wells) and inter-day variability in MALDI-MS data. The spectrum from each well was obtained by averaging four composite mass spectra.

		Mean Percent Relative Intensities (%CV)			
		<i>m/z</i> = 1478	<i>m/z</i> = 1808	<i>m/z</i> = 1829	<i>m/z</i> = 3612
Day 1					
	n = 3	43.8 (14.0)	27.0 (21.8)	12.6 (25.4)	84.5 (9.2)
Day 2					
	n = 3	11.4 (18.8)	5.6 (27.6)	18.6 (15.3)	57.6 (17.9)
Day 3					
	n = 3	14.6 (10.3)	3.5 (63.3)	21.9 (19.1)	43.7 (9.5)
Day 4					
	n = 3	53.1 (17.6)	27.1 (20.1)	13.1 (27.9)	77.1 (5.6)

3.4.2. Partial least squares modeling of *C. burnetii* MALDI-TOF MS data at the strain level (Model I)

A strain-level PLS-DA model was first created using the full preprocessed mass spectral profiles. Initial attempts to distinguish by PCA between all *C. burnetii* strains using the MALDI-TOF MS data with identical preprocessing was unsuccessful with an explained variance of only 80.15% for a four principal component model. No clear clusters grouping each strain were observed, with samples from the same strain, which were collected on different days placed on different clusters (Figure 3-2).

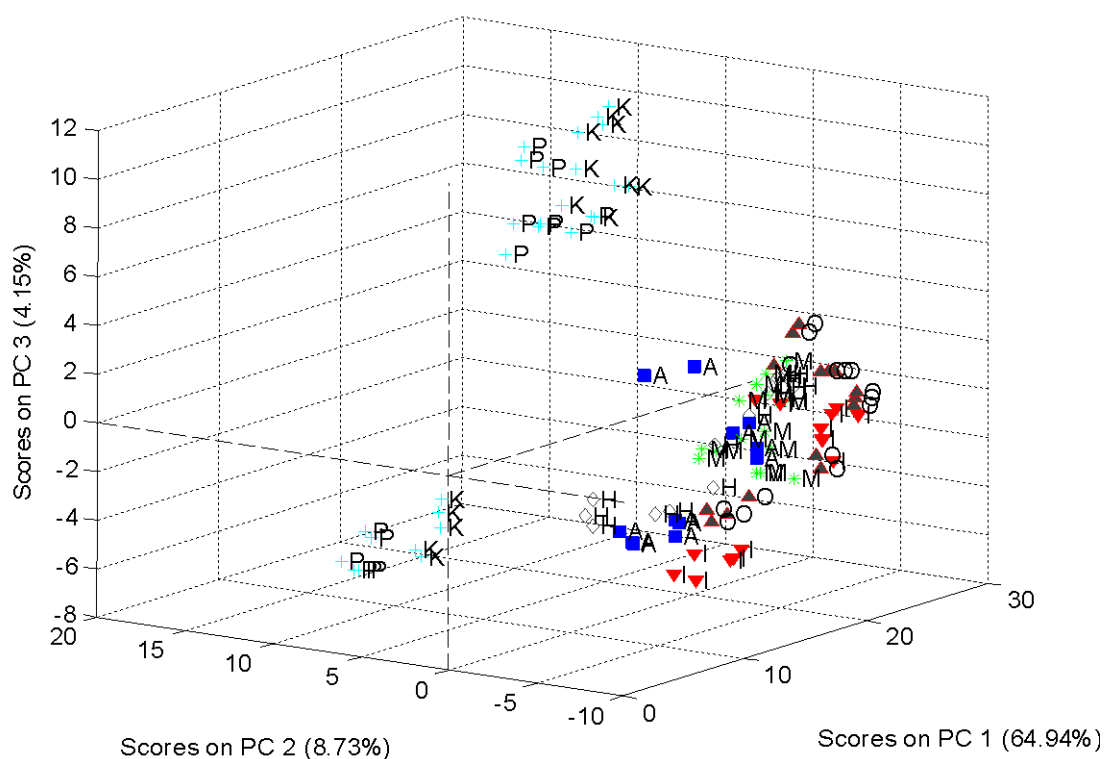


Figure 3-2 PCA scores plot for MALDI-TOF MS *C. burnetii* data. The symbol labels are as follows: I=Nine Mile I, M=M 44, A=Australian QD, K-P=KAV/PAV, H=Henzerling, O=Ohio.

We followed by investigating a single PLS-DA model to classify all strains (PLS2-DA, multivariate Y-block). The KAV and PAV strains were considered members of a single class, due to their high degree of spectral similarity. Figure 3-3 describes the effect of adding an increasing number of LVs to this PLS-DA model under crossvalidation conditions. The optimum number of LVs was chosen to simultaneously maximize the percentage of explained systematic variation in the data while minimizing the influence of MALDI variability reflected in Tables 3-3 and 3-4.

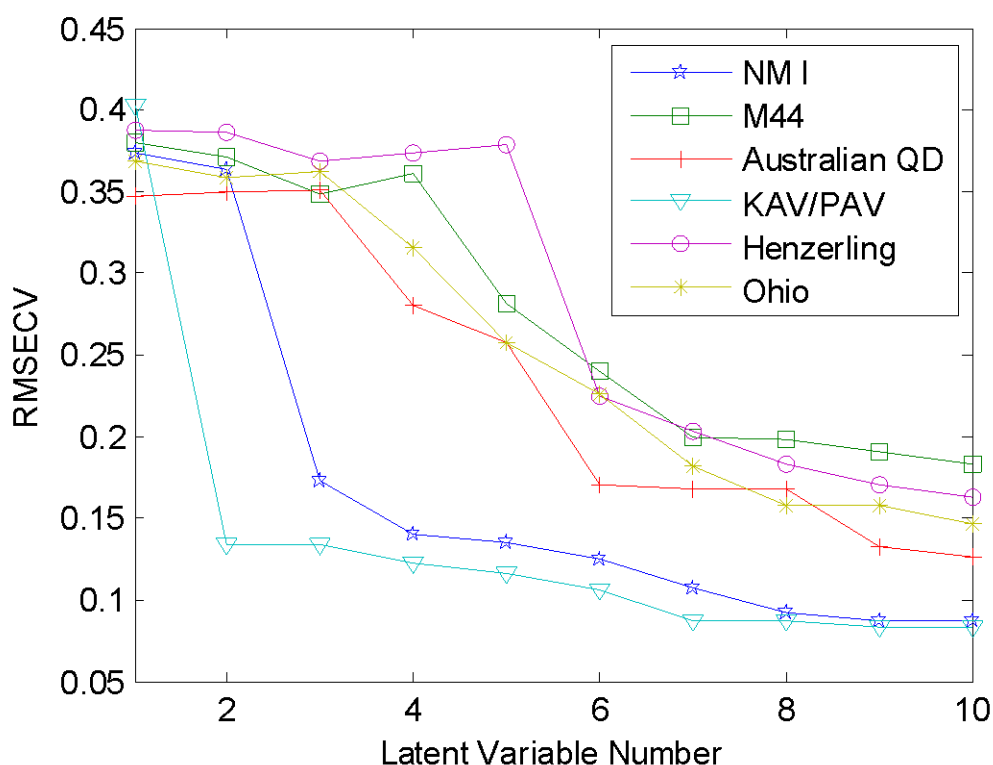


Figure 3-3 Root mean squared error of crossvalidation (RMSECV) as a function of the number of LVs added to the PLS-DA Model I (strain level model). Leave-one-out crossvalidation was used. The optimum number of LVs chosen was 8.

Figure 3-3 indicates that the KAV/PAV and NM I classes behaved differently than the remaining classes. In the case of the KAV/PAV class, predictive models with RMSECV lower than 0.15 were obtained with as low as two LVs. On the same trend, it was possible to classify the NM I strain with as low as four LVs. A second inspection of a selection of unique markers from these two strains (Table 3-2) suggests that the differences in ease of classification can be attributed to differences in their MALDI fingerprints, as both of these strains show the highest number of strain-specific peaks (7 and 12, respectively) and that Table 2, which was manually compiled for investigational purposes, was useful in evaluating PLS-DA model performances and trends that are seen among strains. After binarization, the complete signal profile centered around those

peaks is used by PLS-DA. The remaining M44, Australian QD, Henzerling, and Ohio strains required between six and eight LVs, a number larger than that for KAV/PAV and NM I. The selected 8-LV PLS-DA model captured more than 92% of the Y-block variance of the training data set under crossvalidation.

Crossvalidation was followed by external validation, i.e. prediction of an independent test set not analyzed during model building. The 8-LV PLS-DA Model I was successful in classifying all six strain classes present in the *C. burnetii* test set, correctly placing 20 out of 21 test objects, with only one false negative. Figure 3-4 presents the classification results for six *C. burnetii* strain classes.

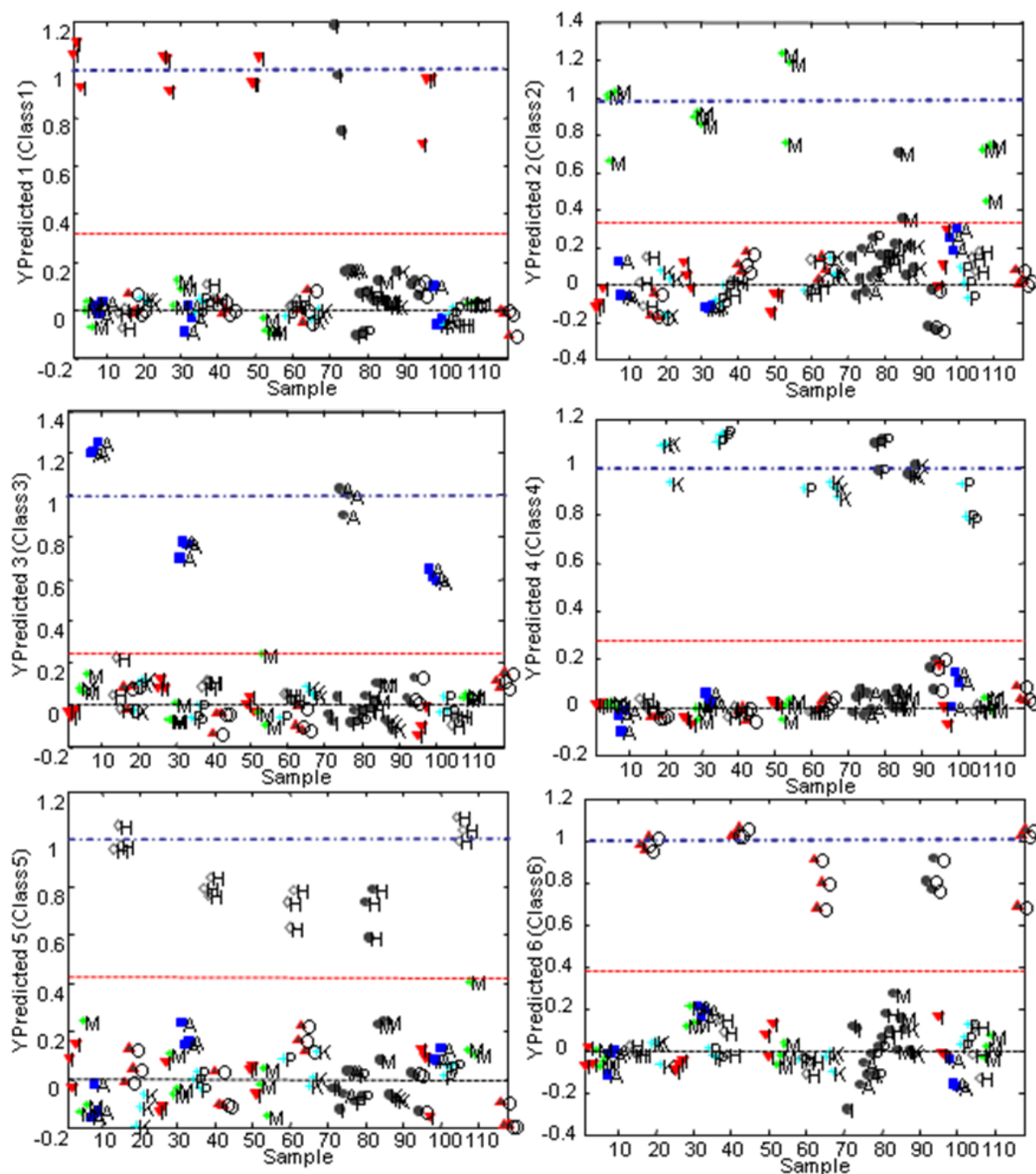


Figure 3-4 Y-predicted value as a function of sample number for six *C. burnetii* strain classes. The filled circular symbols correspond to objects used as unknowns in the test set. Test set objects have been marked with its own class label to demonstrate the PLS-DA model's accuracy to discriminate at the strain level (I=Nine Mile I, M=M44, A=Australian QD, K-P=KAV/PAV, H=Henzerling, O=Ohio). All other objects were used as part of the training set. The dashed red line represents the classification decision threshold. Unknown samples falling above this threshold have a statistically-significant probability of belonging to the same class as the corresponding training objects.

The decision threshold shown in each case (middle dashed line), is calculated using the distribution of predicted Y values obtained during model building. The observed dispersion of individual samples around the Y=1 line at the top of each plot is a measure of the inter-day and inter-well MALDI variability of the preprocessed data. During the PLS-DA model building stage (training), the Y value for each object is assigned as either 0 or 1, depending on class membership. The observed Y value after crossvalidation, may differ from the expected Y=1 value, reflecting the goodness of fit, and thus a Y prediction threshold based on Bayesian statistics²⁴⁸ is used to make a decision as to whether a future unknown would belong to a given class or not. During prediction of the test set, each sample which is a member of the correct strain class would be placed above the decision line and as close as possible to the Y-predicted value of 1 (one). Inversely, each sample not a member of the expected class would be placed below the threshold line and close to 0 (zero). In this ideal case, the discrimination between the classes in the test set would be completely accurate. As seen in Figure 3-4, the test objects were placed above the decision threshold line in most cases. PLS-DA sensitivity and specificity were 100% in all cases, except for the M44 strain (75% sensitivity, 100% specificity), which shows a larger dispersion on the Y-predicted axis. The high degree of success of this PLS-DA model is caused by its ability to separate the information required to discriminate between classes from the MALDI variability still remaining in the data after preprocessing, as shown in Figure 3-5. This variability is captured in LVs not used to build the model, and encompasses the remaining 8% of the overall Y-block variance observed under crossvalidation.

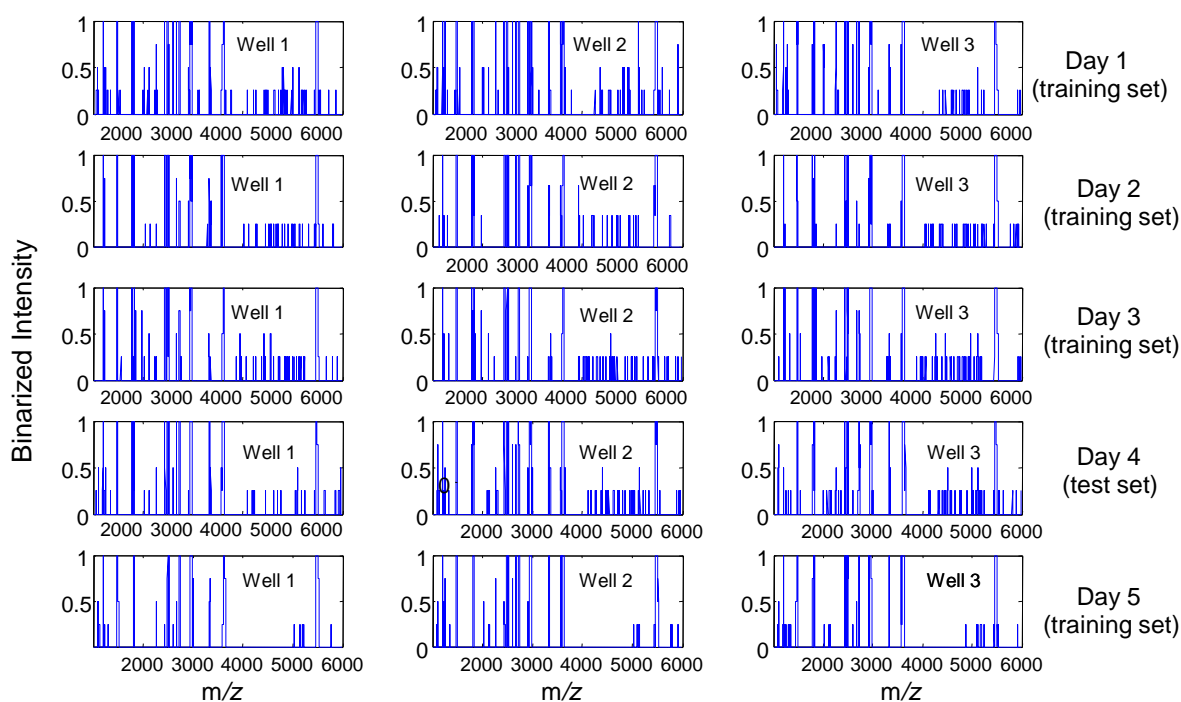


Figure 3-5 Preprocessed (normalized, smoothed, denoised, binarized and averaged) mass spectral data used for building PLS-DA Model I (strain level). The data shown corresponds to the Nine Mile I strain samples.

Only one false negative result was observed for one of the M44 test samples (i.e. this particular sample was placed below the threshold line). The MALDI-TOF MS mass spectrum for this sample was carefully investigated, but no significant spectral differences were found when compared with the other two M44 samples run on the same day and no clear instrumental sources of variability were detected. Thus this sample was not discarded from the test set. As noted by Wahl et al., classification of microorganisms at the strain level poses one of the main challenging tasks in microbial taxonomy by MS²³⁶, particularly, if the investigated microorganisms do not present strongly-distinctive features such as the M44 strain.

3.4.3. Partial least squares modeling of *C. burnetii* MALDI-TOF MS data at the phase level (Model II)

Due to the success of the strain-level model, a second classification scheme was explored, which would have the ability to distinguish antigenic phase differences between the strains investigated in this study. Figure 3-6 shows the RMSECV as a function of LV number for Model II. With only 4 LVs, model II produces an RMSECV equal to 0.2, and an explained Y-variance of 95.95%.

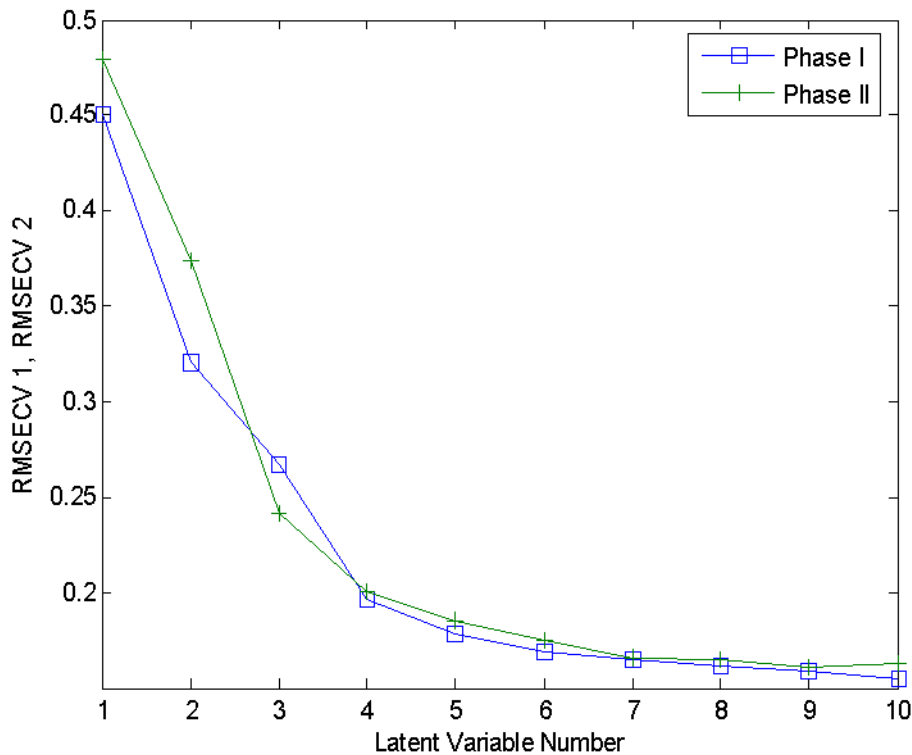


Figure 3-6 Root mean squared error of crossvalidation (RMSECV) as a function of the number of LVs added to the PLS-DA Model II (phase level model). Leave-one-out crossvalidation was used. The optimum number of LVs chosen was 4.

Model building was followed by the prediction of an independent test set. Figure 3-7 shows the predicted class membership for each unknown sample. All phase I unknown samples (NM I, KAV/PAV, Henzerling and Ohio) were correctly classified, whereas all

the Australian QD and most of the M44 unknowns (except for one false positive) were correctly placed below the threshold line. A statistical sensitivity of 100% and specificity of 83% were observed.

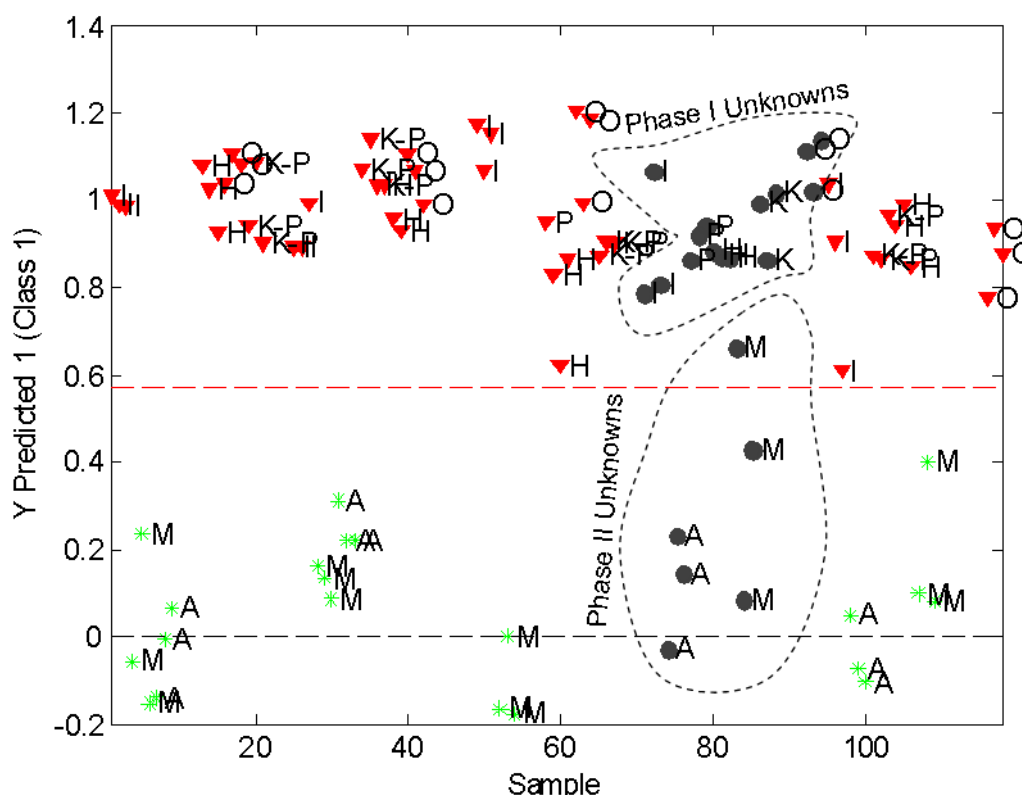


Figure 3-7 Y-predicted value as a function of sample number for different *C. burnetii* antigenic phases. The filled circular symbols correspond to objects used as unknowns in the test set. Unknown samples falling above the decision threshold have a statistically-significant probability of belonging to class I (phase I), whereas objects below the line, most probably belong to class II (phase II). The symbol labels are as follows: I=Nine Mile I, M=M44, A=Australian QD, K-P=KAV/PAV, H=Henzerling, O=Ohio.

The PLS-DA scores on different LVs for different strains and the loadings of the m/z variables on each LV contain valuable information regarding the regions of the mass spectrum that contribute to distinguish between classes. Because whole m/z regions, not peak maxima, are used to differentiate between classes, it was investigated which m/z regions were given more weight in PLS-DA Model II for classifying a given sample as phase I or II. Figure 3.8 shows a score plot of LV 2 vs. LV 4. A positive score on LV 2

greater than 2.7 discriminates phase II samples from phase I samples. Upon inspection of the LV 2 loadings (Figure 3-9, top panel), it is found that several spectral regions have positive loadings in this latent variable. In particular, some variable regions show large positive contributions for LV 2, in coincidence with mass spectral signals in the regions with m/z 1286-1300, 1450-1532, and 3564-3644 (highlighted as A, B and C respectively in Figure 3-9, top panel). These spectral regions coincide with mass spectral features that are observed only for the M44 or Australian QD strains, but not for Nine Mile I, Henzerling, Ohio, KAV and PAV strains, as shown in Table 3-2. Positive loading contributions were also observed for the 5439-5488 m/z region (region “D”, Figure 3-9, top panel).

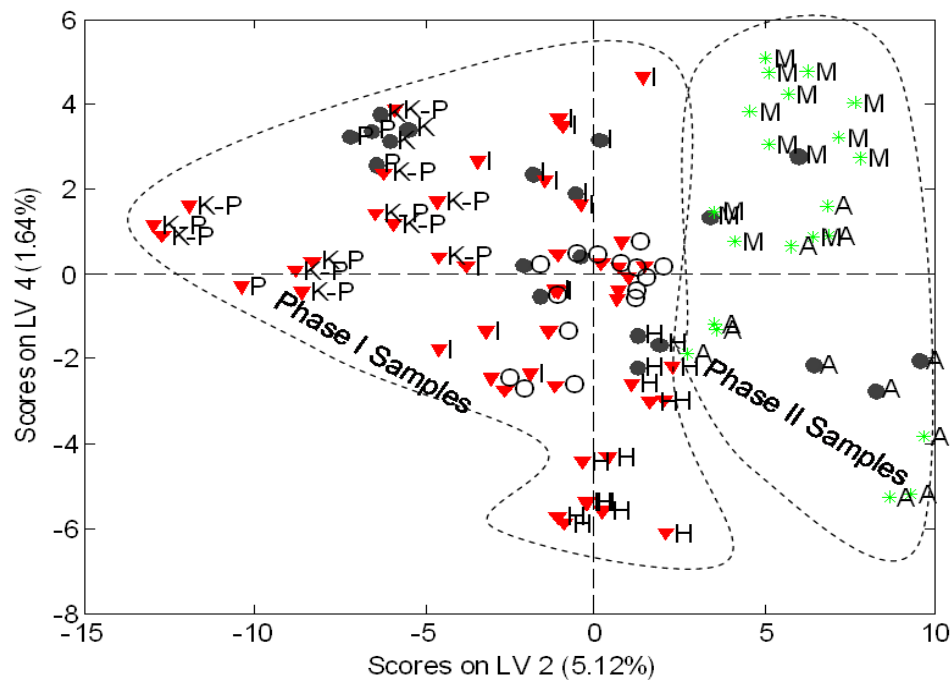


Figure 3-8 Scores plot (LV 2 vs. LV 4) for PLS-DA Model II (phase level model). The symbol labels are as follows: I=Nine Mile I, M=M44, A=Australian QD, K-P=KAV/PAV, H=Henzerling, O=Ohio. The explained Y-variance for each latent variable is expressed between parentheses.

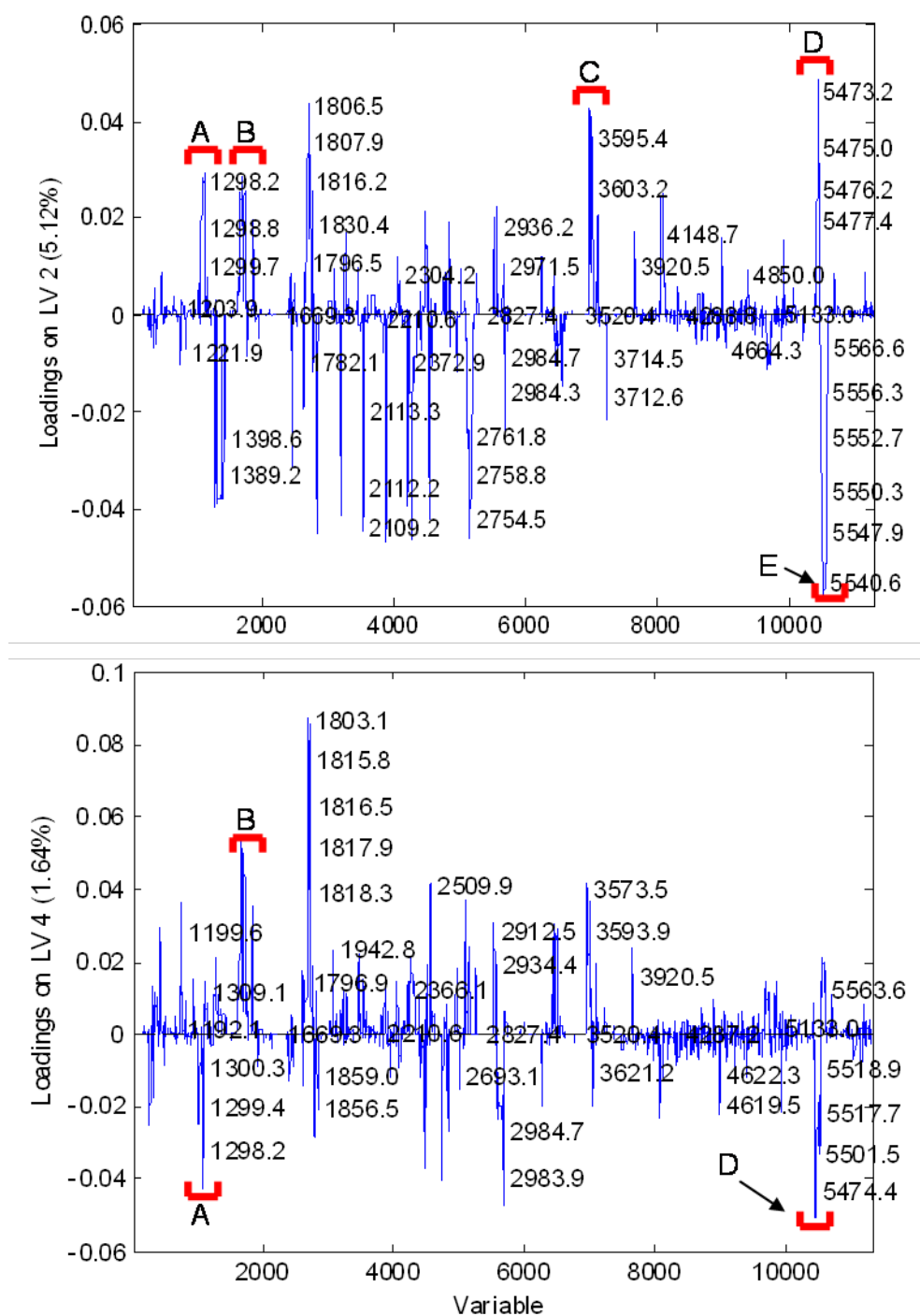


Figure 3-9 Loadings for latent variable 2 (top) and 4 (bottom) in PLS-DA Model II. The highlighted mass-to-charge regions correspond to: A=1286-1300, B=1450-1532, C=3564-3644, D=5439-5488, E=5488-5566.

As shown in detail in Figure 3-10, the Australian strain (phase II) presents the most intense mass spectral features in that range. Large negative LV 2 loadings were observed in the m/z 5488-5566 region (region “E”, Figure 3-9, top panel). This coincides with intense features for the KAV/PAV strain group (Figure 3-10). It is important to emphasize that although the mass spectral data are binarized, intensity information is still preserved, as more intense mass spectral peaks, translate into broader features after binarization, and it is thus natural to observe larger loading values in those spectral regions with more prominent features. In other words, negative loadings in the m/z 5488-5566 region imply that the phase II strains are distinguished from the markedly different KAV/PAV phase I strain class by their almost complete absence of signals in that range.

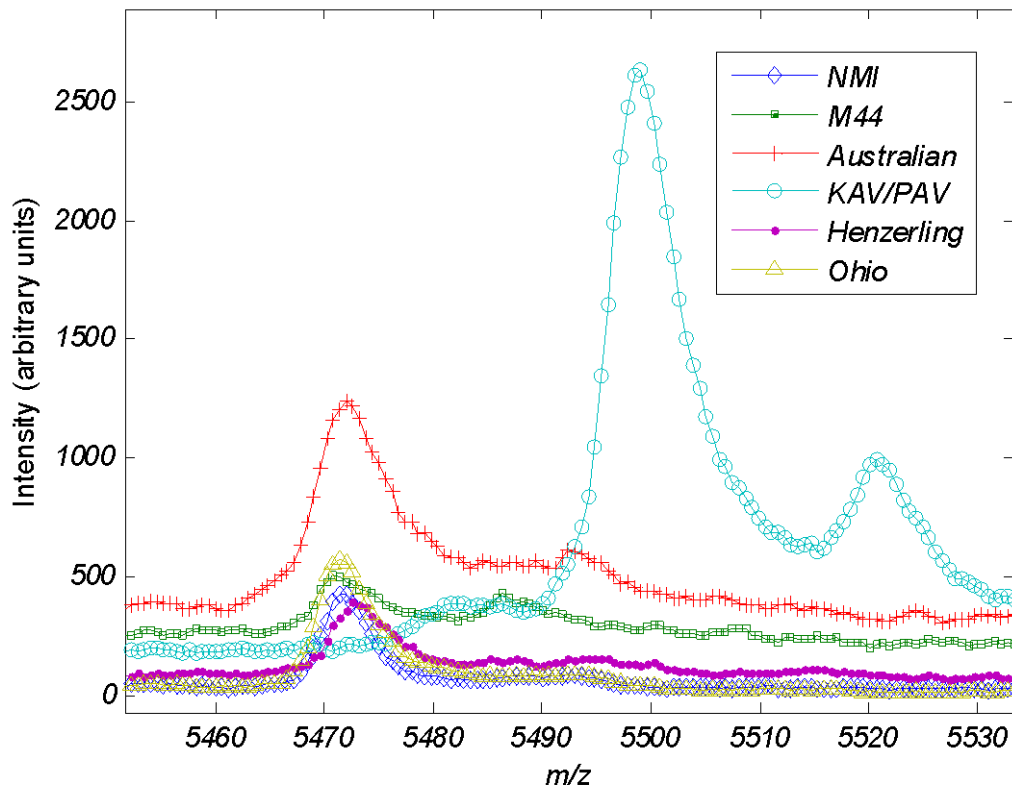


Figure 3-10 Detail of the mass spectral region between m/z 5420 and 5560. The spectra shown correspond to the first day of experiments.

The intra-class differences between phase II objects belonging to the M44 and Australian QD strains are modeled by LV 4. Although there is a certain degree of overlap between both strains, most M44 objects score positively on this LV, while most of the Australian QD objects score negatively (Figure 3-8). The loadings for LV 4 show a negative contribution from the m/z 1286-1300 region and a positive contribution from the region with m/z 1450-1532 (Figure 3-9), bottom panel, regions “A” and “B” respectively). This implies that within the phase II class, M44 samples can be distinguished from the Australian QD samples by the absence of features in the m/z 1286-1300 region, and the presence of mass spectral features in the m/z 1450-1532 region. The sign of the LV 4 loadings in the m/z 5420-5560 region is negative, opposite to the sign observed for the LV 2 loadings in the same variable range (Figure 3-9, region “D”). Samples from the Australian QD strain, which score negatively on LV 4 (Figure 3.8), y-axis), show more intense spectral features in the 5439-5488 range than the M44 samples (Figure 3-10), and thus negative LV 4 loadings serve the purpose of separating between these two strains.

3.5. Conclusions

The feasibility of using MALDI-TOF MS in combination with PLS-DA modeling for the rapid confirmation of the identity of purified cultures of the *C. burnetii* pathogen to the strain level has been demonstrated. PLS-DA’s performance was compared to that of PCA. Although both methods provided a fast and straightforward approach for data interpretation, PLS-DA modeling routinely achieved higher percentages of explained Y-

variance, specificity, and sensitivity. Even though these strains are closely related, they could be differentiated on the basis of their mass spectral differences which were modeled by PLS-DA. The KAV and PAV isolates were found to be identical, in agreement with the fact that both of these isolates were from aortic heart valves of humans with endocarditis, with the KAV strain isolated in Oregon in 1976 and the PAV strain from California in 1979. Therefore, the similarity between these two isolates was not surprising. For the spectral dataset studied in this work, results indicate that decomposition of the denoised and binarized mass spectra into latent variables generates robust models that can be later used for prediction of unknowns without the need for reanalyzing training samples or applying spectral correction methods. These results encourage us to pursue, in the future, the investigation of strains not yet characterized with this method (such as NM phase II) and to investigate the applicability of higher-order PLS approaches to samples containing mixtures of different *Coxiella* strains or other concomitant microorganisms. Additional future experiments include the application of PLS-DA pattern recognition to data sets from two similar MALDI TOF instruments from the same manufacturer, and to datasets obtained under different culture conditions.

CHAPTER 4. RAPID DETECTION OF STAPHYLOCOCCUS AUREUS USING ^{15}N -LABELED BACTERIOPHAGE AMPLIFICATION COUPLED WITH MATRIX-ASSISTED LASER DESORPTION/IONIZATION TIME-OF-FLIGHT MASS SPECTROMETRY

4.1. Abstract

This chapter describes a novel approach to rapid bacterial detection using an isotopically labeled ^{15}N bacteriophage and MALDI-TOF MS. Current phage amplification detection (PAD) via mass spectrometric analysis is limited because host bacteria must be inoculated with low phage titers in such a way that initial infecting phage concentrations must be below the detection limit of the instrument, thus lengthening incubation times. Additionally, PAD techniques cannot distinguish inoculate input phage from output phage which can increase the possibility of false positive results. This chapter describes a rapid and accurate PAD approach for identification of *S. aureus* via detection of bacteriophage capsid proteins. This approach uses both a wild-type ^{14}N and a ^{15}N – isotopically labeled *S. aureus*-specific bacteriophage. High ^{15}N phage titers, above the instrument's detection limits, were used to inoculate *S. aureus*. MALDI-TOF MS detection of the ^{14}N progeny capsid proteins in the phage-amplified culture indicated the presence of the host bacteria. Successful phage amplification was observed after 90 min incubation. The amplification was observed by both MALDI-TOF MS analysis and by standard plaque assay measurements. This method overcomes current limitations by

improving analysis times while increasing selectivity when compared to previously reported PAD methodologies.

4.2. Introduction

S. aureus is an important human pathogen³⁰ that is the leading cause of community-acquired infections³²⁻³⁴. The severity of *S. aureus* infections varies from local benign wounds to severe systemic diseases²⁵⁷. *S. aureus* is the dominant species recovered in positive blood cultures²⁵⁸ and is responsible for a high burden of disease in healthcare and hospital settings^{259, 260}. Early diagnosis is central for infection control and may lead to decreased morbidity and mortality, reduced transmission, shortened hospital stays, and lower hospitalization costs^{39, 40}. Because of *S. aureus*'s increasing prevalence and its association with severe infection and high mortality rates, rapid testing methodologies have been recently developed to aid in efforts to reduce bacterial transmission and limit the spread of disease.

Existing conventional methods, such as traditional culture-based assays, have significant turnaround times (2–4 days) before final results are available. However, implementation of rapid detection techniques has shown to provide results reporting in hours^{30, 260}. Existing rapid methods either eliminate the need for primary culture—the time-limiting step—or shorten the incubation times when compared to traditional procedures³⁰. Rapid molecular methods without culture for identification of *S. aureus* are primarily PCR-based (quantitative and real-time) that allow direct detection from patients' samples with turnaround times in the range of 1 to 5 h. PCR-based methods provide time-saving advantages along with high sensitivity and specificity²⁶¹⁻²⁶³, but can

be impaired by false-positive results requiring confirmation with culture. Rapid culture-based techniques differ from traditional culturing techniques by not relying on detection of discernible colonies growing on primary plates. Rather, rapid culture-based techniques feature shortened and/or modified growth incubation times, coupled with rapid *S. aureus* diagnostic methodologies, and can achieve results in a few hours²⁶⁴⁻²⁶⁶ without the need for additional confirmatory analysis.

The use of phages for bacterial detection is well documented²⁶⁷. Bacteriophages are useful for bacterial detection as they are specific to their target host, self replicate, have extensive shelf lives, are inexpensive²⁶⁸, and are infectious only with metabolically active cells²⁶⁹. More recently, bacteriophage amplification technology has emerged as a means of rapid bacterial detection, using modern protein analytical techniques to monitor changes in sample bacteriophage concentration^{62, 140, 270, 271}. Current phage amplification detection (PAD) techniques are robust, but the progeny phage produced through infection cannot be differentiated from the input parent phage initially added to the sample. For this reason, current techniques must use low-level concentrations of input phage, thus increasing incubation time, increasing detection limits, and allowing for the possibility of false positive results.

MALDI-TOF MS, a well established tool for protein analysis^{106, 272-275}, can readily detect bacteriophage proteins. MALDI-TOF MS has been successful for bacterial identification^{69, 96, 97, 108, 135} but has limitations including data interpretation of complex protein patterns, changes in protein expression with culture techniques, sensitivity, and difficulties with mixed-microorganism community analysis capabilities¹⁰⁸. Bacterial detection via PAD MALDI-TOF MS overcomes some limitations associated with

conventional bacterial MALDI by exploiting the unique attributes of phages for more sensitive and selective mass spectrometric detection. Because phages are robust and have a relatively simple protein constituency, their MALDI MS spectra are less dependent on factors that commonly influence bacterial protein expression such as sample preparation, growth media, growth time, and growth temperature conditions. When mixed flora and/or complex matrices are present in an unknown sample, bacteriophage amplification is selective for the targeted bacteria, resulting in mass spectra that are easier to interpret¹⁴⁰. The number of infectious plaque-forming units generated per bacterial cell (i.e., burst size) serves as signal amplification in which infected bacterium can release 10–1,000 progeny phages per cell lysis event²⁷⁶, resulting in lower detection limits. Additionally, bacteriophage structures are amenable to MALDI analysis because the outer capsid sheath of the particles is typically constructed of numerous copies of repeat proteins¹⁴⁰, further amplifying the mass spectrometric signal. Because bacteriophages are as ecologically diverse as their bacterial counterparts, a variety of bacteriophages specific for various species of bacteria are available.

A rapid *S. aureus* detection method using *Staphylococcus* bacteriophage 53, grown in ¹⁵N-labeled media, to infect the targeted *S. aureus* strain (ATCC 27694) has been developed. Following exposure, each infected *S. aureus* bacterium mass produces wild-type ¹⁴N progeny from the introduced ¹⁵N phage until a threshold is reached and the cells burst. Detection of the target bacterium is then based on assaying the sample medium for the ¹⁴N progeny phage, which is present only if the target bacterium is present. The benefits of the method are two-fold: (i) incubation times are reduced by infecting *S. aureus* with a high titer of ¹⁵N phage, thus decreasing overall analysis time;

and (ii) by isotopically modifying the bacteriophage, the ^{15}N input phage is distinguishable from the wild-type ^{14}N output phage used for detection, thus enhancing the selectivity of the PAD platform.

4.3. Experimental

4.3.1. *S. aureus* and bacteriophage 53

Stock cultures of lyophilized *S. aureus* (ATCC 27694) and bacteriophage 53 (ATCC 27694-B1) were obtained from the American Type Culture Collection (ATCC, Manassas, VA). All microbiological procedures were performed in a US biological safety level 2 (BSL2) facility following standard biosafety protocols. The initial inoculi of ^{14}N *S. aureus* cells were obtained from cultures grown in tryptic soy broth (TSB) (Bacto™ TSB, BD Diagnostics, Franklin, NJ) by overnight incubation at 37 °C with constant rotation. *S. aureus* concentrations were determined by standard bacterial plate counting; the count yielded an average *S. aureus* concentration of 6.7×10^8 CFU mL⁻¹ (9.8 % CV) from triplicate overnight incubations performed on different days. ^{15}N *S. aureus* cells were grown in Bioexpress Cell Growth Media U- ^{15}N , 98% (Cambridge Isotope Laboratories, Inc., Andover, MA) according to manufacturer's instructions with only minor modifications. Bacteriophages were propagated overnight in their respective hosts. ^{14}N bacteriophage 53 was grown via culture with ^{14}N *S. aureus*. ^{15}N bacteriophage 53 was grown in ^{15}N media with ^{15}N *S. aureus*. Phage were recovered after overnight propagation, centrifuged, (15 min at 5,000 g), and supernatants filtered through an Autovial 0.2 µm PVDF membrane syringeless filter device (Whatman, Inc, Clifton, NJ) to remove any bacterial debris. Stock suspensions were stored at 2-5 °C for further analyses. MALDI bacteriophage detection limits were determined by making serial

dilutions of the phage preparations, centrifuging through 30-kDa molecular weight cutoff filters (Amicon Ultra; Millipore, Billerica, MA), selectively reducing disulfide bonds with 2 μ L of 200 mM tris(2-carboxyethyl)phosphine HCl (TCEP) (Sigma Aldrich, St. Louis, MO) in 0.1 M PBS, and submitting the samples to MALDI-TOF MS analysis.

4.3.2. ^{15}N Bacteriophage 53 infection/amplification

Phage-infected bacterial samples were examined for phage amplification by MALDI-TOF MS and were run in parallel with standard plaque assays. Phage titers presented were determined by standard plaque assay²⁷⁷ that used ATCC 27694 as the bacterial host cell. Standard plaque assay concentrations were compared with acquired MALDI signals to corroborate results. In order to optimize ^{15}N infection conditions, a solvent exchange was performed. A 500 μ L aliquot of the ^{15}N bacteriophage stock solution (8.0×10^8 PFU mL^{-1}) was added to a 30-kDa molecular weight cut-off filter, centrifuged, (5 min at 14,000 g) and washed with 500 μ L of TSB (x2). The ^{15}N phage filtrate (20 μ L) was recovered and resuspended in 400 μ L TSB. To this phage media, 50 μ L of the ^{14}N *S. aureus* (6.7×10^8 CFU mL^{-1}) and 50 μ L of a 100 mM magnesium chloride solution were added to achieve a final infection volume of 500 μ L. The infected medium was incubated at 37 °C with gentle rotation for 5 h. Sampling was conducted from $t = 0$ h to $t = 5$ h at 30 min time intervals. Following incubation, samples were centrifuged (5 min at 10,000 g) to pellet bacteria out of solution. The supernatant was recovered and phage samples were centrifuged with washing (5 min at 14,000 g), using 30-kDa molecular weight cutoff filters and 500 μ L of 1 M ammonium bicarbonate, pH 9 (x3). The filtrate (20 μ L) was recovered, treated with 2 μ L of 200 mM TCEP in 0.1 M

PBS, and incubated at 60 °C for 1 h to cleave disulfide bridges. Following reduction, samples were spotted and analyzed by MALDI-TOF MS. ^{14}N bacteriophage infection was performed almost identically to the ^{15}N infection (*vide supra*). The only required modification was to set the ^{14}N infecting phage titer at 1.0×10^6 PFU mL^{-1} , which was experimentally determined to be below the detection limit of the MALDI instrument.

S. aureus detection limits were determined by ten-fold serial dilutions (6.7×10^7 to 6.7×10^4 CFU mL^{-1}) of bacterial preparations and infection with a fixed bacteriophage concentration of 2.0×10^8 PFU mL^{-1} . The infected bacteria were incubated for 5 h at 37 °C and each concentration was sampled at 1 h time intervals. Samples were prepared for MALDI-TOF MS analysis identically, as described above.

4.3.3. Bioluminescence-based detection assay

After *S. aureus* overnight culture, the cells and bacteriophage 53 were mixed and measured over time using a Biotek Synergy II multiplate detection reader. A luciferase-based assay (BacTiter-Glo™, Promega, Madison, WI) was modified to exclude the lysing agent, thus ensuring that any luminescence signal would be related only to host bacterial cell lysis associated with phage infection. Triplicate aliquots of *S. aureus* culture (20 μL) were dispensed into 96-well plates, followed by 20 μL of bacteriophage 53, 20 μL of luciferase, and 20 μL of 1 M magnesium chloride. Each well's final volume was diluted to 200 μL with TSB. Bacterial controls consisted of cells alone. Results presented are the averages from triplicate samples

4.3.4. Tryptic digest of bacteriophage 53

Phage suspensions (500 μ L) were filtered through a 30-kDa molecular weight cut-off filter with centrifugation (10 min at 14,000 g) and washed with 500 μ L of a 50 mM ammonium bicarbonate solution (x3) to remove TSB. The retentate (~20 μ L) was resuspended in 500 μ L of 50 mM ammonium bicarbonate. A 10 μ L (~172 pmol) aliquot of sequence grade modified trypsin beads (Sigma Aldrich) was added to the phage sample and allowed to incubate overnight at 37 °C with constant rotation. Following digestion, trypsin beads were removed by centrifugation (5 min at 7,000 g).

4.3.5. Nano-LC-MS/MS

Protein identification of digested samples was performed using nano-flow liquid chromatography electrospray ionization tandem mass spectrometry (nano-LC-ESI-MS/MS) followed by database searching. A 5 μ L digested sample was injected onto a Waters NanoAquity liquid chromatography system (Waters Corporation, Milford, MA, USA) utilizing a 100 μ m x 100 mm BEH130 C₁₈ analytical column (1.7 μ m particle size) (Waters Corporation). The aqueous mobile phase (A) consisted of HPLC-grade water with 0.2% formic acid (FA) and 0.005% trifluoroacetic acid (TFA), while the organic phase (B) was acetonitrile (ACN) with 0.2% FA and 0.005% TFA. A gradient profile was used at a flow rate of 400 nL min⁻¹. Initially, the mobile phase consisted of 5 % B and 95 % A. After 5 min, the gradient was ramped to 30% B over the next 100 min, continuing up to 90 % B over the next 5 min and holding for 2 min. After 112 min total run time, the gradient was returned to 5 % B and 95 % A for the next 20 min to equilibrate the column to initial conditions. The total run time was 132 min.

The column eluent was introduced into a Thermo Scientific LTQ-Orbitrap Velos mass spectrometer (Thermo Scientific, Waltham, MA) equipped with an electrospray interface. The LTQ-Orbitrap instrument performed data-dependent acquisition of precursor and product ion spectra. The nominal resolution of the Orbitrap analyzer was set at 60,000 with scan range from m/z 400 to 1600. The top 9 most intense ions were selected for fragmentation; the selection window was set at $m/z = 2$. Conventional collision induced dissociation (CID) was used for ion activation purposes. Dynamic exclusion was enabled with a repeat count of 1 and an exclusion duration of 120 sec. Charge state screening and monoisotopic precursor ion selection were enabled along with charge state rejection, whereby singly charged ions were not selected for MS/MS analysis.

4.3.6. Database searching and protein ID validation

Protein identification was performed by matching acquired peptide tandem mass spectra to theoretical digests found in a protein database. Prior to database searching, MS/MS spectra were converted to Mascot generic format by using Mascot Distiller v.2.3.2.0 (Matrix Science, London, UK). Charge state deconvolution and de-isotoping were not performed. Database searching utilized the Mascot v. 2.2.0 algorithm (Matrix Science, London, UK) with the following parameters: fragment ion mass tolerance of 0.50 Da, parent ion tolerance of 200 ppm, trypsin enzyme, and deamidation of asparagine and oxidation of methionine specified as variable modifications. A database of 24,384 entries was generated by extracting sequences from the National Center for Biotechnology (NCBI) protein database (downloaded on November 8, 2009) that

contained at least one of the following strings in the entry description; “staphylococcus phage”, “aureus”, “trypsin”, “keratin”.

To validate MS/MS-based peptide and protein identification, Scaffold v. 3.00.02 (Proteome Software Inc., Portland, OR) with PeptideProphet²⁷⁸ and ProteinProphet²⁷⁹ algorithms was used. Peptide identifications were accepted if they could be established at greater than 95.0% probability as specified by PeptideProphet™. Protein identifications were accepted if they could be established at a 99.0% probability based on ProteinProphet™ and if they contained at least 3 peptide matches. Proteins containing similar peptides and that could not be differentiated based on MS/MS analysis alone were grouped as a single match.

4.3.7. MALDI-TOF MS analysis

A matrix solution consisting of 20 mg mL⁻¹ ferulic acid in a 17:33:50 (v/v) mixture of formic acid, acetonitrile, and deionized water was used for all analyses. MALDI-TOF MS samples were spotted onto a 192-spot MALDI plate (Applied Biosystems, Framingham, MA). Mass spectra of each spot were acquired by scanning from 25 kDa to 40 kDa in linear positive ion mode on an Applied Biosystems 4800 MALDI-TOF/TOF mass spectrometer equipped with a UV nitrogen laser (337-nm, 30 ns pulse width). Each sample was spotted in triplicate and each spectrum stored was an average of 6000 accumulated laser shots.

4.4. Results and Discussion

Unambiguous identification of a bacteriophage biomarker protein is a necessary PAD requirement. Figure 4-1a shows MALDI-TOF MS spectra of bacteriophage 53 after filtration of the bacteriophage lysate using a 30 kDa molecular weight cutoff filter. A significant $[M+H]^+$ peak is observed at 35.04 kDa. Plaque assays of the filter retentate showed that the molecular weight cutoff filter retains intact, viable bacteriophage 53. MALDI-TOF MS analyses of filtered preparations containing solely *S. aureus* showed no significant peaks in the mass range near 35.04 kDa. The 35.04 kDa signal was identified by digesting the filter retentate with trypsin followed by LC-MS/MS analysis and database searching using the MASCOT algorithm. MASCOT results revealed that the highest scoring protein of the digested bacteriophage sample was gi|66395381, labeled as “ORF011” of “Staphylococcus phage 53” and a “major head protein”. A total of 12 unique peptides were identified as belonging to gi|66395381 after validation, resulting in 47% sequence coverage. The identification of this protein corroborated the predicted outcome that detection of a major head protein of bacteriophage can be expected by use of MALDI-TOF MS. While the dominant peak in Figure 4-1a is 35.04 kDa, as opposed to the calculated molecular weight of gi|66395381 at 36.8 kDa, it is important to note that the database results are theoretical calculations of the precursor form that use the entire amino acid compositions based on genome sequencing and do not reflect modifications made subsequent to translation. Thus, through combining MALDI-TOF MS analysis with the LC/MS/MS results and the labeling experiments (*vide infra*), confidence was attained that the MALDI analysis accurately reflects a bacteriophage 53 biomarker.

Figure 4-1b shows MALDI-TOF MS spectra of the ^{15}N -labeled bacteriophage generated by growing bacteria and phage in ^{15}N growth media. An $[\text{M}+\text{H}]^+$ peak similar to that seen in the wild-type bacteriophage is observed at 35.46 kDa, a mass shift of 420 Da. Using the amino acid sequence of the precursor gi|66395381, there are 428 possible nitrogen atoms in which a ^{15}N may replace a ^{14}N ; thus, the experimentally observed mass shift of 420 Da is consistent with a mature ^{15}N labeled head protein of bacteriophage 53. Further, LC-MS/MS analysis of a tryptically-cleaved ^{15}N -labeled bacteriophage preparation coupled with a MASCOT search using 15.0001 Da as the molecular weight of nitrogen returned gi|66395381 as the protein with the highest score. Additionally, database searching identified 14 tryptic peptides from the ^{15}N labeled bacteriophage preparation that matched the homologous counterparts in the wild-type ^{14}N bacteriophage.

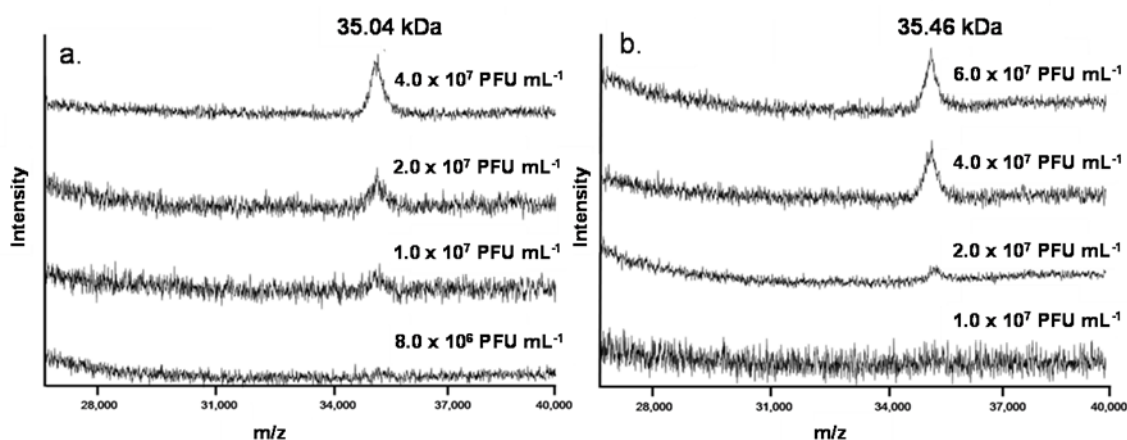


Figure 4-1 MALDI-TOF MS spectra of capsid protein peaks for (a) ^{14}N cultured bacteriophage 53 and (b) ^{15}N cultured bacteriophage 53 as the 35.04 and 35.46 kDa biomarkers, respectively, approach the instrument's detection limit. Samples were spotted in triplicate, and each mass spectrum corresponds to 6000 accumulated laser shots. Data were acquired in the 25,000 to 40,000 m/z range.

Standard PAD MS-based methods require establishment of the instrument's detection limit for the phage preparation being used^{140, 270}. Figures 4-1a and 4-1b show

MALDI-TOF MS spectra of the dilution series for the wild-type ^{14}N bacteriophage and the ^{15}N labeled bacteriophage. The MALDI-TOF mass spectra for the ^{15}N -labeled bacteriophage exceed the signal-to-noise (S/N) = 3 threshold between 4.0×10^7 PFU mL^{-1} and 2.0×10^7 PFU mL^{-1} while the ^{14}N wild type spectra exceed the S/N = 3 threshold between 2.0×10^7 PFU mL^{-1} and 1.0×10^7 PFU mL^{-1} . Because standard PAD methods require the initial concentration of input phage to be distinguishable from newly amplified phage, these experiments would require an initial ^{14}N phage concentration below 1.0×10^7 PFU mL^{-1} .

On the basis of the detection limits derived from the results shown in Figure 4-1a, a conventional PAD experiment was conducted wherein the starting bacterial concentration was 6.7×10^7 CFU mL^{-1} and the starting ^{14}N bacteriophage concentration was 1.0×10^6 PFU mL^{-1} . Figure 4-2 shows MALDI-TOF mass spectral time series obtained at 30 min intervals. From $t = 0$ min through $t = 120$ min, only background signal was observed, and the ^{14}N phage protein was not detectable (Figure 4-2a, 4-2b). At $t = 150$ min, a weak signal consistent with the ^{14}N phage capsid protein peak begins to emerge (Figure 4-2c), indicative of progeny phage amplification; however the signal is weak, and falls below the method's detection limit. At $t = 180$ min, the 35.04 kDa protein signal has intensified so that it can be unambiguously detected (Figure 4-2d). At $t = 210$ min and $t = 240$ min, the ^{14}N progeny phage biomarker dominates the spectra (Figure 4-2e, 4-2f). Therefore, for this set of experimental conditions, detection of *S. aureus* can be achieved at 180 min.

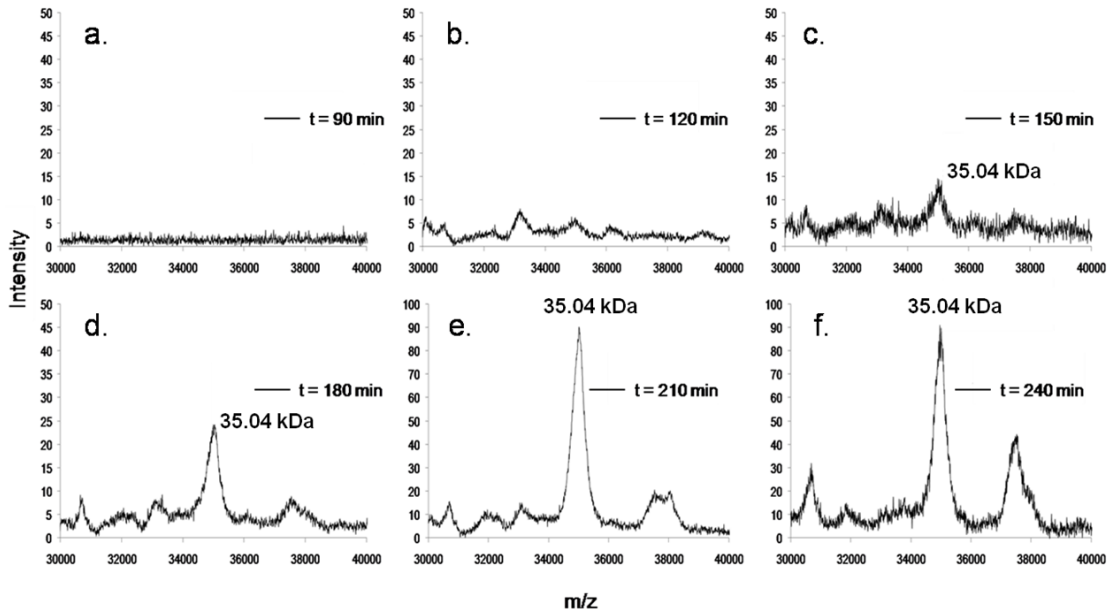


Figure 4-2 MALDI-TOF mass spectra acquired at various time points during conventional ^{14}N *in vitro* phage infection of *S. aureus* performed at 37 °C; (a) 90-, (b) 120-, (c) 150-, (d) 180-, (e) 210-, (f) 240-min infection time. Initial *S. aureus* bacterial concentrations and initial ^{14}N phage concentrations were 6.7×10^7 CFU mL $^{-1}$ and 1.0×10^6 PFU mL $^{-1}$, respectively.

While a standard PAD experiment with an initial phage concentration well below the detection limit of the MALDI-TOF MS still induces productive and detectable phage amplification, the time necessary to achieve such amplification is prolonged by the lower initial concentration of the input phage. To investigate this phage dose-dependency on the bacteria, bioluminescence was monitored for phage-mediated amplification and cell lysis. Bioluminescence is routinely used for the detection of bacteria via ATP monitoring in living cells⁷⁶. In this study, bioluminescence changes reflect the attack of *S. aureus* by the phage and the subsequent ATP release associated with phage-host infection, replication, and cell lysis. To ensure ^{15}N phage amplification did not differ from a naturally occurring host infection, equal concentrations (8.0×10^7 PFU mL $^{-1}$) of ^{14}N and ^{15}N phage were used to infect separate *S. aureus* samples (6.7×10^7 CFU mL $^{-1}$), and

bioluminescence was monitored. The overlaying traces in Figure 4-3a (inset) verify that phage-mediated bioluminescence detection of *S. aureus* was comparable for both ^{15}N and ^{14}N phage and that ^{15}N phage was able to bind to the bacterial cells effectively and succeed in carrying out the normal cycle of replication and lysis of the host cell. Furthermore, the bioluminescence data included in Figure 4-3b indicated that more rapid results can be obtained by use of higher initial concentrations of bacteriophage, provided that such high concentrations do not result in “lysis from without”²⁸⁰, which is a non-productive phage amplification event.

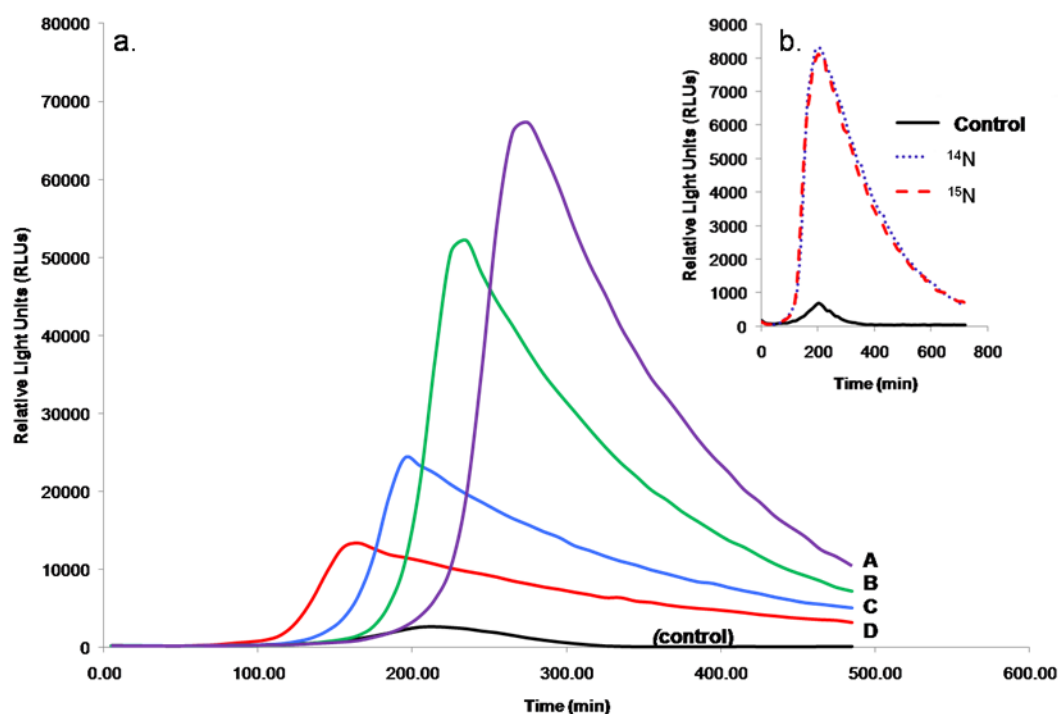


Figure 4-3 Phage-mediated bioluminescent detection of *S. aureus*. Bioluminescence (RLU) was measured over time following addition of bacteriophage. A fixed *S. aureus* concentration of 6.7×10^7 CFU mL⁻¹ was used for all samples. The black solid line corresponds to the *S. aureus* phage-free control. Data were acquired in triplicate and the mean values are plotted. (a) Signal response times for ^{14}N and ^{15}N bacteriophage at a fixed concentration of 8.0×10^7 PFU mL⁻¹. (b) Average relative bioluminescence as a function of time showing dose-dependent detection. Samples were labeled A through D, with the corresponding light emission profiles similarly labeled in the graph. Bacteriophage 53 concentrations were A) 8.0×10^4 PFU mL⁻¹; B) 8.0×10^5 PFU mL⁻¹; C) 8.0×10^6 PFU mL⁻¹; D) 8.0×10^7 PFU mL⁻¹. To establish the onset of phage amplification in luminescence experiments via an objective metric, a sample was deemed as having bacteriophage amplification if the point-by-point second derivative ratios of the phage-containing vs. control curves were greater than or equal to 3. *S. aureus* samples infected with higher phage concentrations, bacteriophage amplification is detected well before the onset of bacteriophage amplification in *S. aureus* samples with lower bacteriophage concentrations. As phage concentration was increased from 10^4 to 10^7 PFU mL⁻¹, response times needed to observe an increase in RLUs decreased. Ranging from the highest concentration of bacteriophage to the lowest, the times from infection to initiation of bacteriophage amplification were 81.5 min, 141.5 min, 161.5 min, and 251.5 min, respectively.

MALDI-TOF mass spectra for the time course of a ^{15}N labeled PAD experiment are shown in Figure 4-4, where ^{15}N bacteriophage was added to *S. aureus* so that the final concentration of bacteriophage was $2.0 \times 10^8 \text{ PFU mL}^{-1}$ and the bacteria concentration was $6.7 \times 10^7 \text{ CFU mL}^{-1}$. At $t = 0 \text{ min}$, a significant peak indicative of the ^{15}N labeled bacteriophage capsid protein can be seen (Figure 4-4a), consistent with the features shown in Figure 1b. When compared with the bioluminescence-derived detection times at $t = 30 \text{ min}$ and an inoculate phage titer of $2.0 \times 10^8 \text{ PFU mL}^{-1}$, MALDI detection may be expected. However, no change in the resulting mass spectrum was yet observed (Figure 4-4b). At $t = 60 \text{ min}$, a shoulder of the ^{14}N phage capsid protein peak emerges (Figure 4-4c), indicative of progeny phage amplification. However the S/N is less than 3; thus, the presence of *S. aureus* can be inferred but not confirmed. At $t = 90 \text{ min}$, a clear $^{14}\text{N}/^{15}\text{N}$ doublet can be observed at $m/z = 35.04$ and 35.46 kDa , confirming a positive *S. aureus* detection (Figure 4-4d). As the experiment proceeds to 120 min and 150 min, the ^{14}N progeny phage protein signal intensifies so that it dominates the spectra and the ^{15}N labeled signal can no longer be seen (Figure 4-4e, 4-4f). No major increase in ^{14}N signal was observed with infection times greater than 240 min. Therefore, for this set of experimental conditions, detection of *S. aureus* occurred at 90 min. The ability of the method to inoculate with high ^{15}N -labeled phage titers at an initial infection concentration higher than the MALDI detection limit demonstrated a clear time-saving advantage over traditional ^{14}N phage inoculation methods, and it allowed unambiguous detection in 90 min incubation time—1.5 h sooner than in the standard ^{14}N PAD experiment.

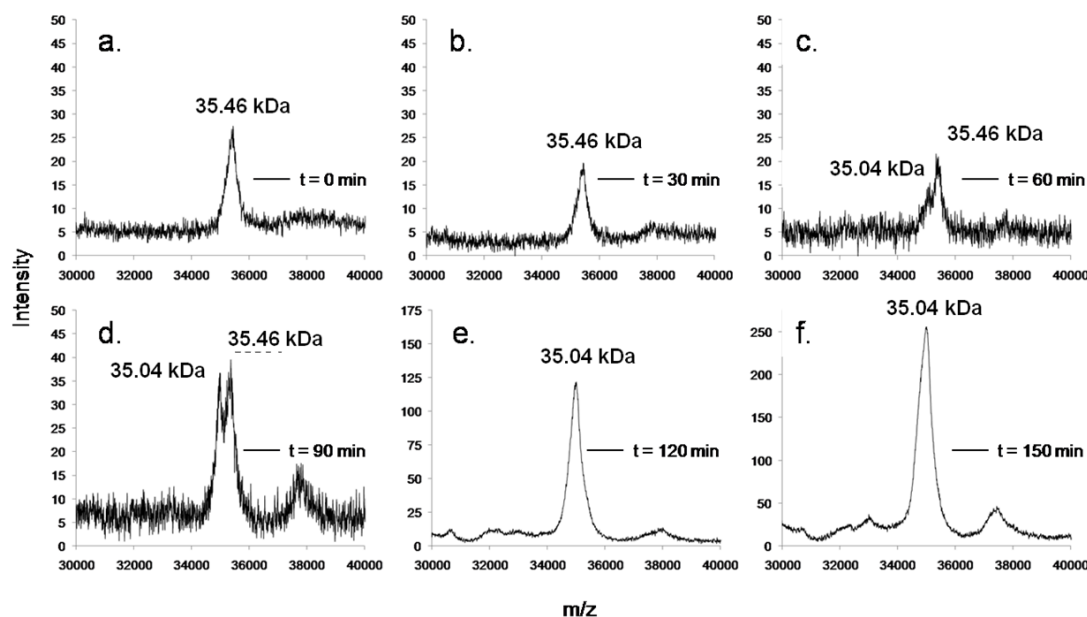


Figure 4-4 MALDI-TOF mass spectra acquired at various time points during ^{15}N *in vitro* phage infection of *S. aureus* performed at 37°C ; (a) 0-, (initial infection); (b) 30-, (c) 60-, (d) 90-, (e) 120-, (f) 150-min infection time. Initial *S. aureus* bacterial concentrations and initial ^{15}N phage concentrations were 6.7×10^7 CFU mL^{-1} and 2.0×10^8 PFU mL^{-1} , respectively.

To determine the sensitivity of this *S. aureus* detection method, ^{15}N PAD experiments were conducted. In these experiments, the initial bacteriophage concentration was held constant at 2.0×10^8 PFU mL^{-1} and a tenfold dilution series of bacteria were added to respective vials, beginning at 6.7×10^7 CFU mL^{-1} and ending at 6.7×10^4 CFU mL^{-1} . Normalized mass spectra of ^{15}N phage-infected *S. aureus* suspensions are shown in Figure 4-5. As seen previously, a bacteria concentration of 6.7×10^7 CFU mL^{-1} , when combined with a high concentration of ^{15}N labeled bacteriophage, generates an abundant ^{14}N bacteriophage signal after 2 h incubation time when analyzed by MALDI-TOF MS (Figure 4-5a). At a bacteria concentration of 6.7×10^6 CFU mL^{-1} , the ^{15}N method can also positively detect the presence of *S. aureus*, although only a shoulder corresponding to the ^{14}N protein is seen at 2 h (Figure 4-5b). The two lower dilutions showed no peak at 2 h (spectra not shown). However, when analyzed after 5 h

of incubation time, the MALDI-TOF spectrum of 6.7×10^5 CFU mL⁻¹ bacteria shows the emergence of a ¹⁴N shoulder at 35.04 kDa (Figure 4-5c). Similar analysis of the 6.7×10^4 CFU mL⁻¹ *S. aureus* dilution t = 0 h and t = 5 h detected only the ¹⁵N capsid peak at both time points and did not generate a discernable ion signal for the ¹⁴N capsid protein (Figure 4-5d). Thus, the detection limit of the phage amplification procedure was established at 6.7×10^6 CFU mL⁻¹ at t = 2 h and 6.7×10^5 CFU mL⁻¹ at t = 5 h. If rapid ¹⁵N PAD detection of low-abundance *S. aureus* is required at t = 90 min incubation time, a sample preconcentration step can be incorporated prior to ¹⁵N infection.

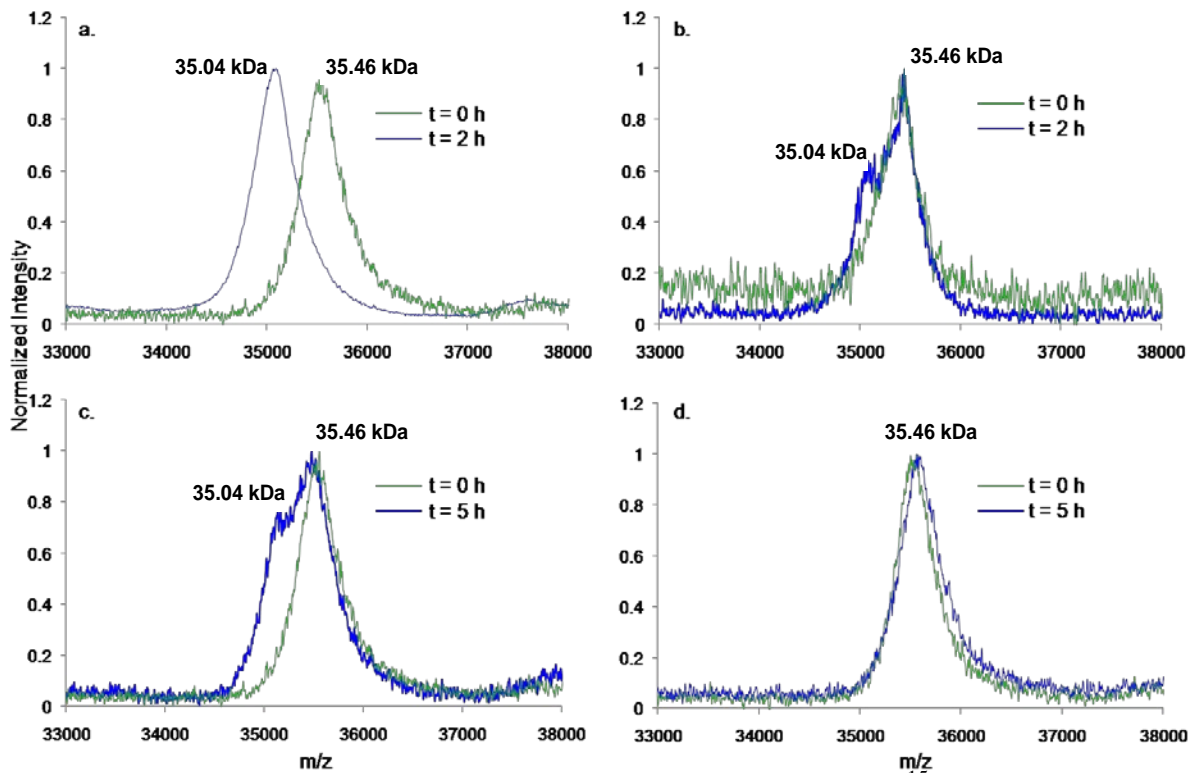


Figure 4-5 Resulting MALDI mass spectra acquired from analysis of ¹⁵N bacteriophage amplified media. Samples were prepared as serial dilutions of *S. aureus* culture in TSB with a bacteriophage concentration of 2.0×10^8 PFU mL⁻¹. Spectral peaks have been normalized to the base peak in each spectrum, and spectra have been overlaid for comparative purposes. (a) 6.7×10^7 CFU mL⁻¹; (b) 6.7×10^6 CFU mL⁻¹; (c) 6.7×10^5 CFU mL⁻¹; (d) 6.7×10^4 CFU mL⁻¹.

Isotopically labeled PAD to detect pathogenic bacteria possesses unique properties for routine clinical microbiology testing. PAD will only detect viable, live bacteria whereas PCR tests will return a positive result whether the bacteria is alive or not. PCR can be prone to ambiguous test results and often requires confirmatory analysis while PAD may not require additional testing. The cost of reagents for PAD can be rendered negligible when compared to PCR, as bacteriophage are easily cultured and can be incorporated into a kit with little cost. MALDI instrumentation and advanced sample preparation methodologies are becoming more common in clinical laboratories and can be used in a wide range of clinical applications. The PAD MS analysis is compatible with high throughput automation and requires little hands-on time for laboratory technicians. When compared to rapid culture methods, PAD does not require clean sample matrices or single colony isolation to produce a rapid result. Clearly, a well-developed PAD assay can augment the information produced by a clinical microbiology laboratory, and in some cases replace expensive or labor-intensive testing.

4.5. Conclusions

The goal of this research was to provide the foundation for a rapid PAD MS-based method that incorporates a “heavy”-labeled ^{15}N bacteriophage that can quickly infect its host bacteria and produce a distinct ^{14}N mass spectrometric signal indicative of host bacterial detection. The feasibility of this approach has been demonstrated using cultivated *S. aureus*, Staphylococcal bacteriophage 53 and MALDI-TOF MS. These data encourage the continued development and use of isotopically labeled PAD MS-based methods for rapid bacterial detection. Further development of PAD methodologies should

investigate the plausibility of incorporating ^{13}C isotopes into the bacteriophage proteome (in the place of ^{15}N) to increase the observed mass shift from the parent/progeny peaks. The 35 kDa phage capsid protein that contains 428 nitrogen molecules available for ^{15}N enrichment contains 1645 carbon molecules that can be enriched for ^{13}C , thus the resulting mass shift should be nearly 4 times greater than the shift resulting from ^{15}N labeling. This increased mass shift could potentially resolve the parent/progeny peaks, increase sensitivity of the measurements, and allow for a more rapid PAD method. Future studies will be aimed at evaluating the clinical impact of rapid PAD MS-based methods for identification of additional *S. aureus* bacterial strains and will incorporate antibiotic susceptibility testing into the PAD workflow for detecting methicillin-type resistant (MRSA) and methicillin-type susceptible (MSSA) *S. aureus* isolates.

CHAPTER 5. VIABLE STAPHYLOCOCCUS AUREUS QUANTITATION USING ^{15}N METABOLICALLY-LABELED BACTERIOPHAGE AMPLIFICATION COUPLED WITH A MULTIPLE REACTION MONITORING PROTEOMICS WORKFLOW

5.1. Abstract

Chapter 4 evaluated the performance of MALDI-TOF MS for analysis of wild-type and ^{15}N bacteriophage intact proteins for *S. aureus* detection and described how this research was able to overcome limitations associated with existing PAD techniques, advancing MS-based strategies for bacterial detection. Chapter 5 extends the idea of using isotopically labeled bacteriophage amplification by implementing a “bottom-up” proteomics approach that not only identifies *S. aureus* in a sample, but also quantitates the bacterial concentration. This chapter presents a multiple reaction monitoring (MRM) LC method with MS/MS detection for quantitation of *S. aureus* via isotopically labeled PAD. This PAD method enables rapid and accurate quantitation of viable *S. aureus* by detecting an amplified capsid protein from a specific phage. A known amount of metabolically-labeled ^{15}N reference bacteriophage, utilized as the input phage and as the internal standard for quantitation, was spiked into *S. aureus* samples. Following a 2-h incubation, the sample was subjected to a 3-min rapid trypsin digest and analyzed by high-throughput LC-MS/MS targeting peptides unique to both the ^{15}N (input phage) and ^{14}N (progeny phage) capsid proteins. Quantitation was achieved by comparing peak areas

of target peptides from the metabolically labeled ^{15}N bacteriophage peptide internal standard with that of the wild-type ^{14}N peptides that were produced by phage amplification and subsequent digestion when the host bacteria was present. This approach is based on the fact that a labeled species differs from the unlabeled one in terms of its mass but exhibits almost identical chemical properties such as ion yields and retention times. A 6-point calibration curve for *S. aureus* concentration was constructed with standards ranging from 5.0×10^4 CFU mL $^{-1}$ to 2.0×10^6 CFU mL $^{-1}$, with the ^{15}N reference phage spiked at a concentration of 1.0×10^9 PFU mL $^{-1}$. Amplification with ^{15}N bacteriophage coupled with LC-MS/MS detection offers speed, accuracy, sensitivity, and precision for *S. aureus* quantitation.

5.2. Introduction

S. aureus is a versatile pathogenic bacterium²⁹ responsible for a significant number of healthcare-associated and community-acquired infections³¹. It causes a broad spectrum of infections ranging from acute to chronic disease^{35,36} and is a common etiological agent of opportunistic infections. An increasing prevalence of *S. aureus* strains that are resistant to antibiotics are emerging, posing an even greater threat to the general public worldwide³⁸. For these reasons, the development and improvement of diagnostic methods that allow rapid identification and quantitation of this bacterium are highly critical³¹.

Several methods are available for definitive identification of *S. aureus*. Traditional identification through plate-culture (requires 2-3 days), can require sub-culturing, or biochemical analysis⁵⁶, and necessitates blood sample volumes difficult to

obtain in pediatric patients²⁸¹. Molecular methods, such as polymerase chain reaction, reverse transcription-polymerase chain reaction, and quantitative reverse transcription-polymerase chain reaction (PCR, RT-PCR, and qRT-PCR) are primarily based on particular genes specific to *S. aureus*³¹ and offer the most sensitive measurements in the least amount of time, with the least amount of sample, but can be prone to ambiguous results that can only be resolved through sample cultivation³⁸. Additionally PCR is unable to distinguish dead bacteria from live cells, and the required reagents are relatively costly. Gene probe assays are promising in that they offer simple, rapid and sensitive measurements and are lower in cost than PCR techniques^{31, 56}. Several rapid methods (culture-based and molecular-based screening methods) for *S. aureus* are also available, allowing diagnostics within hours of collection time; however these tests can be costly and the majority yield qualitative, not quantitative results²⁸²⁻²⁸⁴.

Isotope labeling MS has long been used for quantitation of small molecules in a variety of matrices¹⁸⁷. More recently, MS-based stable isotope tagging of proteins and peptides followed by MS/MS experiments²⁸⁵, has emerged as a popular tool in quantitative proteomic experiments^{125, 126, 174, 286-289}. Quantitation is achieved by adding a known amount of stable isotope-labeled protein or peptide to a sample as an internal standard and comparing instrument response to an unlabeled counterpart. Because species tagged with heavy isotopes differ from the unlabeled light ones in terms of their mass but exhibit almost identical chemical properties such as ion yields and retention times¹⁸⁶, ionic signals from tagged ion pairs can be accurately compared independently from instrument response. Labeling strategies include the use of chemical reactions to introduce an isotopic or isobaric tag at specific functional groups on polypeptides²⁹⁰⁻²⁹³,

metabolic isotope labeling using heavy amino acids^{190, 294-297}, and methods that introduce stable isotope tags via enzymatic reactions^{298, 299,300}. Each of these methods has specific strengths and weaknesses³⁰⁰; however, metabolic incorporation of stable isotopes in whole organisms using cell culturing in heavy media has proven to be a favorite³⁰¹. Heavy isotopes, such as ¹⁵N and ¹³C, in nutrients fed to organisms during growth result in incorporation of heavy labels into all proteins over the course of doubling³⁰². Labeled samples and unlabeled controls are then combined prior to sample preparation, providing an internal control to reduce variability in the comparison of two proteomes³⁰³.

The use of phages for bacterial detection is well documented²⁶⁷. Bacteriophages are specific to their target host, self-replicate, have extensive shelf lives, are inexpensive²⁶⁸, and infect only metabolically-active cells²⁶⁹. Bacteriophage amplification technology has emerged as a means of rapid bacterial detection, using modern protein analytical techniques to monitor changes in sample bacteriophage concentration^{62, 140, 270, 271}. Standard PAD techniques are highly specific, but the progeny phage produced through infection cannot be differentiated from the input parent phage initially added to the sample. For this reason, standard PAD techniques must use low-level concentrations of input phage --well below the detection limit of the mass spectrometer-- thus prolonging incubation time prior to analysis, decreasing analysis frequency, increasing detection limits, and potentially increasing the probability of false positive results. To overcome these limitations, we have recently developed a rapid ¹⁵N PAD approach for analysis of intact phage proteins as a means of detecting *S. aureus* via top-down MALDI-TOF MS³⁰⁴. While this ¹⁵N PAD MALDI-TOF MS method has proven successful for detecting viable *S. aureus* via amplified phage capsid proteins, it is unable to quantify *S.*

aureus concentration due to the inherent problems in obtaining quantitative MALDI results.

Here, we present a “bottom-up” approach that combines PAD, stable isotope metabolic labeling, and LC-MRM MS/MS to quantify Staphylococcal bacteriophage 53 peptides from a phage capsid head protein, which when present, are indicative of the concentrations of viable host *S. aureus* bacteria (ATCC 27694). We show that our ^{15}N PAD LC-MS/MS method offers good accuracy, precision, and sensitivity for high-throughput quantitation of viable *S. aureus*. To our knowledge, this is the first study employing ^{15}N PAD combined with LC-MS/MS to quantify target bacteria.

5.3. Experimental

5.3.1. *S. aureus* and bacteriophage 53

Stock cultures of lyophilized *S. aureus* (ATCC 27694) and bacteriophage 53 (ATCC 27694-B1) were obtained from the American Type Culture Collection (ATCC, Manassas, VA). All microbiological procedures were performed in a US biological safety level 2 (BSL2) facility following standard biosafety protocols. ^{14}N bacteriophage stocks were generated by combining 500 μL of dense ATCC 27694 culture with 500 μL of wild type bacteriophage 53 (1.0×10^6 PFU mL^{-1}) in a test tube, pouring the contents onto a tryptic soy agar plate, and incubating the plate overnight at 37 °C. Following incubation, the plate's content was collected into a 50 mL conical tube by washing with tryptic soy broth (TSB) (Bacto™ TSB, BD Diagnostics, Franklin, NJ), scraping with a sterile plastic loop, and aspirating with a pipette. The conical tube was then centrifuged for 20 minutes at 3500 rpm to pellet out the debris, and the supernatant was filtered

through an Autovial 0.2 µm PVDF membrane syringeless filter device (Whatman, Inc, Clifton, NJ) to remove extraneous debris. The final phage filtrate was quantified using a traditional plaque assay²⁷⁷.

5.3.2. Biosynthetic production of ¹⁵N *S. aureus* and ¹⁵N bacteriophage 53

¹⁵N *S. aureus* cells were grown in Bioexpress Cell Growth Media U-¹⁵N, 98% (Cambridge Isotope Laboratories, Inc., Andover, MA) according to manufacturer's instructions with only minor modifications. A 1-mL sample of ¹⁵N cell growth media was added to 9 mL of 0.1 M phosphate buffered saline (PBS), inoculated with 500 µL of *S. aureus* ATCC 27694, and allowed to grow overnight at 37 °C. Following overnight culture, the same procedure was repeated with the exception of inoculating the fresh ¹⁵N cell growth media with 500 µL of the dense overnight bacterial growth. This double-round inoculation of ATCC 27694 with ¹⁵N cell growth media ensured maximum labeling efficiency. Following the second overnight incubation, the dense ¹⁵N labeled bacteria were combined with 500 µL of wild type bacteriophage (1.0x10⁶ PFU mL⁻¹) and added to a ¹⁵N-labeled agar plate. The ¹⁵N-labeled agar plates were made by combining 10 mL of ¹⁵N cell growth media, 90 mL of de-ionized water, and 1.5 grams of agar. The solution was autoclaved for 60 minutes and poured into sterile Petri dishes. After allowing the ¹⁵N *S. aureus* and ¹⁵N bacteriophage to incubate overnight on the ¹⁵N-labeled agar plate, the plate's contents was collected into a 50 mL conical tube by washing with 5 mL TSB, scraping with a sterile plastic loop, and aspirating with a pipette. The conical tube was then centrifuged for 20 minutes at 3500 rpm to pellet out the debris, and the supernatant was filtered through an Autovial 0.2 µm PVDF membrane

syringeless filter device to remove extraneous debris. The ^{15}N -labeled bacteriophages were quantified using a standard plaque assay²⁷⁷. Phage stock suspensions (2.1×10^9 PFU mL^{-1}) were stored at 4 °C for further analyses.

5.3.3. Nano-LC-MS/MS

Protein identification was performed as previously reported³⁰⁴. Briefly, tryptic digests of the ^{14}N and ^{15}N phage stock solutions were analyzed using using a Waters NanoAquity liquid chromatography system (Waters Corporation, Milford, MA) utilizing a 100 μm x 100 mm BEH130 C_{18} analytical column (1.7 μm particle size) (Waters Corporation). A 5- μL digested sample was injected onto a Waters NanoAquity liquid chromatography system (Waters Corporation, Milford, MA, USA) utilizing a 100 μm x 100 mm BEH130 C_{18} analytical column (1.7 μm particle size) (Waters Corporation). The aqueous mobile phase (A) consisted of HPLC-grade water with 0.2% formic acid (FA) and 0.005% trifluoroacetic acid (TFA), while the organic phase (B) was acetonitrile (ACN) with 0.2% FA and 0.005% TFA. A gradient profile was used at a flow rate of 400 nL min^{-1} . Initially, the mobile phase consisted of 5 % B and 95 % A. After 5 min, the gradient was ramped to 30% B over the next 100 min, continuing up to 90 % B over the next 5 min and holding for 2 min. After 112 min total run time, the gradient was returned to 5 % B and 95 % A for the next 20 min to equilibrate the column to initial conditions. The total run time was 132 min.

The column eluent was introduced into a Thermo Scientific LTQ-Orbitrap Velos mass spectrometer (Thermo Scientific, Waltham, MA, USA) equipped with an electrospray interface. The LTQ-Orbitrap instrument performed data-dependent

acquisition of precursor and product ion spectra. The nominal resolution of the Orbitrap analyzer was set at 60,000 with scan range from m/z 400 to 1600. The top 9 most intense ions were selected for fragmentation; the selection window was set at $m/z = 2$. Conventional collision induced dissociation (CID) was used for ion activation purposes. Dynamic exclusion was enabled with a repeat count of 1 and an exclusion duration of 120 sec. Charge state screening and monoisotopic precursor ion selection were enabled along with charge state rejection, whereby singly charged ions were not selected for MS/MS analysis.

5.3.4. Protein identification and target peptide determination

Protein identification was performed by matching acquired peptide tandem mass spectra to theoretical digests found in a protein database. Prior to database searching, MS/MS spectra were converted to Mascot generic format by using Mascot Distiller v.2.3.2.0 (Matrix Science, London, UK). Charge state deconvolution and de-isotoping were not performed. Database searching utilized the Mascot v.2.2.0 algorithm (Matrix Science, London, UK) with the following parameters: fragment ion mass tolerance of 0.50 Da, parent ion tolerance of 200 ppm, trypsin enzyme, and deamidation of asparagine and oxidation of methionine specified as variable modifications. A database of 24,384 entries was generated by extracting sequences from the National Center for Biotechnology (NCBI) protein database (downloaded on November 08, 2009) that contained at least one of the following strings in the entry description; “staphylococcus phage”, “aureus”, “trypsin”, “keratin”. To validate MS/MS-based peptide and protein identification, Scaffold v.3.00.02 (Proteome Software Inc., Portland, OR) with

PeptideProphet^{TM278} and ProteinProphet^{TM279} algorithms was used. Peptide identifications were accepted if they could be established at greater than 95.0% probability as specified by PeptideProphetTM. Protein identifications were accepted if they could be established at a 99.0% probability based on ProteinProphetTM, and if they were based on at least 3 peptide matches. Proteins containing similar peptides and that could not be differentiated based on MS/MS analysis alone were grouped into a single match.

The peptide sequences SIAQSIEK, LGVILPVTk, and LIYGIPQLIEYK were selected for quantitation purposes. The metabolically labeled SIAQSIEK and LGVILPVTk were 10 Da heavier than the naturally-occurring peptides, due to incorporation of serine, isoleucine, alanine, glutamic acid, leucine, glycine, valine, proline, and threonine each with a ¹⁵N nitrogen count of 1, and glutamine and lysine amino acids with a ¹⁵N nitrogen count of 2. Similarly, labeled LIYGIPQLIEYK was 14 Da heavier than the naturally-occurring peptide.

5.3.5. Preparation of *S. aureus* working stock and standard solutions

To determine the *S. aureus* concentration (CFU mL⁻¹) and to prepare calibrated standards, serial dilutions of *S. aureus* concentrated overnight suspensions (working stocks) were made and absorbance spectra for each dilution were recorded at 650 nm using a SpectraMax 2 (Molecular Devices, Inc., Sunnyvale, CA) spectrophotometer. The bacterial dilutions were then plated for viable cell counting. After overnight growth at 37 °C, the relationship between absorbance and the CFU mL⁻¹ was graphed and values in the linear range of this graph were used to calculate the concentration of *S. aureus* working

stocks solutions. This calibration curve was then used in daily analyses to calculate the number of viable cells in the *S. aureus* working stock by optical density readings.

For quantitation, an initial absorbance reading was taken of the *S. aureus* working stock solution and was used as the starting point when making serial dilutions for calibration curves. From the working stock, six 1-mL serial dilutions in TSB were prepared ranging from 5.0×10^5 CFU mL⁻¹ to 2.0×10^6 CFU mL⁻¹. The six 0.5-mL calibration standards, ranging from 5.0×10^4 CFU mL⁻¹ to 2.0×10^5 CFU mL⁻¹, were prepared by adding 50 µL of the corresponding *S. aureus* dilution, 250 µL of stock ¹⁵N phage (2.1×10^9 PFU mL⁻¹), 50 µL of 1 M magnesium chloride, and 150 µL TSB, to make the final volume, 0.5 mL. The 250 µL 500 mL⁻¹ of stock ¹⁵N phage was used as the internal standard (ISTD).

5.3.6. ¹⁵N bacteriophage 53 infection/amplification procedures

The infected medium was incubated at 37 °C with gentle rotation for 2 h. Following incubation, samples were centrifuged (5 min at 10,000 g) to pellet bacteria out of solution. The supernatant was recovered and phage samples were centrifuged with washing (5 min at 14,000 g), using 30-kDa molecular weight cutoff filters (Amicon Ultra; Millipore, Billerica, MA) and 500 µL of 1 M ammonium bicarbonate, pH 9 (x2). The filtrate (20 µL) was recovered for subsequent enzymatic digestion.

5.3.7. Rapid enzymatic digestion procedure

In-solution digestion was performed using 20 µL aliquots of the phage/bacteria filtered samples. A modification of an acid-labile surfactant digestion method described

before³⁰⁴ was used. The modification included incubation at a higher temperature (52 °C) for a short period of time (3 min) and the use of a thermocycler (Applied Biosystems) as described originally by Turapov *et al.*⁴⁴ and later by Moura *et al.*⁴⁵. Briefly, a volume of 10 µL of a 0.1 % solution of sodium 3-[(2-methyl-2-undecyl-1,3-dioxolan-4-yl)methoxyl]-1-propanesulfonate (Rapigest, Waters Corporation, Milford, MA) in 50 mM ammonium bicarbonate digestion buffer was added to each 20 µL phage aliquot to solubilize proteins and facilitate protein digestion^{305, 306}. The solution was then incubated at 100 °C for 5 minutes and rapidly cooled to room temperature. A 10 µL aliquot (~172 pmol) of sequence-grade Promega trypsin was added, and samples were incubated in a thermocycler at 52 °C for 3 min to achieve complete digestion. Following digestion, the samples were allowed to cool, 10 µl of 450 mM HCl were added, and the samples were incubated for 30 min at 37 °C to reduce the pH and cleave the acid-labile surfactant. The digested samples were then transferred to autosampler vials for LC-MS/MS analysis.

5.3.8. LC-MS/MS instrumentation and methodology

An Agilent 1200 series LC system (Agilent Technologies, Inc., Santa Clara, CA) was configured for alternating column regeneration to increase sample throughput. A dual column, dual pump system coupled to an Agilent 1200 Series 2 position/10 port valve allowed simultaneous analysis of one column eluent while a second identical column was flushed and equilibrated (Figure 5-1). The analytical columns utilized were 150 mm x 1 mm i.d. Symmetry300 reverse phase C₁₈ (3.5 µm particle size, Waters Corporation, Milford, MA). The injection volume was 8 µL, and a 2-µL full loop injection with three-time loop overfill was utilized for injections. The aqueous mobile

phase (A) consisted of 0.1% formic acid in HPLC-grade water, while the organic mobile phase (B) was 0.1% formic acid in acetonitrile. A gradient profile for the analysis column was utilized at a flow rate of 75 $\mu\text{L min}^{-1}$. Initially, the mobile phase consisted of 98% A and 2% B. At 3 min the gradient was stepped to 80% A and 20% B over the next 7 min. After 10 min the gradient was stepped to 75% A and 25% B over the next 5 min and then held constant for 2 min. After 17 min total the gradient was stepped to 2% A and 98% B for 7 min to clean the column, then stepped to 98% A and 2% B for the next 3 min to begin equilibrating the column to initial conditions. The isocratic gradient for the regeneration column utilized a 50 $\mu\text{L min}^{-1}$ flow rate and consisted of a constant eluent composition of 98% A and 2% B. The total analysis run time was 28 min.

The column eluent was introduced into a Thermo Scientific Vantage TSQ triple quadrupole tandem mass spectrometer with an electrospray interface (Thermo Scientific, Waltham, MA). The instrument was operated in positive ion multiple reaction monitoring mode. The precursor→fragment ion transitions were m/z 438.2 → 675.4, m/z 470.3 → 670.5, and m/z 725.4 → 890.5 for the native peptides and m/z 443.2 → 683.4, m/z 475.4 → 677.4, and m/z 732.4 → 899.5 for the ^{15}N corresponding labeled peptides. For each peptide, two additional transitions were monitored for confirmation purposes (Table 5-1). Instrument parameters were as follows: spray voltage 4000 V, sheath gas 4, auxiliary gas 2, capillary tube temperature 300 °C, and collision gas pressure of 1.5 mTorr. Collision energies and tube lens settings were optimized for each peptide. Data processing and instrument control were performed via the Thermo Scientific Xcalibur software.

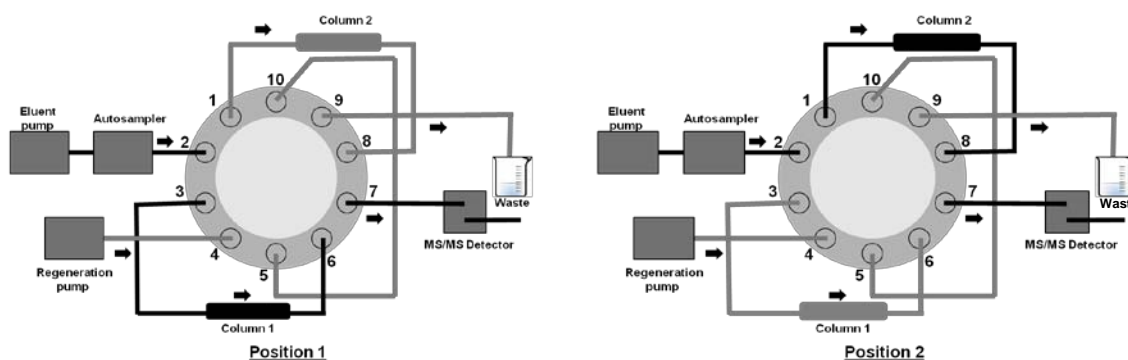


Figure 5-1 Schematic of the alternate column regeneration configuration for chromatographic separation prior to mass spectrometric detection.

5.4. Results and Discussion

A specific biomarker of Bacteriophage 53 is the 35 kDa bacteriophage 53 major capsid protein identified by MALDI-TOF MS of the intact protein and LC-MS/MS analysis of the tryptic digestion of the phage followed by database searching³⁰⁴. Of the tryptic peptides identified, three candidates for MRM analysis were selected for further investigation: SIAQSIEK, LGVILPVTk, and LIYGIPQLIEYK. The amino acid sequence of the main capsid protein in Figure 5-2 highlights peptide coverage (47%) and indicates candidate peptides in red, bolded font. These particular peptides were selected based on their signal intensities and absence of methionine, tryptophan, and cysteine residues. The presence of these residues is not desirable because they tend to be reactive and are prone to oxidation which would modify the peptide's molecular mass³⁰⁷⁻³⁰⁹, leading to inconsistent MRM analyses.

MEQTQKLKLN	LQHFASNNVK	PQVFNPDNVM	MHEK KDGTLM	NEFTTPILQE
VMENSK IMQL	GKYEPMEGTE	KKFTFWADKP	GAYWVGEGQK	IETSK KATWVN
ATMRAFK LGV	ILPVTK EFLN	YTYSQFF EEM	KPMIAEAFYK	KFDEAGILNQ
GNNPFGK SIA	QSIEK TNKVI	KGDF TQDNII	DLEALLEDE	LEANAFISK T
QNRSLLRKIV	DPETKERI YD	RNSDSL DGLP	VVNLK SSNLK	RGELITG DFD
KLIYGIPQLI	EYKID ETAQL	STVKNE DGTP	VNLFEQ DMVA	LRATMH VALH
IADDKA FAKL	VPADKRTDSV	PGEV		

Figure 5-2 Amino acid sequence of the major capsid head protein of interest present in Staphylococcal bacteriophage 53. The sequence coverage (47%) is highlighted and the three target peptides used for quantitation of *S. aureus* are indicated in bold red font. The sequence (gi | 66395381) was obtained from the National Center for Biotechnology Information database.

Stable ^{15}N isotope bacteriophage labeling was achieved by inoculating the wild type bacteriophage with a ^{15}N -enriched broth, producing a stable isotope-labeled bacteriophage 53 internal standard. Under the conditions employed, all nitrogen-containing amino acids biosynthesized were ^{15}N -labeled. Following tryptic digest, the resulting heavy peptide mixture was analyzed by LC-MS/MS to determine the completion of ^{15}N labeling. The SIAQSIEK and LGVILPVTK labeled peptides were shifted by 10 Da and the LIYGIPQLIEYK peptide was shifted by 14 Da from its unlabeled counterpart. These results were expected since SIAQSIEK and LGVILPVTK both have 10 nitrogen atoms while LIYGIPQLIEYK contains 14 nitrogen atoms. No evidence was seen for unlabeled or partially labeled peptides in the analysis.

To evaluate mass spectrometric instrument response for the wild-type phage tryptic peptides of interest, and to establish the analytical limit of detection, two-fold dilution series of the wild-type ^{14}N bacteriophage-derived peptides were analyzed using the MRM transitions described in Table 5-1.

Table 5-1 Target Staphylococcal bacteriophage 53 capsid protein peptide sequences and their corresponding ^{15}N metabolically labeled counterparts. The unique peptide sequences were chosen to identify the 35 kDa (^{14}N) and 35.5 kDa (^{15}N) capsid protein from Staphylococcal bacteriophage 53. MS/MS = mass spectrometry/mass spectrometry.

Target peptide	Actual Mass Da	Precursor Ion m/z	Fragment Ion (quantitation)	Fragment Ion (confirmation)	Fragment Ion (confirmation)
SIAQSIEK- ^{14}N	874.5	438.2 (+2)	675.4 (y6)	476.3 (y4)	604.3 (y5)
SIAQSIEK- ^{15}N	884.5	443.2 (+2)	683.4 (y6)	481.3 (y4)	611.3 (y5)
LGVILPVTK- ^{14}N	938.6	470.3 (+2)	670.5 (y6)	557.4 (y5)	444.3 (y4)
LGVILPVTK- ^{15}N	948.8	475.4 (+2)	677.4 (y6)	563.3 (y5)	449.3 (y4)
LIYGIPQLIEYK- ^{14}N	1448.8	725.4 (+2)	890.5 (y7)	1223.7 (y10)	1060.6 (y9)
LIYGIPQLIEYK- ^{15}N	1462.8	732.4 (+2)	899.5 (y7)	1235.7 (y10)	1071.6 (y9)

Typical chromatographic traces for quantitation and confirmation transitions are shown in Figure 5-3. The resulting curves from the dilution series confirmed that the instrument response was proportional to the ^{14}N bacteriophage concentration for the MRM quantitative transitions (Figure 5-4) with a detection limit of approximately 5.0×10^5 PFU mL^{-1} , based upon the observed S/N of at least 1000 for the SIAQSIEK quantitative transition (Figure 5-3). This is 100 times more sensitive than the previously reported ^{15}N PAD MALDI method³⁰⁴.

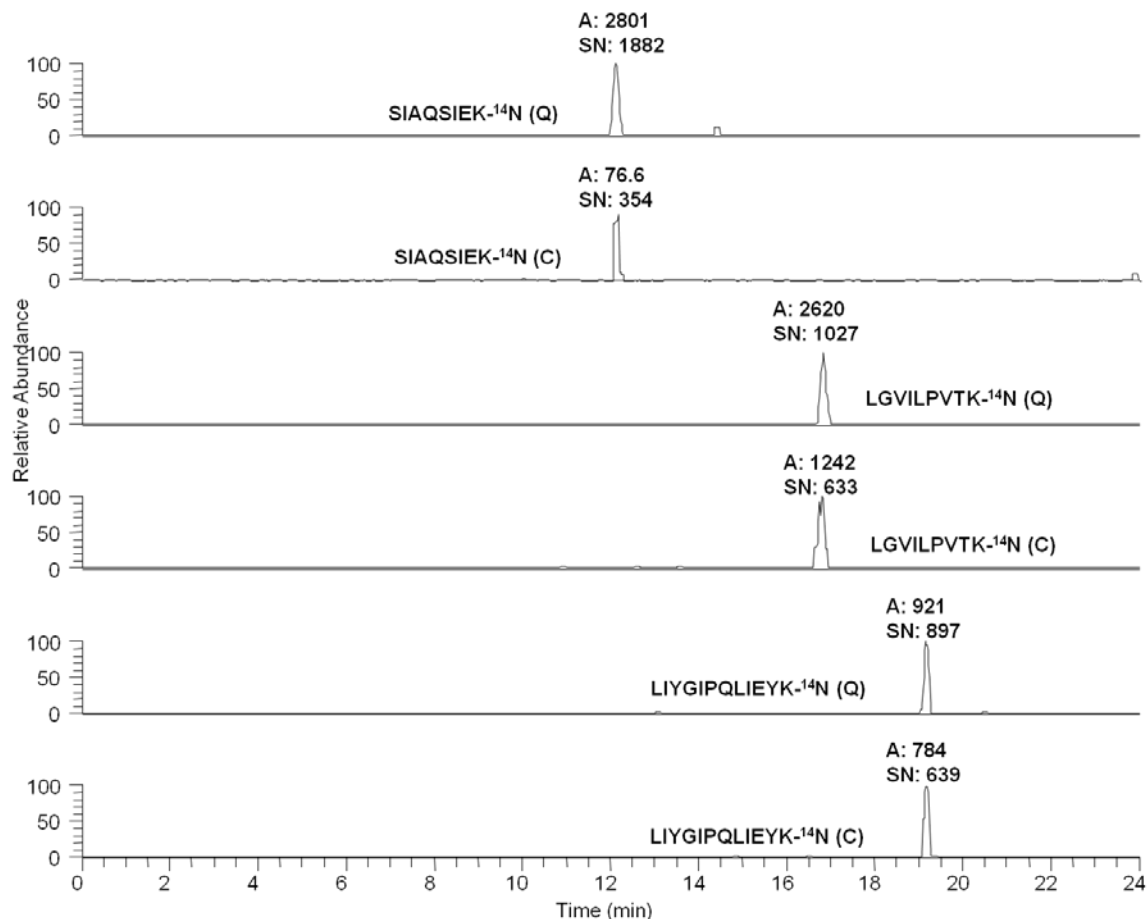


Figure 5-3 Liquid chromatography tandem mass spectrometry (LC-MS/MS) extracted ion chromatograms of target ^{14}N transitions (quantitative and confirmation) monitored for peptides from a major capsid head protein unique to bacteriophage 53. A stock solution with 5.0×10^5 PFU mL^{-1} concentration of ^{14}N phage was analyzed to determine the instrument's sensitivity for the target peptides (no phage amplification). The chromatograms demonstrate a typical response as the ^{14}N phage concentration approaches the instrument's limit of detection. Data were acquired on a Thermo Scientific TSQ Vantage.

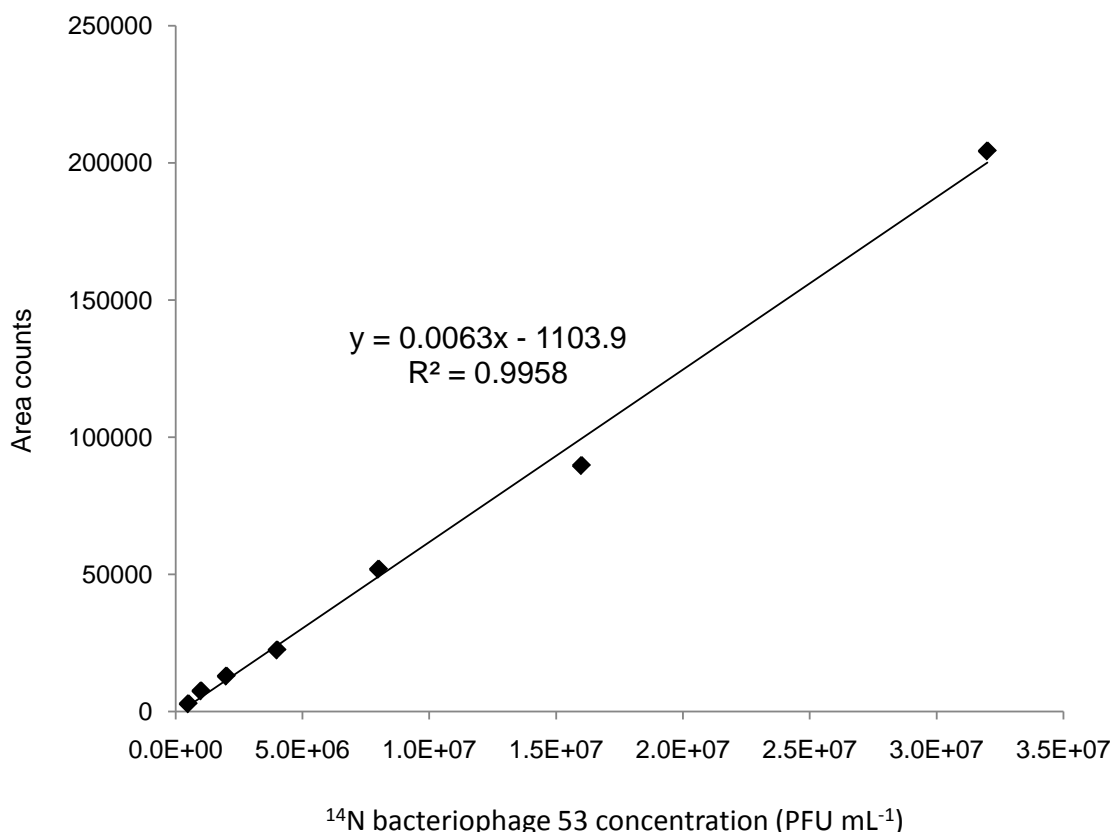


Figure 5-4 Calibration curve generated for two-fold serial dilutions of the ^{14}N wild type bacteriophage stock solution without amplification or ^{15}N label. The observed area counts for the SIAQSIEK quantitative MRM transition were plotted against expected ^{14}N phage concentration (PFU mL $^{-1}$). The resulting calibration curve for the SIAQSIEK quantitative peptide was linear (0.99) in the 5.0×10^5 PFU mL $^{-1}$ to 3.2×10^7 PFU mL $^{-1}$ range.

A ^{15}N PAD experiment was conducted to confirm that the developed MRM instrumental method could detect an increase in progeny phage concentration, thereby implying the presence of *S. aureus*. In this experiment, duplicate samples containing 1.0×10^9 PFU mL $^{-1}$ of ^{15}N labeled bacteriophage and 2.0×10^5 CFU mL $^{-1}$ of *S. aureus* were prepared. Following addition of the labeled bacteriophage, one replicate was immediately filtered, digested, and analyzed ($t = 0$ h), while the second replicate was subjected to a 2-h incubation period at 37°C. Figure 5 -5 shows extracted ion chromatograms for this experiment. Figure 5-5a ($t = 0$ h) shows high signal intensities for

each ^{15}N quantitative transition, while instrument response to the native bacteriophage (^{14}N progeny) quantitative transition is negligible. Following the 2-h incubation, no significant differences were observed in ^{15}N signal intensities, however, relative to the $t = 0$ h extracted ion chromatograms (Figure 5-5a), a dramatic increase in signal intensity was observed for all three ^{14}N quantitative transitions (Figure 5-5b). Because the only means of generating the ^{14}N phage peptides is through amplification of the progeny bacteriophage by a viable strain of *S. aureus*, these results confirm that the ^{15}N PAD LC-MS/MS method can be used to positively detect the presence of *S. aureus*. Additionally, to look for background levels of the ^{14}N phage peptides and to test for interferences, a $t = 0$ h *S. aureus* control sample was incorporated into each experimental sample set. This control sample was prepared identically to samples for ^{15}N PAD, with the exception that it was not subjected to the $t = 2$ h phage amplification event. Following sample preparation, this control was immediately filtered, washed, digested and analyzed by LC-MS/MS. Daily analyses showed no background levels ($< 5.0 \times 10^4$ CFU mL^{-1}) of ^{14}N phage peptides present in any of the unamplified samples, and that there were not interferences to the analysis (Figure 5-5a).

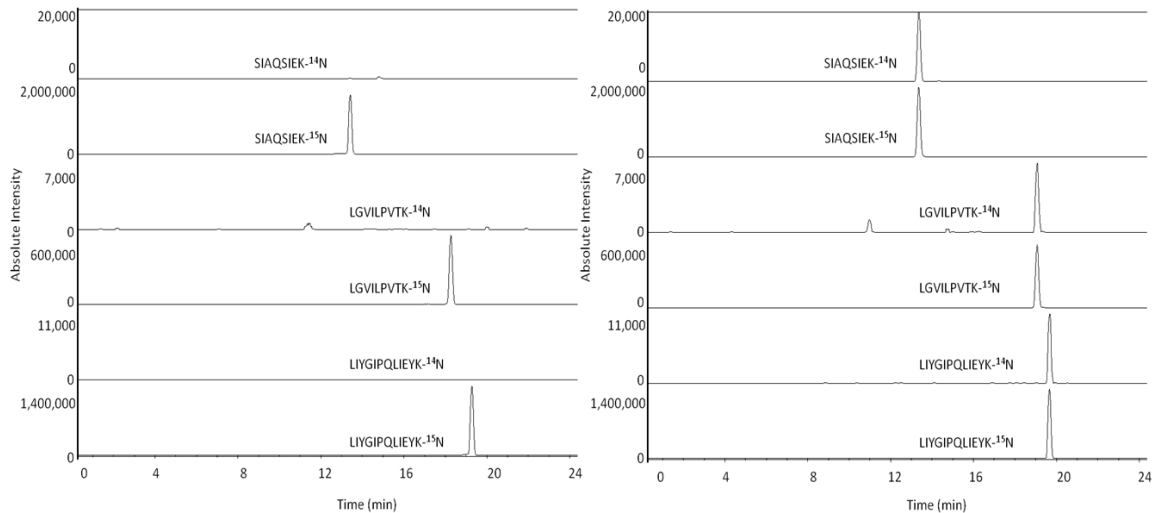


Figure 5-5 Liquid chromatography tandem mass spectrometry (LC-MS/MS) extracted ion chromatograms of the quantitative transitions monitored. The chromatograms show a standard solution (2.0×10^5 CFU mL^{-1}) a) $t = 0$ h; prior to the phage amplification event and b) $t = 2$ h; the end point of the infection. The $t = 0$ h and $t = 2$ h chromatograms are displayed on identical scales based on ion counts.

The purpose of using ^{15}N labeled bacteriophage in PAD experiments is two-fold. First, to distinguish parent bacteriophage (^{15}N labeled input) from progeny bacteriophage (^{14}N wild type output) by their mass differences. The use of a heavy phage provides more confidence in the mass spectrometric analyses since the parent and progeny can be differentiated by mass. Secondly, by using the ^{15}N labeled phage as an internal standard and a standard growth parameter, the number of bacteria can be quantified. To quantify the bacteria in culture, a high concentration of ^{15}N bacteriophage must be used to ensure conditions where at least one infective ^{15}N bacteriophage is attached to each *S. aureus* bacterium, preventing any further bacterial growth. For this condition to be met, a high multiplicity of infection (MOI); i.e. the ratio of infectious bacteriophage to bacteria, and a sufficiently dense concentration of bacteriophage must exist³¹⁰. The number of

bacteriophages that infect a given bacterial cell can be calculated from the Poisson distribution, given as:

$$P(n) = m^n e^{-m}/n! \quad (\text{Eq. 5.1})$$

where, $P(n)$ is the probability of bacterial cells being infected by n phage, and m is the MOI. Using overnight cultures, our experimentally determined mean bacterial density was found to be $3.6 \times 10^8 \text{ CFU mL}^{-1} \pm 5\%$ over the course of five different days. For the given ^{15}N bacteriophage concentration of $1 \times 10^9 \text{ PFU mL}^{-1}$ used in this study, the lowest theoretical MOI that would be encountered in the experimental design is 2.77. Figure 5-6 plots $P(n)$ versus n for a MOI of 2.77. From the plot it can be seen that $\geq 95\%$ of all bacteria will have at least one infectious bacteriophage attached for a sample of *S. aureus* at a concentration of the $3.6 \times 10^8 \text{ CFU mL}^{-1}$. Thus, if concentrations of bacteria are kept below $3.6 \times 10^8 \text{ CFU mL}^{-1}$, all bacteria can be assumed phage-infected, leading to accurate quantification.

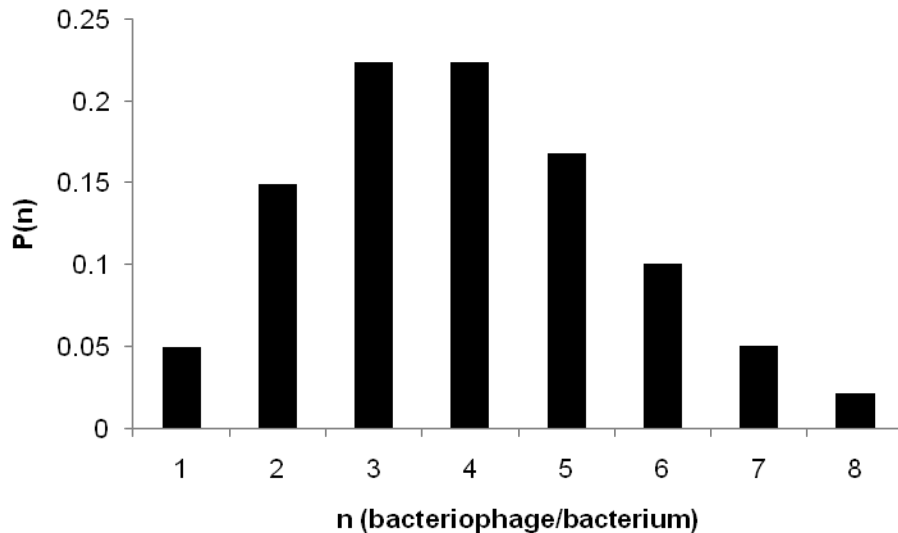
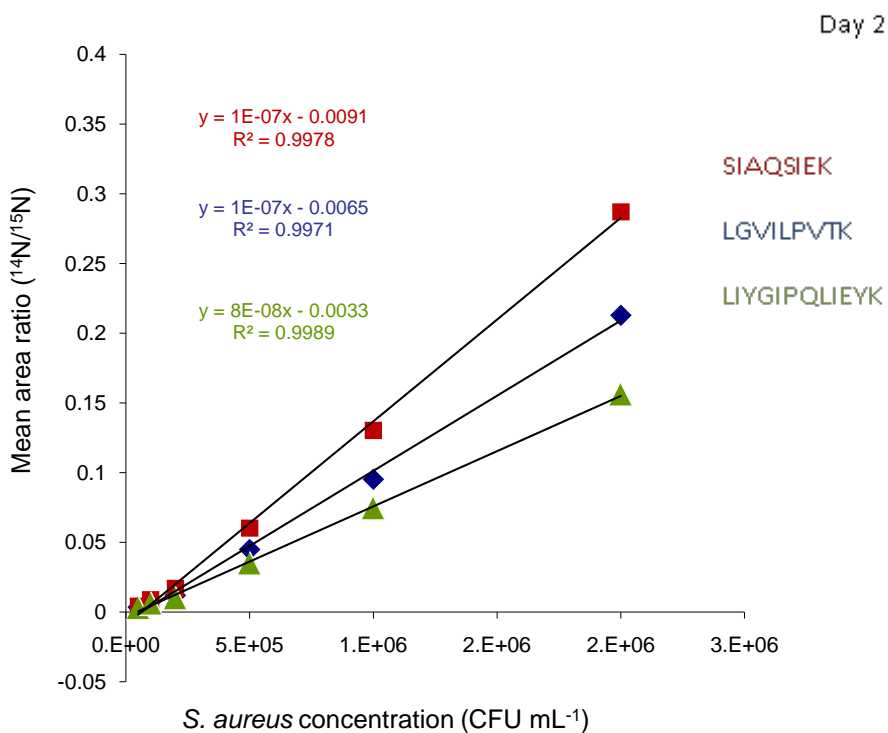
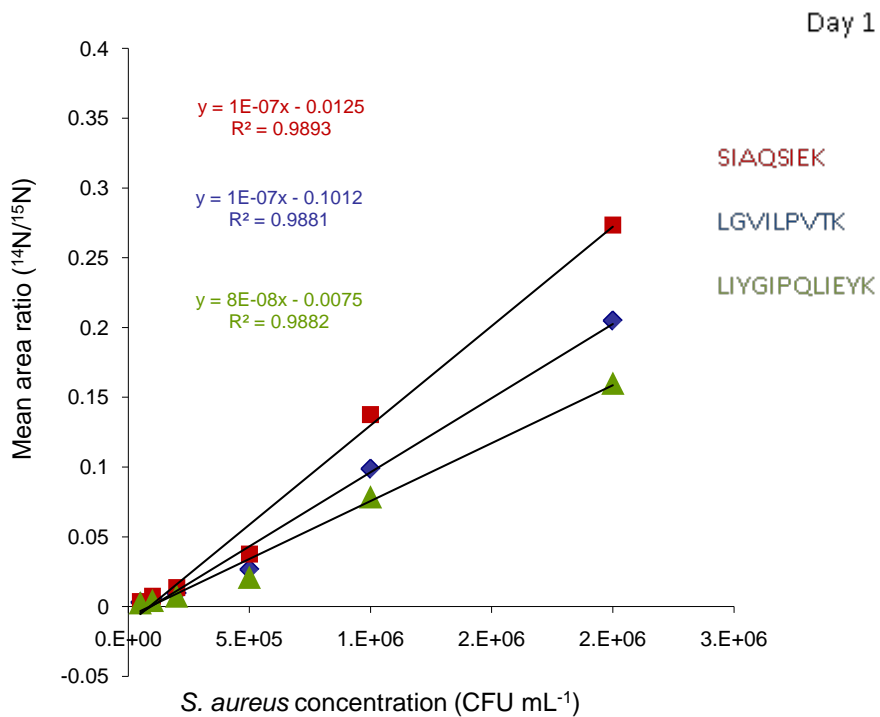


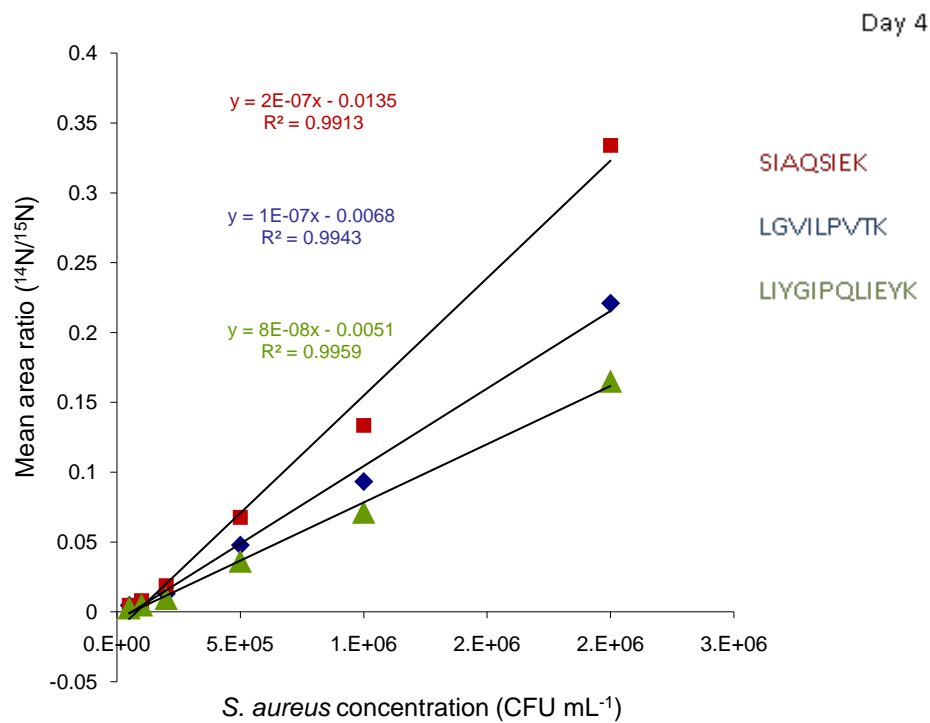
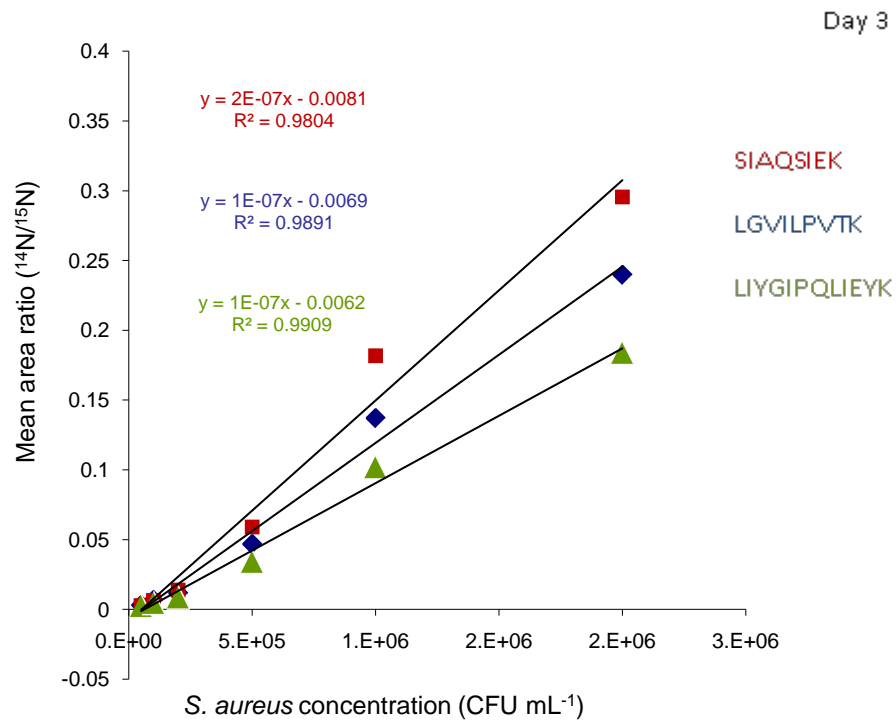
Figure 5-6 Plot showing the probability $P(n)$ of bacteria cells being infected by n phage using equation 1, a bacteriophage concentration of $1.0 \times 10^9 \text{ PFU mL}^{-1}$, and a multiplicity of infection (MOI) of 2.77 $\geq 95\%$ of all bacteria will have at least one infectious phage attached for a sample of *S. aureus* at a concentration of $3.6 \times 10^8 \text{ CFU mL}^{-1}$.

Various modeling and experimental studies have been conducted that describe bacteriophage and bacteria proliferation concentration thresholds that must be met for a productive phage infection event³¹¹. To ensure that at high phage concentrations effectively all bacteria are infected immediately after inoculation, various concentrations of bacteria (1×10^4 - 1×10^7 CFU mL⁻¹) were inoculated at 1.0×10^9 PFU mL⁻¹ bacteriophage, and allowed to incubate for 15 minutes. Following incubation, each sample was serially diluted and plated onto tryptic soy agar. After culturing the plates overnight, colonies on each plate were counted and compared against control plates that contained the same bacterial concentrations without bacteriophage infection. At each bacterial concentration tested, the cultures infected with 1.0×10^9 PFU mL⁻¹ bacteriophage showed no bacterial growth, suggesting that all *S. aureus* were rapidly infected within the first minutes of phage infection.

Following these preliminary method characterization studies, 6-point calibration curves ranging from 5.0×10^4 CFU mL⁻¹ to 2.0×10^6 CFU mL⁻¹ were generated on five different days with three replicate LC-MS/MS injections for each standard. The metabolically ¹⁵N reference phage was spiked at a concentration of 1×10^9 PFU mL⁻¹. The mean unlabeled/labeled MRM area ratios for each quantitative transition were plotted against expected *S. aureus* concentrations for each standard. Regression analysis showed good linearity ($R^2 = 0.99$) over the 5×10^4 CFU mL⁻¹ to 2.0×10^5 CFU mL⁻¹ range for each quantitative peptide transition (Figure 5-7) for all 5 days. As can be seen in Figure 5-7, the calibration curves were highly reproducible from day to day, which allowed us to generate highly specific, sensitive, and reproducible data, yielding more confidence in our analyses. The concentrations of unknown samples were then determined using the

slope and y-intercept calculated by linear regression analysis of the calibration curves constructed from each quantitative transition analyzed on that given day.





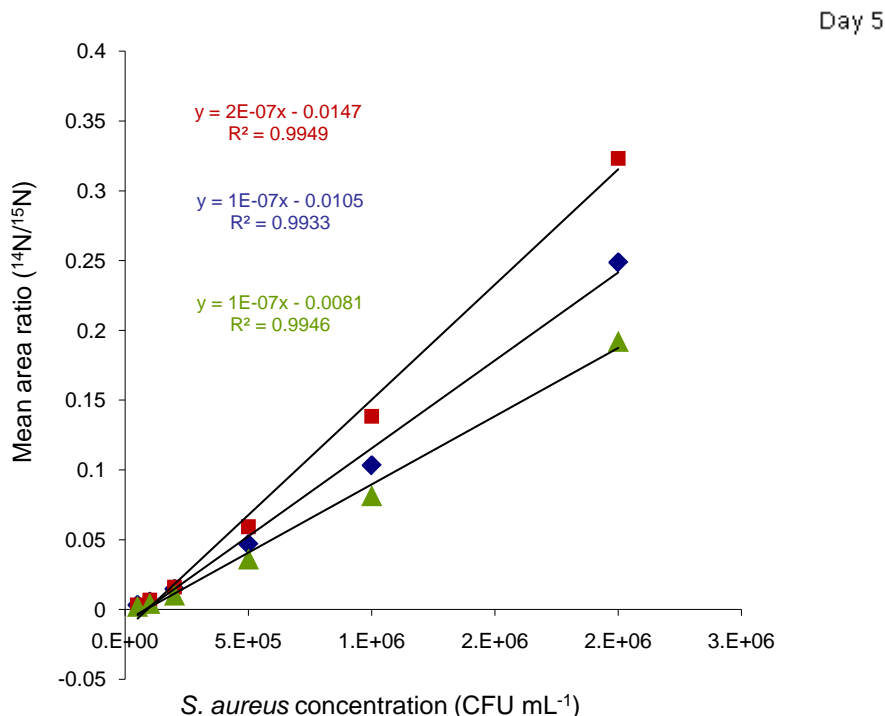


Figure 5-7 Calibration curves generated for *S. aureus* quantitation. Triplicate instrument runs were performed for each standard and the mean area ratios (unlabeled phage/¹⁵N phage) for each quantitative peptide transition were plotted against expected *S. aureus* concentration. Calibration curves for n = 5 days were compared to evaluate reproducibility. The resulting calibration curves for SIAQSIEK, LGVILPVTk, and LIYGIPQLIEYK were linear (0.98-0.99) in the 5.0×10^4 CFU mL⁻¹ to 2.0×10^6 mL⁻¹ range.

To further evaluate precision and accuracy, samples with known amounts of *S. aureus* were spiked at low (1.0×10^5 CFU mL⁻¹) and high levels (1.0×10^6 CFU mL⁻¹), subjected to the 2-h phage amplification event, proteolytically digested, and analyzed by LC-ESI-MS/MS. Each sample preparation was analyzed in triplicate. The intra- and inter-peptide mean concentrations, standard deviations, and % RSDs are reported in Table 5-2. Mean *S. aureus* concentrations for five replicates spiked at 1.0×10^5 CFU mL⁻¹ and 1.0×10^6 CFU mL⁻¹ levels produced highly reproducible results with % RSDs of ≤ 15%, for all three quantitative transitions, demonstrating the effectiveness of the method. Similarly, inter-peptide %RSDs of ≤ 2% and ≤ 9% for 1.0×10^5 CFU mL⁻¹ and 1.0×10^6

CFU mL⁻¹, respectively, show significant agreement among the three transitions used for quantification, indicating that the evaluated peptides did not differ with respect to precision. To determine the accuracy of the measurements the experimentally-determined *S. aureus* concentration was compared against the amount spiked. Inter-peptide accuracies were determined to be 31% and 1% for the 1.0x10⁵ CFU mL⁻¹ and 1.0x10⁶ CFU mL⁻¹ concentrations, respectively. Although the accuracy of the low-level spike appears to have a slight high bias, CFUs are only an estimate of the number of cells present³¹², as the accuracy of the method is dependent on the reference curve obtained via direct plate count and optical density readings. Despite the limitations of plate counting and optical density readings we have rigorously standardized all steps in our ¹⁵N PAD method to control and minimize error in the analyses.

Table 5-2 Precision and accuracy of *S. aureus* quantitative measurements. Three technical replicates were performed for n = 5 identical samples at two concentration levels. Std. dev. = standard deviation; %RSD = % relative standard deviation.

<i>S. aureus</i> Measurements (CFU mL ⁻¹)						
	Spike Concentration (CFU mL ⁻¹)	Intra-peptide concentration (mean ± st. dev.) (%RSD)	Inter-peptide concentration (mean ± st. dev.) (% RSD)	Spike Concentration (CFU mL ⁻¹)	Intra-peptide concentration (mean ± st. dev.) (%RSD)	Inter-peptide concentration (mean ± st. dev.) (% RSD)
n = 5						
SIAQSIEK	1.00x10 ⁵	1.30x10 ⁵ ± 1.16x10 ⁴ (8.9)		1.00x10 ⁶	9.70x10 ⁵ ± 1.04x10 ⁵ (10.7)	
LGVILPVTK	1.00x10 ⁵	1.33x10 ⁵ ± 2.00x10 ⁴ (15.0)	1.31x10 ⁵ ± 1.73x10 ³ (1.3)	1.00x10 ⁶	1.02x10 ⁶ ± 1.35x10 ⁵ (13.2)	1.01x10 ⁶ ± 1.16x10 ⁴ (8.9)
LIYGIPQLIEYK	1.00x10 ⁵	1.30x10 ⁵ ± 1.70x10 ⁴ (13.1)		1.00x10 ⁶	1.04x10 ⁶ ± 1.53x10 ⁵ (14.7)	

Finally, verification that complete digestion has been achieved is essential for accurately quantifying proteins using MS³¹³, and to ensure long term stability of the quantification method. Digestion parameters, including incubation time and temperature, amount of trypsin, and amount of acid-labile detergent, were varied and peptide recoveries were determined. Maximum peptide yields were assumed to have been achieved when no further increase in ¹⁴N or ¹⁵N peptide amounts could be observed.

Three specific peptides from different regions of the protein were quantified to ensure complete digestion of the protein and accuracy of the measurements. Three digestion protocols were compared 1) overnight tryptic digestion at 37 °C; 2) 2-h tryptic digestion at 37 °C; and 3) 3-min tryptic digestion at 52 °C. For each protocol, triplicate *S. aureus* samples at 5.0×10^5 CFU mL⁻¹, were subjected to the 2-h phage amplification event, proteolytically digested, and analyzed by LC-ESI-MS/MS. Each sample preparation was analyzed in triplicate. Table 5-3 shows the comparison of the different digestion conditions. The number of live *S. aureus* cells obtained from three independent analyses of a standard solution of 5.0×10^5 CFU mL⁻¹ following phage infection were determined to be 5.0×10^5 CFU mL⁻¹, 4.7×10^5 CFU mL⁻¹, and 5.6×10^5 CFU mL⁻¹ for the 3 minute/52 °C, 2 hour/37 °C and 18 h/37 °C digestion protocols, respectively, indicating that all digestion techniques yielded good precision and accuracy (Table 5-3). Means for the three quantitative peptide transitions, at each digest condition, were reproducible with %RSDs of $\leq 13\%$. Inter-peptide agreement at each digest condition resulted in %RSDs of $\leq 5\%$, indicating that each protocol was robust and suitable for the peptides evaluated. The inter-peptide accuracy of the 3-min ¹⁵N PAD MS method was calculated to be 100%, indicating that the rapid 3-min digest incubated at 52 °C was a good, rapid alternative to the longer traditional tryptic digestion methods that use 37°C incubation temperature and 2-18 h digestion times. Furthermore, the accuracy of the method and the good agreement between values obtained independently on the three peptides suggests that all three digestion techniques yielded complete digestion of the major capsid protein of Bacteriophage 53.

Table 5-3 Verification of completeness of digestion for the SIAQSIEK, LGVILPVTk, and LIYGIPQLIEYK quantitative peptide transitions. For ^{15}N PAD MS measurements, 5.0×10^5 CFU mL^{-1} of spiked *S. aureus* was subjected to phage amplification, tryptic digest, and LC-MS/MS analysis. Triplicate results for each preparation are shown and intra-peptide and inter-peptide means (CFU mL^{-1} tested), standard deviations, and percent relative standard deviations (%RSDs) for $n = 3$ sample preparations is reported. Std. dev. = standard deviation; %RSD = % relative standard deviation.

3-min Digestion Protocol (5x10 ⁵ CFU mL ⁻¹ spiked <i>S. aureus</i>)					
	3-min	3-min	3 -min	3-min ¹⁵ N PAD Digest Intra-peptide (mean ± st. dev.) (%RSD)	3-min ¹⁵ N PAD Digest Inter-peptide (mean ± st. dev.) (%RSD)
n = 3	¹⁵ N PAD Digest 1	¹⁵ N PAD Digest 2	¹⁵ N PAD Digest 3		
SIAQSIEK	5.33x10 ⁵	5.55x10 ⁵	4.84x10 ⁵	5.24x10 ⁵ ± 3.64x10 ⁴ (6.95)	5.00x10 ⁵ ± 2.09x10 ⁴ (4.18)
LGVILPVTK	4.83x10 ⁵	5.03x10 ⁵	4.86x10 ⁵	4.91x10 ⁵ ± 1.06x10 ⁴ (2.18)	
LIYGIPQLIEYK	4.72x10 ⁵	5.20x10 ⁵	4.64x10 ⁵	4.85x10 ⁵ ± 3.05x10 ⁴ (6.29)	
2-h Digestion Protocol (5x10 ⁵ CFU mL ⁻¹ spiked <i>S. aureus</i>)					
	2-h	2-h	2-h	2-h ¹⁵ N PAD Digest Intra-peptide (mean ± st. dev.) (%RSD)	2-h ¹⁵ N PAD Digest Inter-peptide (mean ± st. dev.) (%RSD)
n = 3	¹⁵ N PAD Digest 1	¹⁵ N PAD Digest 2	¹⁵ N PAD Digest 3		
SIAQSIEK	4.74x10 ⁵	4.19x10 ⁵	4.73x0 ⁵	4.56x10 ⁵ ± 3.13x10 ⁴ (6.86)	4.74x10 ⁵ ± 1.82x10 ⁴ (3.83)
LGVILPVTK	4.96x10 ⁵	4.66x10 ⁵	5.14x10 ⁵	4.92x10 ⁵ ± 2.39x10 ⁴ (4.85)	
LIYGIPQLIEYK	4.80x10 ⁵	4.57x10 ⁵	4.90x10 ⁵	4.76x10 ⁵ ± 1.69x10 ⁴ (3.56)	
Overnight Digestion Protocol (5x10 ⁵ CFU mL ⁻¹ spiked <i>S. aureus</i>)					
	Overnight	Overnight	Overnight	Overnight ¹⁵ N PAD Digest Intra-peptide (mean ± st. dev.) (%RSD)	Overnight ¹⁵ N PAD Digest Inter-peptide (mean ± st. dev.) (%RSD)
n = 3	¹⁵ N PAD Digest 1	¹⁵ N PAD Digest 2	¹⁵ N PAD Digest 3		
SIAQSIEK	5.42x10 ⁵	6.47x10 ⁵	5.60x10 ⁵	5.83x10 ⁵ ± 5.64x10 ⁴ (9.67)	5.67x10 ⁵ ± 1.48x10 ⁴ (2.61)
LGVILPVTK	5.06x10 ⁵	6.38x10 ⁵	5.53x10 ⁵	5.66x10 ⁵ ± 6.70x10 ⁴ (11.84)	
LIYGIPQLIEYK	5.04x10 ⁵	6.30x10 ⁵	5.26x10 ⁵	5.54x10 ⁵ ± 6.74x10 ⁴ (12.17)	

5.5. Conclusions

Rapid, accurate, and sensitive quantitation of *S. aureus* has been achieved by ^{15}N PAD and LC-MS/MS. To fulfill this goal we focused on 1) developing a rapid ^{15}N phage amplification step that could simultaneously infect all *S. aureus* cells; 2) developing a

rapid and efficient proteolytic digestion method; and 3) employing high-throughput LC-ESI-MS/MS for rapid, sensitive, and specific quantitation. The ability of our method to inoculate with high ^{15}N -labeled phage titers (higher than the LC-MS/MS detection limit) allows *S. aureus* cells to be infected simultaneously, permitting *S. aureus* quantitation and offering time-saving advantages over standard PAD methodologies. Traditional digestion protocols often include reduction and alkylation steps followed by lengthy trypsin incubation times that range from several hours to overnight. The rapid 3-min digest produced maximum peptide yields that showed no significant difference in peptide recoveries when compared to traditional digest preparations, thereby enhancing the rapidity of the method. Phage-amplified digest samples were quantified by LC-MS/MS configured for alternating column regeneration to further increase sample throughput. Using two columns, two pumps, and one 2-position 10-port valve allowed switching between columns for short cycle times from injection to injection. Extracted ion chromatograms of the labeled and unlabeled peptide isoforms showed co-elution of the peptide pairs with high retention time reproducibility and allowed the ^{15}N signals to be used as retention time indicators for the native peptide signals, thus improving precision for quantifying peptide abundances. MRM MS allowed simultaneous quantitation of peptides from the phage capsid protein as a measure of *S. aureus* concentration and method specificity was enhanced by monitoring three ion transitional pairs for each peptide for a total of 12 independent ion transitions used for quantitation and confirmation of the phage protein of interest.

While we have demonstrated the feasibility of this approach using cultivated *S. aureus*, Staphylococcal bacteriophage 53 and LC-MS/MS, this quantitative technique

should be broadly applicable to other bacteria. The presented data encourages the continued development and use of isotopically labeled PAD MS-based methods for rapid bacterial quantification.

There are many possible applications to the ^{15}N PAD MS quantification method. The method uses the specificity of the bacteriophage to identify the bacteria of interest and should be able to accurately quantify a target bacteria in mixed cultures. Traditional techniques require an enrichment culture followed by plating and subsequent culturing of single colonies to obtain pure cultures. The use of the ^{15}N PAD MS method would allow direct detection and accurate quantification of a target bacteria in the enrichment culture and perhaps directly from some clinical samples. Furthermore, since phage only amplify with live bacterial cells, there is the possibility of testing the effectiveness of antibiotics on a culture or clinical isolate. Antibiotic susceptibility testing should only require the addition of different classes and different concentrations of antibiotics to split enrichment cultures prior to phage infection, and following phage amplification the number of viable bacterial cells can be quantified by the ^{15}N PAD MS method.

CHAPTER 6. CONCLUSIONS AND OUTLOOK

6.1. Abstract

This chapter reviews the current progress of MS for clinical diagnostics and discusses trends and future developments. This chapter concludes with a discussion of potential future directions to further expand this dissertation work.

6.2. Mass spectrometry for clinical diagnostics

Magnetic Resonance Imaging (MRI) spectroscopy, a harmless and noninvasive diagnostic tool, is frequently used to detect abnormalities in the body and to produce images that can later lead to effective treatments. Magnetic resonance was first studied in the 1940s and 1950s, and in 1952 Edward Purcell and Felix Bloch were awarded the Nobel Prize for their 1946 work demonstrating successful magnetic resonance in bulk matter³¹⁴. The first MRI scanner was invented by Raymond Vahan Damadian in 1971³¹⁵. For nearly seven years skeptics claimed it could not be done, but in 1977, the first human MRI body scan was performed³¹⁶⁻³¹⁸. The set-up took almost five hours to produce a single image, the images were, by modern standards, rudimentary, and these first imaging techniques were never incorporated into practicable, functional methodologies in what is considered MR imaging as we know it today. Nevertheless, in the early 1980s, 40 years following Purcell and Bloch's award-winning work, MRI instrumentation began its ascent towards becoming widely adopted as a diagnostic resource. To accomplish this goal, tremendous reach and development has been made since its emergence, and

limitations have been overcome to advance MRI technology for use in the medical community in routine clinical diagnostics. Today, functional MRI spectroscopy is an extensively used tool, helping diagnosis of anything from brain tumors to torn ligaments³¹⁹, imaging in seconds what used to take hours³¹⁹. While MRI equipment is expensive to buy, about \$1-2 million, and to operate, \$400 to \$3,500 per procedure, 10,000 MRI scanners around the world perform 75 million scans annually³¹⁸. MRI is considered one of the most useful diagnostics tools of our time.

Comparatively, the field of MS is in its infancy and faces similar challenges to render clinical diagnostic applications substantially more simple and efficient in the near future. While MS has been around for over a century and is well established in the physical, chemical, and biochemical sciences³²⁰, it has only come of age in the biological and life sciences during the past two decades, following ESI and MALDI ionization³²¹. During this brief history of success, MS has made significant improvements, including speed, sensitivity, resolution, mass accuracy, cost, ease-of-use, and availability. Today, while the price for a mass spectrometer is relatively high, on average \$270,000, there are over 250,000 active MS systems worldwide and the market is rapidly maturing³²². Concurrently, the “omics” disciplines (metabolomics, proteomics, genomics, and transcriptomics) have emerged and are beginning to impact diagnostics, therapeutics, and drug development³²³. Recently, the field of neonatal screening for metabolic disorders has emerged as the first broadly accepted routine use of MS in clinical diagnostics, allowing more than 30 different metabolic disorders to be simultaneously quantified using MS/MS³²⁴. MS in clinical diagnosis is also prevalent in toxicant and drugs-of-abuse screening, endocrinology and hormone analysis, therapeutic drug monitoring, oncology

drug testing, and anti-viral drug testing³²⁵⁻³³⁰. Still, protein-based assays developed on novel or complex platforms such as MS have not been well established in the clinical context³³¹ and MS is not yet routinely used in clinical diagnostics for the detection of disease-related proteins or peptides³³².

So what clinical utility does MS-based diagnostics hold today and what are the future trends of tomorrow? Constructive communication, interpretation, translation, and cooperation between laboratorians and clinicians is paramount to realize the potential and limitations of MS-based medical diagnostics. The emerging field of MS-based metabolomics has greatly risen in prominence over the past few years and holds immense potential for clinical diagnostics, along with vast progress in the fields of MS-based genomics and proteomics³³³. MS-based technologies for conventional proteomics are likely to play similarly important roles in clinical discovery applications and clinical proteomics, however the potential of its future applications for novel diagnostics is uncertain³³⁴. For clinical diagnostics, sensitivity, reproducibility and robustness all have to be optimized while still allowing high-throughput and automated analysis³³⁴, and it remains to be determined which MS-based technologies may provide the decisive advantages in clinical diagnosis³³⁴. LC-ESI-MS/MS appears to be the instrument of choice at the discovery stage but due to its complexity and lengthy times of analysis, to date, LC-ESI-MS/MS has only played a minor role in clinical diagnostics³³⁴. Further, its sensitivity is competitively challenged when compared to traditional techniques and it can require technically-difficult sample preparations that don't exist in present workflows. However, LC-ESI-MS/MS's speed of assay development, relatively low cost-per-sample, and high specificity³³⁵, coupled with its successful history for validation and

quantitation of small molecules, is currently influencing its role in peptide and protein detection, validation and quantitation in clinical samples. Because MALDI-TOF MS has a faster acquisition system, making it more suitable for high-throughput analyses, and is less technically sophisticated than LC-ESI-MS/MS, it has a high potential for improving clinical diagnostics³³² and is often preferred over LC-ESI-MS/MS for routine measurements³³². MALDI-TOF MS's offline operation also has the additional advantage of allowing simultaneous preparation of hundreds of samples in a clinical setting³³².

MS for microbial diagnostics is in its formative years³³⁶ and requires substantial work, however, recent progress is encouraging and the future appears bright³³⁷. Metabolic profiling by gas chromatography (GC)-TOF MS has recently been explored as a tool to detect and discriminate pathogenic organisms³³⁸. MALDI-TOF MS has been recently described as a rapid, reliable, and cost-effective alternative for bacteria, mycobacteria, and fungi identification³³⁹⁻³⁴⁴ and large diagnostic centers already exist for MALDI-TOF MS bacterial identification³⁴⁵. Bruker Daltonic's commercially available MALDI Biotyper (Bruker Daltonics, Bremen, Germany) is designed to rapidly identify bacteria, yeasts, and fungi³⁴⁶ and offers rapidity, high specificity, low false positives, low operational costs, and low technical barriers for new operators^{347, 348}. The initial preparations are from a cultured colonies and identification is performed by matching protein fingerprint spectra to a database, allowing 30-60 identifications per hour^{346, 349}. Currently, Bruker Diagnostics is taking steps to file its MALDI Biotyper TOF MS with the US Food and Drug Administration (FDA)³⁴⁹ for approval to run clinical samples, and has already installed over 150 of such systems worldwide in routine laboratories for microbiology³⁴⁷. As MALDI-TOF MS technology has not been approved in the US to run

clinical samples, such an approval would be a milestone for clinical diagnostics and would have major implications for the clinical lab community³⁴⁹. A recent comparative analysis of the Bruker Biotyper MALDI-TOF MS with the BD Phoenix automated microbiology system (Becton Dickinson, Franklin Lakes, NJ), which utilizes biochemical and enzymatic substrates with a variety of colorimetric and fluorescent indicators,³⁵⁰ was performed with over 400 Gram-negative bacilli collected from multiple clinical sources³⁵¹. The study concluded that the Bruker MALDI Biotyper either performed equivalently or outperformed the Phoenix and with the improved turnaround time and cost-effectiveness provided, advanced bacterial identification in the clinical microbiology laboratory³⁵¹. This methodology may become the method of choice for high-throughput testing in clinical microbiology, proving accurate, fast, automatable, and cost-efficient results³³⁶. However, it is our view that the approaches described herein do not compete but actually complement each other for their ability to provide information³²⁴ and will be recognized as such in future novel diagnostics. Clinical specimen screening via mass profiling coupled with sequence-based confirmatory analysis provides confidence in microbial identification. Given the complementary nature of proteomic information provided by top-down and bottom-up strategies, both will continue to be employed for protein identification and characterization and a melding of the two strategies is already in progress with the emergence of “middle-down” proteomics³⁵². Similarly, proteomics offers highly complementary information to genomics, and integrating genotypic and proteomics applications with MS can provide an even more powerful approach for bacterial identification. Improvements and new approaches in technology are now emerging that open up the possibility for the development of multiparameter detection

methods. These multiparametric analyses offer tailored procedures that can, for instance, take advantage of the sensitivity associated with performance of immunoassays and nucleic acid amplification and couple these techniques with the high-analytical attributes of MS (i.e immuno-MS, PCR-MS)^{336, 353}. The commercially available Ibis T5000™ “universal” Biosensor System (Ibis Biosciences, Abbott Molecular, Inc., Abbott Park, IL) couples nucleic acid amplification to high performance ESI-MS and base-composition analysis (PCR-ESI-TOF MS) for identification of bacteria, viruses, fungi, and protozoa in clinical and environmental matrices^{354, 355}. The latest Ibis T5000 automated platform, the PLEX-ID, is based on technology developed for the Department of Defense (DOD) known as T.I.G.E.R. (Triangulation Identification for the Genetic Evaluation of Risks) for pathogen surveillance²²⁹. The PLEX-ID workflow can analyze up to 180 samples in 24 hours and allows detection and characterization of known and previously unknown organisms³⁵⁶ by determination of base composition fingerprints and subsequent identification by matching fingerprint spectra to a reference amplicon database, without any prior knowledge of the sample³⁵⁵. The PLEX-ID System is currently pending FDA approval for clinical diagnostics and is already employed by the Federal Bureau of Investigation (FBI) for routine forensics analyses³⁵⁶. These hybrid MS-based applications also hold great promise for stepwise replacing or complementing culture-based, biochemical, traditional serological, and traditional molecular methodologies in microbiology laboratories³³⁶ and have the potential to play a significant role in the future of modern diagnostic microbiology.

6.3. Proposed Future Directions

Bacterial identification and characterization is used in a wide variety of applications, and while many traditional approaches for detection exist, perhaps MS-based methods can offer faster and more definitive answers. The results presented here demonstrate the potential and advantages of using MS for bacterial detection and quantification. A relatively large amount of research needs to be completed in order to overcome recognized limitations. The following studies are recommended for future research:

6.3.1. *C. burnetii* analysis and strain-level discrimination by MS

1. Bacterial diversity studies, and in particular bacterial profiling techniques, for taxonomical classification involve recognition of similarities, differences, and relationships. Thus, it is of importance that a sufficient number of strains and adequate sample sizes are included into analyses in order to reduce uncertainty in statistical analyses. Incorporating additional *C. burnetii* strains into these MS-based techniques could be undertaken as an incremental project to further confirm and strengthen these findings.
2. Bacterial analyses of cellular proteins by MS generally does not have the sensitivity of PCR-based DNA methods or immunoassays^{332, 357}. To increase sensitivity, the bulk of past work has focused on bacterial identification following culture (as a means of multiplying and isolating the organism). A limitation of the projects described in Chapters 2 and 3 was that traditional culture of a slow-growing organism was necessary to overcome sensitivity issues, thus hindering

rapid analysis. Current progress should expand to more sensitive methodologies involving biodetection without pre-enrichment, thus encouraging timeliness and reducing sample preparation complexity. The ^{15}N PAD MS methodology, described in Chapters 4 and 5, is an alternative approach that possesses enormous potential to help overcome this challenge. Immunoassays are currently among the most sensitive detection methods available, thus, immuno-MS assays techniques that do not require cultivation should be taken into consideration. Such MS-based immunoassays use antibodies to isolate and separate bacterial targets from other flora and matrix constituents, and once isolated, captured bacteria are concentrated and detected by MS^{141, 332, 358}. MS techniques that analyze PCR products (PCR-MS) have also been shown to produce more sensitive, vastly quicker, and higher throughput approaches^{359, 360} and should also be explored.

6.3.2. *S. aureus* detection and quantitation by MS

1. ^{15}N PAD coupled with mass spectrometric detection possesses characteristics suitable for everyday use for bacterial detection in the clinical microbiology laboratory and the simplicity of the analysis combined with inexpensive sample reagents makes implementation of this methodology foreseeable in a clinical setting. Working towards this mean, future goals should focus on optimizing the experimental design in order to execute high throughput parallel laboratory automation that will further reduce detect-to-protect response times. Transferring the technology to a multi-well plate format and taking advantage of the already developed field of robotics handling, would be ideal for performing ^{15}N PAD

inoculation and incubation, automated parallel trypsin digestion, and sample handling directly to the autosampler for LC-ESI-MS/MS analysis. Direct sample infusion into the mass spectrometer should be explored, thus eliminating the need for the time-consuming aspect of the LC separation and rendering this method more amenable to a high-throughput workflow. Similarly, MALDI-TOF MS's characteristic off-line analysis capability makes it is easily adaptable for automated parallel analysis, creating the possibility of analyzing hundreds of samples per hour following incubation. Overall, integrating faster and more user-friendly technology would minimize human involvement in the sample work-flow and would require less technical skill and expertise.

2. As discussed in Chapter 4, further development of PAD MS methodologies should investigate alternative labeling strategies. Incorporating ^{13}C isotopes into the bacteriophage proteome to increase the observed MALDI mass shift from the parent/progeny peaks could potentially resolve the parent/progeny peaks, increasing sensitivity of the measurements, and allowing for a more rapid PAD method.
3. As discussed in Chapters 4 and 5, current concerns of emerging antibiotic-resistant bacteria, and in particular strains of *S. aureus*, has provoked initial work that will incorporate antibiotic susceptibility testing into the ^{15}N PAD MS workflow for detecting methicillin-type resistant (MRSA) and methicillin-type susceptible (MSSA) *S. aureus* isolates. Because bacteriophage will only infect and replicate in viable host cells, PAD has the ability to rapidly determine antibiotic resistant bacterial strains. A potential antibiotic susceptibility

experiment would involve addition of antibiotics to live bacterial cells, infection of the bacterial sample with its proper phage, and analysis by MS. Relative to the control (phage + bacteria – antibiotic), if a successful phage amplification event is observed in the presence of the antibiotic-treated cells, that particular bacterial strain would be classified as antibiotic resistant. Whereas, if the phage does not propagate relative to the control, the bacterium in the sample would be classified as antibiotic susceptible.

4. A multiplex-¹⁵N PAD MS approach for specific and simultaneous detection and accurate quantification of bacteria that are common human pathogens would be of importance for faster disease diagnosis, treatment of infection, and prevention of outbreaks from potential medical, environmental, or terroristic sources. A potential experimental protocol would allow multiple identification of different target pathogenic bacteria (*S. aureus*, *S. pyogenes*, *E. coli*, *Salmonella typhi*, *Bordetella pertussis*, *Clostridium difficile*...) by detection of their respective phage. Following the phage amplification step, samples would be analyzed via MALDI-TOF MS or LC-ESI/MS/MS for proteins or peptide fragments unique to each of the host-specific phages. Thus, if phage propagation was only ascertained for T4, a phage that specifically infects *E. coli*, the source of bacterial infection would be determined and the possibility of co-infection by other multiplexed pathogens would be eliminated.

REFERENCES

1. Alzheimer, A., Ein Fall von leutischer Meningomyelitis und -encephalitis [A case of leutic meningomyelitis and encephalitis]. *Archiv fuer Psychiatrie* **1897**, 29, (63), 1-17.
2. Emerson, D.; Agulto, L.; Liu, H.; Liu, L., Identifying and Characterizing Bacteria in an Era of Genomics and Proteomics. *BioScience* 2008, pp 925-36.
3. Wilkins, C. L.; Lay, J. O., *Identification of Microorganisms by Mass Spectrometry*. John Wiley and Sons: Hoboken, NJ, 2006; Vol. 169, p 352.
4. Sintchenko, V.; Iredell, J. R.; Gilbert, G. L., Pathogen profiling for disease management and surveillance. *Nat Rev Microbiol* **2007**, 5, (6), 464-70.
5. Beck, R., *A Chronology of Microbiology in Historical Context*. ASM Press: Washington DC, 2000.
6. Rosati, L. A., The microbe, creator of the pathologist: an inter-related history of pathology, microbiology, and infectious disease. *Ann Diagn Pathol* **2001**, 5, (3), 184-89.
7. Kjelle, M., *Louis Pasteur: Fighter Against Contagious Disease (Uncharted, Unexplored, Unexplained)*. Mitchell Lane: USA, 2005; p 48.
8. Baxby, D., *Jenner's Smallpox Vaccine: The Riddle of Vaccinia Virus and Its Origin*. Heinemann Educational Books: London, 1981.
9. Jenn, E., *Inquiry into the Causes and Effects of the Variolae Vaccine*. Sampson Low: London, 1798; p 45.
10. Robert Koch, B. Robert Koch - Biography, Nobelprize.org, Accessed Jan 25, 2011.
11. Stern, A. M.; Markel, H., The history of vaccines and immunization: familiar patterns, new challenges. *Health Aff (Millwood)* **2005**, 24, (3), 611-21.
12. Mangili, A.; Gendreau, M. A., Transmission of infectious diseases during commercial air travel. *Lancet* **2005**, 365, (9463), 989-96.
13. Webster, C. H., Airline operating realities and the global spread of infectious diseases. *Asia Pac J Public Health* **2010**, 22, (3 Suppl), 137S-143S.
14. Kourkine, I. V.; Ristic-Petrovic, M.; Davis, E.; Ruffolo, C. G.; Kapsalis, A.; Barron, A. E., Detection of Escherichia coli O157:H7 bacteria by a combination of immunofluorescent staining and capillary electrophoresis. *Electrophoresis* **2003**, 24, (4), 655-61.

15. Chugh, T. D., Emerging and re-emerging bacterial diseases in India. *J Biosci* **2008**, 33, (4), 549-55.
16. Howard, B.; Keisser, J., *Clinical and Pathogenic Microbiology*. 2nd ed.; Mosby: St. Louis, 1994.
17. Malone, D. L.; Genuit, T.; Tracy, J. K.; Gannon, C.; Napolitano, L. M., Surgical site infections: reanalysis of risk factors. *J Surg Res* **2002**, 103, (1), 89-95.
18. Tasota, F. J.; Fisher, E. M.; Coulson, C. F.; Hoffman, L. A., Protecting ICU patients from nosocomial infections: practical measures for favorable outcomes. *Crit Care Nurse* **1998**, 18, (1), 54-65; quiz 66-67.
19. *Biological and chemical terrorism: strategic plan for preparedness and response. Recommendations of the CDC Strategic Planning Workgroup.* ; MMWQ Recomm Rep: 2000; pp 1-14.
20. Weapons of Mass Destruction: An Encyclopedia of Worldwide Policy, Technology, and History. In Croddy, E.; Wirtz, J.; Larsen, J., Eds. ABC-CLIO, Inc.: Santa Barbara, 2005; Vol. 2, p 600.
21. Karwa, M.; Currie, B.; Kvetan, V., Bioterrorism: Preparing for the impossible or the improbable. *Crit Care Med* **2005**, 33, (1 Suppl), S75-95.
22. Fraser, C. M.; Dando, M. R., Genomics and future biological weapons: the need for preventive action by the biomedical community. *Nat Genet* **2001**, 29, (3), 253-56.
23. Wallin, A.; Luksiene, Z.; Zagminas, K.; Surkiene, G., Public health and bioterrorism: renewed threat of anthrax and smallpox. *Medicina (Kaunas)* **2007**, 43, (4), 278-84.
24. Jernigan, D. B.; Raghunathan, P. L.; Bell, B. P.; Brechner, R.; Bresnitz, E. A.; Butler, J. C.; Cetron, M.; Cohen, M.; Doyle, T.; Fischer, M.; Greene, C.; Griffith, K. S.; Guarner, J.; Hadler, J. L.; Hayslett, J. A.; Meyer, R.; Petersen, L. R.; Phillips, M.; Pinner, R.; Popovic, T.; Quinn, C. P.; Reefhuis, J.; Reissman, D.; Rosenstein, N.; Schuchat, A.; Shieh, W. J.; Siegal, L.; Swerdlow, D. L.; Tenover, F. C.; Traeger, M.; Ward, J. W.; Weisfuse, I.; Wiersma, S.; Yeskey, K.; Zaki, S.; Ashford, D. A.; Perkins, B. A.; Ostroff, S.; Hughes, J.; Fleming, D.; Koplan, J. P.; Gerberding, J. L., Investigation of bioterrorism-related anthrax, United States, 2001: epidemiologic findings. *Emerg Infect Dis* **2002**, 8, (10), 1019-28.
25. Gerberding, J. L.; Hughes, J. M.; Koplan, J. P., Bioterrorism preparedness and response: clinicians and public health agencies as essential partners. *JAMA* **2002**, 287, (7), 898-900.
26. Marrie, T. J., Raoult, D. , *Antimicrob Agents* **1997**, 8, 145-161.

27. Thompson, H. A.; Hoover, T. A.; Vodkin, M. H.; Shaw, E. I., Do chromosomal deletions in the lipopolysaccharide biosynthetic regions explain all cases of phase variation in *Coxiella burnetii* strains? An update. *Annl NY Acad Sci* **2003**, 990, 664-70.
28. Samuel, J. E.; Frazier, M. E.; Mallavia, L. P., Correlation of plasmid type and disease caused by *Coxiella burnetii*. *Infect Immun* **1985**, 49, (3), 775-79.
29. Schmidt, F.; Scharf, S. S.; Hildebrandt, P.; Burian, M.; Bernhardt, J.; Dhople, V.; Kalinka, J.; Gutjahr, M.; Hammer, E.; Volker, U., Time-resolved quantitative proteome profiling of host-pathogen interactions: the response of *Staphylococcus aureus* RN1HG to internalisation by human airway epithelial cells. *Proteomics* **2010**, 10, (15), 2801-11.
30. Sturenburg, E., Rapid detection of methicillin-resistant *Staphylococcus aureus* directly from clinical samples: methods, effectiveness and cost considerations. *Ger Med Sci* **2009**, 7, Doc06.
31. Kurlenda, J.; Grinholc, M., Current diagnostic tools for methicillin-resistant *Staphylococcus aureus* infections. *Mol Diagn Ther* **2010**, 14, (2), 73-80.
32. Cattoir, V.; Merabet, L.; Djibo, N.; Rioux, C.; Legrand, P.; Girou, E.; Lesprit, P., Clinical impact of a real-time PCR assay for rapid identification of *Staphylococcus aureus* and determination of methicillin resistance from positive blood cultures. *Clin Microbiol Infect* **2011**, 17 (3), 425-31.
33. Cosgrove, S. E.; Sakoulas, G.; Perencevich, E. N.; Schwaber, M. J.; Karchmer, A. W.; Carmeli, Y., Comparison of mortality associated with methicillin-resistant and methicillin-susceptible *Staphylococcus aureus* bacteremia: a meta-analysis. *Clin Infect Dis* **2003**, 36, (1), 53-59.
34. Khatib, R.; Schaffer, C.; Johnson, L. B., *Staphylococcus aureus* in a single positive blood culture: causes and outcome. *Scand J Infect Dis* **2002**, 34, (9), 645-47.
35. van den Berg, S.; Bowden, M. G.; Bosma, T.; Buist, G.; van Dijk, J. M.; van Wamel, W. J.; de Vogel, C. P.; van Belkum, A.; Bakker-Woudenberg, I. A., A multiplex assay for the quantification of antibody responses in *Staphylococcus aureus* infections in mice. *J Immunol Methods* **2011**, 365, (1-2), 142-48.
36. Francois, P.; Scherl, A.; Hochstrasser, D.; Schrenzel, J., Proteomic approaches to study *Staphylococcus aureus* pathogenesis. *J Proteomics* **2010**, 73, (4), 701-18.
37. Mann, N. H., The potential of phages to prevent MRSA infections. *Res Microbiol* **2008**, 159, (5), 400-05.
38. Durai, R.; Ng, P. C.; Hoque, H., Methicillin-resistant *Staphylococcus aureus*: an update. *Aorn J* **2010**, 91, (5), 599-606; quiz 607-09.
39. Doern, G. V., Manual blood culture systems and the antimicrobial removal device. *Clin Lab Med* **1994**, 14, (1), 133-47.

40. Barenfanger, J.; Drake, C.; Kacich, G., Clinical and financial benefits of rapid bacterial identification and antimicrobial susceptibility testing. *J Clin Microbiol* **1999**, 37, (5), 1415-18.
41. d'Herrele, Sur un microbe invisible antagoniste des bacilles dysenteriques. *CR Acad Sci* **1917**, 165, 373-75.
42. Sandeep, K., Bacteriophage precision drug against bacterial infections. *Current Sci* **2006**, 90, (5), 631-33.
43. Kutter, E.; De Vos, D.; Gvasalia, G.; Alavidze, Z.; Gogokhia, L.; Kuhl, S.; Abedon, S. T., Phage therapy in clinical practice: treatment of human infections. *Curr Pharm Biotechnol* **2010**, 11, (1), 69-86.
44. Ackermann, H. W.; Azizbekyan, R. R.; Bernier, R. L.; de Barjac, H.; Saindoux, S.; Valero, J. R.; Yu, M. X., Phage typing of *Bacillus subtilis* and *B. thuringiensis*. *Res Microbiol* **1995**, 146, (8), 643-57.
45. Vaisanen, O. M.; Mwaisumo, N. J.; Salkinoja-Salonen, M. S., Differentiation of dairy strains of the *Bacillus cereus* group by phage typing, minimum growth temperature, and fatty acid analysis. *J Appl Bacteriol* **1991**, 70, (4), 315-24.
46. Brown, E. R.; Cherry, W. B., Specific identification of *Bacillus anthracis* by means of a variant bacteriophage. *J Infect Dis* **1955**, 96, (1), 34-39.
47. van der Mee-Marquet, N.; Loessner, M.; Audurier, A., Evaluation of seven experimental phages for inclusion in the international phage set for the epidemiological typing of *Listeria monocytogenes*. *Appl Environ Microbiol* **1997**, 63, (9), 3374-77.
48. Bannerman, E.; Boerlin, P.; Bille, J., Typing of *Listeria monocytogenes* by monocin and phage receptors. *Int J Food Microbiol* **1996**, 31, (1-3), 245-62.
49. Akinyemi, K. O.; Philipp, W.; Beyer, W.; Bohm, R., Application of phage typing and pulsed-field gel electrophoresis to analyse *Salmonella enterica* isolates from a suspected outbreak in Lagos, Nigeria. *J Infect Dev Ctries* **2010**, 4, (12), 828-33.
50. Ross, I. L.; Davos, D. E.; Mwanri, L.; Raupach, J.; Heuzenroeder, M. W., MLVA and Phage Typing as Complementary Tools in the Epidemiological Investigation of *Salmonella enterica* serovar Typhimurium Clusters. *Curr Microbiol* **2010**, 62, (3), 1034-38.
51. Baggesen, D. L.; Sorensen, G.; Nielsen, E. M.; Wegener, H. C., Phage typing of *Salmonella* Typhimurium - is it still a useful tool for surveillance and outbreak investigation? *Euro Surveill* **2010**, 15, (4), 19471.
52. Wildemauwe, C.; De Brouwer, D.; Godard, C.; Buysens, P.; Dewit, J.; Joseph, R.; Vanhoof, R., The use of spa and phage typing for characterization of a MRSA

population in a Belgian hospital: comparison between 2002 and 2007. *Pathol Biol (Paris)* **2010**, 58, (1), 70-72.

53. el-Ghodban, A.; Ghenghesh, K. S.; Marialigeti, K.; Tawil, A., Enterotoxins and phage typing of *Staphylococcus aureus* isolated from clinical material and food in Libya. *Arch Inst Pasteur Tunis* **1999**, 76, (1-4), 23-25.

54. Konstantinidis, K. T.; Ramette, A.; Tiedje, J. M., The bacterial species definition in the genomic era. *Philos Trans R Soc Lond B Biol Sci* **2006**, 361, (1475), 1929-40.

55. Sauer, S.; Kliem, M., Mass spectrometry tools for the classification and identification of bacteria. *Nat Rev Microbiol* **2010**, 8, (1), 74-82.

56. Oliveira, K.; Procop, G. W.; Wilson, D.; Coull, J.; Stender, H., Rapid identification of *Staphylococcus aureus* directly from blood cultures by fluorescence in situ hybridization with peptide nucleic acid probes. *J Clin Microbiol* **2002**, 40, (1), 247-51.

57. Su, X. L.; Li, Y., Quantum dot biolabeling coupled with immunomagnetic separation for detection of *Escherichia coli* O157:H7. *Anal Chem* **2004**, 76, (16), 4806-10.

58. Hahn, M. A.; Tabb, J. S.; Krauss, T. D., Detection of single bacterial pathogens with semiconductor quantum dots. *Anal Chem* **2005**, 77, (15), 4861-69.

59. Ho, J. A.; Hsu, H. W.; Huang, M. R., Liposome-based microcapillary immunosensor for detection of *Escherichia coli* O157:H7. *Anal Biochem* **2004**, 330, (2), 342-49.

60. Ho, J. A.; Hsu, H. W., Procedures for preparing *Escherichia coli* O157:H7 immunoliposome and its application in liposome immunoassay. *Anal Chem* **2003**, 75, (16), 4330-4.

61. Zhao, X.; Hilliard, L. R.; Mechery, S. J.; Wang, Y.; Bagwe, R. P.; Jin, S.; Tan, W., A rapid bioassay for single bacterial cell quantitation using bioconjugated nanoparticles. *Proc Natl Acad Sci U S A* **2004**, 101, (42), 15027-32.

62. Goodridge, L.; Chen, J.; Griffiths, M., Development and characterization of a fluorescent-bacteriophage assay for detection of *Escherichia coli* O157:H7. *Appl Environ Microbiol* **1999**, 65, (4), 1397-404.

63. Oda, M.; Morita, M.; Unno, H.; Tanji, Y., Rapid detection of *Escherichia coli* O157:H7 by using green fluorescent protein-labeled PP01 bacteriophage. *Appl Environ Microbiol* **2004**, 70, (1), 527-34.

64. Fung, Y. S.; Wong, Y. Y., Self-assembled monolayers as the coating in a quartz piezoelectric crystal immunosensor to detect *Salmonella* in aqueous solution. *Anal Chem* **2001**, 73, (21), 5302-09.

65. Abdel-Hamid, I.; Ivnitski, D.; Atanasov, P.; Wilkins, E., Flow-through immunofiltration assay system for rapid detection of *E. coli* O157:H7. *Biosens Bioelectron* **1999**, 14, (3), 309-16.
66. Dudak, F. C.; Boyaci, I. H., Rapid and label-free bacteria detection by surface plasmon resonance (SPR) biosensors. *Biotechnol J* **2009**, 4, (7), 1003-11.
67. Lowe, C. R.; Hin, B. F.; Cullen, D. C.; Evans, S. E.; Stephens, L. D.; Maynard, P., Biosensors. *J Chromatogr* **1990**, 510, 347-54.
68. Casalnuovo, I. A.; Pierro, D.; Bruno, E.; Francesco, P.; Coletta, M., Experimental use of a new surface acoustic wave sensor for the rapid identification of bacteria and yeasts. *Lett Appl Microbiol* **2006**, 42, (1), 24-29.
69. Lay, J. O., Jr., MALDI-TOF mass spectrometry of bacteria. *Mass Spectrom Rev* **2001**, 20, (4), 172-94.
70. Ye, R. W.; Wang, T.; Bedzyk, L.; Croker, K. M., Applications of DNA microarrays in microbial systems. *J Microbiol Methods* **2001**, 47, (3), 257-72.
71. Call, D. R.; Borucki, M. K.; Loge, F. J., Detection of bacterial pathogens in environmental samples using DNA microarrays. *J Microbiol Methods* **2003**, 53, (2), 235-43.
72. Fox, A., Mass Spectrometry for Species or Strain Identification after Culture or without Culture: Past, Present, and Future. *J Clin Microbiol* **2006**, 44, (8), 2677-80.
73. Foddai, A.; Elliott, C. T.; Grant, I. R., Optimization of a phage amplification assay to permit accurate enumeration of viable *Mycobacterium avium* subsp. paratuberculosis cells. *Appl Environ Microbiol* **2009**, 75, (12), 3896-902.
74. Kutin, R. K.; Alvarez, A.; Jenkins, D. M., Detection of *Ralstonia solanacearum* in natural substrates using phage amplification integrated with real-time PCR assay. *J Microbiol Methods* **2009**, 76, (3), 241-46.
75. Seaman, T.; Trollip, A.; Mole, R.; Albert, H., The use of a novel phage-based technology as a practical tool for the diagnosis of tuberculosis in Africa. *African J Biotechnol* **2003**, 2, (2), 40-45.
76. Squirrell, D.; Price, R.; Murphy, M., Rapid and specific detection of bacteria using bioluminescence. *Anal Chim Acta* **2002**, 457, 109-14.
77. Hillier, K., Babies and bacteria: phage typing, bacteriologists, and the birth of infection control. *Bull Hist Med* **2006**, 80, (4), 733-61.
78. Bettelheim, K. A.; Beutin, L., Rapid laboratory identification and characterization of verocytotoxigenic (Shiga toxin producing) *Escherichia coli* (VTEC/STEC). *J Appl Microbiol* **2003**, 95, (2), 205-17.

79. Kremser, L.; Blaas, D.; Kenndler, E., Capillary electrophoresis of biological particles: viruses, bacteria, and eukaryotic cells. *Electrophoresis* **2004**, 25, (14), 2282-91.
80. Mossoba, M. M.; Al-Khaldi, S. F.; Jacobson, A.; Segarra Crowe, L. I.; Fry, F. S., Application of a disposable transparent filtration membrane to the infrared spectroscopic discrimination among bacterial species. *J Microbiol Methods* **2003**, 55, (1), 311-14.
81. Wenning, M.; Buchl, N. R.; Scherer, S., Species and strain identification of lactic acid bacteria using FTIR spectroscopy and artificial neural networks. *J Biophotonics* **2010**, 3, (8-9), 493-505.
82. Piraino, P.; Ricciardi, A.; Salzano, G.; Zotta, T.; Parente, E., Use of unsupervised and supervised artificial neural networks for the identification of lactic acid bacteria on the basis of SDS-PAGE patterns of whole cell proteins. *J Microbiol Methods* **2006**, 66, (2), 336-46.
83. Rodas, A. M.; Ferrer, S.; Pardo, I., 16S-ARDRA, a tool for identification of lactic acid bacteria isolated from grape must and wine. *Syst Appl Microbiol* **2003**, 26, (3), 412-22.
84. Satokari, R. M.; Vaughan, E. E.; Smidt, H.; Saarela, M.; Matto, J.; de Vos, W. M., Molecular approaches for the detection and identification of bifidobacteria and lactobacilli in the human gastrointestinal tract. *Syst Appl Microbiol* **2003**, 26, (4), 572-84.
85. Aebersold, R.; Mann, M., Mass spectrometry-based proteomics. *Nature* **2003**, 422, (6928), 198-207.
86. Fenn, J. B.; Mann, M.; Meng, C. K.; Wong, S. F.; Whitehouse, C. M., Electrospray ionization for mass spectrometry of large biomolecules. *Science* **1989**, 246, (4926), 64-71.
87. Karas, M.; Hillenkamp, F., Laser desorption ionization of proteins with molecular masses exceeding 10,000 daltons. *Anal Chem* **1988**, 60, (20), 2299-301.
88. Cody, R. B.; Laramée, J. A.; Durst, H. D., Versatile new ion source for the analysis of materials in open air under ambient Conditions. *Anal Chem* **2005**, 77, (8), 2297-302.
89. Takats, Z.; Wiseman, J. M.; Gologan, B.; Cooks, R. G., Mass spectrometry sampling under ambient conditions with desorption electrospray ionization. *Science* **2004**, 306, (5695), 471-3.
90. Kauppila, T. J.; Kotiaho, T.; Kostianen, R.; Bruins, A. P., Negative ion-atmospheric pressure photoionization-mass spectrometry. *J Am Soc Mass Spectrom* **2004**, 15, (2), 203-11.

91. McEwen, C. N.; McKay, R. G.; Larsen, B. S., Analysis of solids, liquids, and biological tissues using solids probe introduction at atmospheric pressure on commercial LC/MS instruments. *Anal Chem* **2005**, 77, (23), 7826-31.
92. Anhalt, J. P.; Fenselau, C., Identification of bacteria using mass spectrometry. *Anal Chem* **1975**, 47, 219-25
93. Dare, D., Rapid bacterial characterization and identification by MALDI-TOF mass spectrometry. In *Advances Techniques in Diagnostic Microbiology*, Springer: New York, 2006; Vol. I, pp 117-133.
94. Lay, J. O., Jr.; Holland, R. D., Rapid identification of bacteria based on spectral patterns using MALDI-TOFMS. *Methods Mol Biol* **2000**, 146, 461-87.
95. Holland, R. D.; Wilkes, J. G.; Rafii, F.; Sutherland, J. B.; Persons, C. C.; Voorhees, K. J.; Lay, J. O., Jr., Rapid identification of intact whole bacteria based on spectral patterns using matrix-assisted laser desorption/ionization with time-of-flight mass spectrometry. *Rapid Commun Mass Spectrom* **1996**, 10, (10), 1227-32.
96. Fenselau, C., The proteomic revolution has changed the capabilities of analytical chemistry. *Anal Chem* **2008**, 80, (21), 7903.
97. Demirev, P. A.; Fenselau, C., Mass spectrometry in biodefense. *J Mass Spectrom* **2008**, 43, (11), 1441-57.
98. Jarman, K. H.; Cebula, S. T.; Saenz, A. J.; Petersen, C. E.; Valentine, N. B.; Kingsley, M. T.; Wahl, K. L., An algorithm for automated bacterial identification using matrix-assisted laser desorption/ionization mass spectrometry. *Anal Chem* **2000**, 72, (6), 1217-23.
99. Pierce, C. Y.; Barr, J. R.; Woolfitt, A. R.; Moura, H.; Shaw, E. I.; Thompson, H. A.; Massung, R. F.; Fernandez, F. M., Strain and phase identification of the U.S. category B agent *Coxiella burnetii* by matrix assisted laser desorption/ionization time-of-flight mass spectrometry and multivariate pattern recognition. *Anal Chim Acta* **2007**, 583, (1), 23-31.
100. Arnold, R. J.; Reilly, J. P., Fingerprint matching of *E. coli* strains with matrix-assisted laser desorption/ionization time-of-flight mass spectrometry of whole cells using a modified correlation approach. *Rapid Commun Mass Spectrom* **1998**, 12, (10), 630-36.
101. Conway, G. C.; Smole, S. C.; Sarracino, D. A.; Arbeit, R. D.; Leopold, P. E., Phyloproteomics: species identification of Enterobacteriaceae using matrix-assisted laser desorption/ionization time-of-flight mass spectrometry. *J Mol Microbiol Biotechnol* **2001**, 3, (1), 103-12.
102. Donohue, M. J.; Smallwood, A. W.; Pfaller, S.; Rodgers, M.; Shoemaker, J. A., The development of a matrix-assisted laser desorption/ionization mass spectrometry-

based method for the protein fingerprinting and identification of *Aeromonas* species using whole cells. *J Microbiol Methods* **2006**, 65, (3), 380-89.

103. Jarman, K.; Cebula, S.; Saenz, A.; Petersen, C.; Valentine, N.; Kingsley, M.; Wahl, K., An algorithm for automated bacterial identification using matrix-assisted laser desorption/ionization mass spectrometry. *Anal Chem* **2000**, 72, (6), 1217-23.

104. DeLuca, S.; Sarver, E. W.; Harrington, P. D.; Voorhees, K. J., Direct analysis of bacterial fatty acids by Curie-point pyrolysis tandem mass spectrometry. *Anal Chem* **1990**, 62, (14), 1465-72.

105. Hathout, Y.; Demirev, P. A.; Ho, Y. P.; Bundy, J. L.; Ryzhov, V.; Sapp, L.; Stutler, J.; Jackman, J.; Fenselau, C., Identification of *Bacillus* spores by matrix-assisted laser desorption ionization-mass spectrometry. *Appl Environ Microbiol* **1999**, 65, (10), 4313-19.

106. Ryzhov, V.; Hathout, Y.; Fenselau, C., Rapid characterization of spores of *Bacillus cereus* group bacteria by matrix-assisted laser desorption-ionization time-of-flight mass spectrometry. *Appl Environ Microbiol* **2000**, 66, (9), 3828-34.

107. Ilina, E. N.; Borovskaya, A. D.; Malakhova, M. M.; Vereshchagin, V. A.; Kubanova, A. A.; Kruglov, A. N.; Svistunova, T. S.; Gazarian, A. O.; Maier, T.; Kostrzewa, M.; Govorun, V. M., Direct bacterial profiling by matrix-assisted laser desorption-ionization time-of-flight mass spectrometry for identification of pathogenic *Neisseria*. *J Mol Diagn* **2009**, 11, (1), 75-86.

108. Fenselau, C.; Demirev, P. A., Characterization of intact microorganisms by MALDI mass spectrometry. *Mass Spectrom Rev* **2001**, 20, (4), 157-71.

109. Whiteaker, J. R.; Warscheid, B.; Pribil, P.; Hathout, Y.; Fenselau, C., Complete sequences of small acid-soluble proteins from *Bacillus globigii*. *J Mass Spectrom* **2004**, 39, (10), 1113-21.

110. Madonna, A. J.; Voorhees, K. J.; Taranenko, N. I.; Laiko, V. V.; Doroshenko, V. M., Detection of cyclic lipopeptide biomarkers from *Bacillus* species using atmospheric pressure matrix-assisted laser desorption/ionization mass spectrometry. *Anal Chem* **2003**, 75, (7), 1628-37.

111. Warscheid, B.; Fenselau, C., A targeted proteomics approach to the rapid identification of bacterial cell mixtures by matrix-assisted laser desorption/ionization mass spectrometry. *Proteomics* **2004**, 4, (10), 2877-92.

112. Dworzanski, J. P.; Snyder, A. P.; Chen, R.; Zhang, H.; Wishart, D.; Li, L., Identification of bacteria using tandem mass spectrometry combined with a proteome database and statistical scoring. *Anal Chem* **2004**, 76, (8), 2355-66.

113. Pribil, P. A.; Patton, E.; Black, G.; Doroshenko, V.; Fenselau, C., Rapid characterization of *Bacillus* spores targeting species-unique peptides produced with an

atmospheric pressure matrix-assisted laser desorption/ionization source. *J Mass Spectrom* **2005**.

114. Jones, J. J.; Stump, M. J.; Fleming, R. C.; Lay, J. O., Jr.; Wilkins, C. L., Investigation of MALDI-TOF and FT-MS techniques for analysis of *Escherichia coli* whole cells. *Anal Chem* **2003**, 75, (6), 1340-47.

115. English, R. D.; Warscheid, B.; Fenselau, C.; Cotter, R. J., *Bacillus* spore identification via proteolytic peptide mapping with a miniaturized MALDI TOF mass spectrometer. *Anal Chem* **2003**, 75, (24), 6886-93.

116. Dworzanski, J. P.; Snyder, A. P., Classification and identification of bacteria using mass spectrometry-based proteomics. *Expert Rev Proteomics* **2005**, 2, (6), 863-78.

117. Zhang, L.; Reilly, J. P., De novo sequencing of tryptic peptides derived from *Deinococcus radiodurans* ribosomal proteins using 157 nm photodissociation MALDI TOF/TOF mass spectrometry. *J Proteome Res* **2010**, 9, (6), 3025-34.

118. Mann, M.; Wilm, M., Error-tolerant identification of peptides in sequence databases by peptide sequence tags. *Anal Chem* **1994**, 66, (24), 4390-99.

119. Washburn, M. P.; Wolters, D.; Yates, J. R., 3rd, Large-scale analysis of the yeast proteome by multidimensional protein identification technology. *Nat Biotechnol* **2001**, 19, (3), 242-47.

120. Link, A. J.; Eng, J.; Schieltz, D. M.; Carmack, E.; Mize, G. J.; Morris, D. R.; Garvik, B. M.; Yates, J. R., 3rd, Direct analysis of protein complexes using mass spectrometry. *Nat Biotechnol* **1999**, 17, (7), 676-82.

121. Hillenkamp, F.; Karas, M.; Beavis, R. C.; Chait, B. T., Matrix-assisted laser desorption/ionization mass spectrometry of biopolymers. *Anal Chem* **1991**, 63, (24), 1193A-1203A.

122. Tanaka, K. W., H.; Ido, Y.; Akita, S.; Yoshida, Y.; Yoshida, T. , Protein and polymer analyses of to 100,000 by laser ionization time-of-flight mass spectrometry. *Rapid Comm Mass Spectrom* **1988**, 2, 151-53.

123. Karas, M.; Bachmann, D.; Hillenkamp, F., Influence of the wavelength in high-irradiance ultraviolet laser desorption mass spectrometry of organic molecules. *Anal Chem* **1985**, 57, (14), 2935-39.

124. Zenobi, R.; Knochenmuss, R., Ion formation in MALDI mass spectrometry. *Mass Spectrom Rev* **1999**, 17, 337-66.

125. Yates, J. R., 3rd; Gilchrist, A.; Howell, K. E.; Bergeron, J. J., Proteomics of organelles and large cellular structures. *Nat Rev Mol Cell Biol* **2005**, 6, (9), 702-14.

126. Jensen, O. N., Interpreting the protein language using proteomics. *Nat Rev Mol Cell Biol* **2006**, 7, (6), 391-403.
127. Demirev PA, F. C., Mass spectrometry for rapid characterization of microorganisms. *Annl Rev Anal Chem* **2008**, 1, (3), 71-93.
128. Ritchie, G.; Harvey, D. J.; Stroehrer, U.; Feldmann, F.; Feldmann, H.; Wahl-Jensen, V.; Royle, L.; Dwek, R. A.; Rudd, P. M., Identification of N-glycans from Ebola virus glycoproteins by matrix-assisted laser desorption/ionisation time-of-flight and negative ion electrospray tandem mass spectrometry. *Rapid Commun Mass Spectrom* **2010**, 24, (5), 571-85.
129. Jang, H. B.; Sung, H. W.; Nho, S. W.; Park, S. B.; Cha, I. S.; Aoki, T.; Jung, T. S., Enhanced Reliability of Avian Influenza Virus (AIV) and Newcastle Disease Virus (NDV) Identification Using Matrix-Assisted Laser Desorption/Ionization-Mass Spectrometry (MALDI-MS). *Anal Chem* **2011**Epub ahead of print.
130. Luan, J.; Yuan, J.; Li, X.; Jin, S.; Yu, L.; Liao, M.; Zhang, H.; Xu, C.; He, Q.; Wen, B.; Zhong, X.; Chen, X.; Chan, H. L.; Sung, J. J.; Zhou, B.; Ding, C., Multiplex detection of 60 hepatitis B virus variants by maldi-tof mass spectrometry. *Clin Chem* **2009**, 55, (8), 1503-09.
131. Kemptner, J.; Marchetti-Deschmann, M.; Mach, R.; Druzhinina, I. S.; Kubicek, C. P.; Allmaier, G., Evaluation of matrix-assisted laser desorption/ionization (MALDI) preparation techniques for surface characterization of intact *Fusarium* spores by MALDI linear time-of-flight mass spectrometry. *Rapid Commun Mass Spectrom* **2009**, 23, (6), 877-84.
132. Santos, C.; Paterson, R. R.; Venancio, A.; Lima, N., Filamentous fungal characterizations by matrix-assisted laser desorption/ionization time-of-flight mass spectrometry. *J Appl Microbiol* **2010**, 108, (2), 375-85.
133. Buskirk, A. D.; Hettick, J. M.; Chipinda, I.; Law, B. F.; Siegel, P. D.; Slaven, J. E.; Green, B. J.; Beezhold, D. H., Fungal pigments inhibit the matrix-assisted laser desorption/ionization time-of-flight mass spectrometry analysis of darkly pigmented fungi. *Anal Biochem* **2011**, 411, (1), 122-28.
134. Shaw, E. I.; Moura, H.; Woolfitt, A. R.; Ospina, M.; Thompson, H. A.; Barr, J. R., Identification of biomarkers of whole *Coxiella burnetii* phase I by MALDI-TOF mass spectrometry. *Anal Chem* **2004**, 76, (14), 4017-22.
135. van Baar, B. L., Characterisation of bacteria by matrix-assisted laser desorption/ionisation and electrospray mass spectrometry. *FEMS Microbiol Rev* **2000**, 24, (2), 193-219.
136. Haag, A. M.; Taylor, S. N.; Johnston, K. H.; Cole, R. B., Rapid identification of *Haemophilus* and other bacteria by matrix-assisted laser desorption ionization time-of-flight mass spectrometry. *Am Clin Lab* **2000**, 19, (3), 20-21.

137. Madonna, A. J.; Basile, F.; Ferrer, I.; Meetani, M. A.; Rees, J. C.; Voorhees, K. J., On-probe sample pretreatment for the detection of proteins above 15 KDa from whole cell bacteria by matrix-assisted laser desorption/ionization time-of-flight mass spectrometry. *Rapid Commun Mass Spectrom* **2000**, 14, (23), 2220-29.
138. Evason, D. J.; Claydon, M. A.; Gordon, D. B., Exploring the limits of bacterial identification by intact cell-mass spectrometry. *J Am Soc Mass Spectrom* **2001**, 12, (1), 49-54.
139. Arnold, R. J.; Karty, J. A.; Ellington, A. D.; Reilly, J. P., Monitoring the growth of a bacteria culture by MALDI-MS of whole cells. *Anal Chem* **1999**, 71, (10), 1990-96.
140. Rees, J. C.; Voorhees, K. J., Simultaneous detection of two bacterial pathogens using bacteriophage amplification coupled with matrix-assisted laser desorption/ionization time-of-flight mass spectrometry. *Rapid Commun Mass Spectrom* **2005**, 19, (19), 2757-61.
141. Madonna, A.; Van Cuyk, S.; Voorhees, K., Detection of Escherichia coli using immunomagnetic separation and bacteriophage amplification coupled with matrix-assisted laser desorption/ionization time-of-flight mass spectrometry. *Rapid Comm Mass Spectrom* **2003**, 17, (3), 257-63.
142. Nilles, J. M.; Connell, T. R.; Durst, H. D., Quantitation of chemical warfare agents using the direct analysis in real time (DART) technique. *Anal Chem* **2009**, 81, (16), 6744-49.
143. Vaclavik, L.; Cajka, T.; Hrbek, V.; Hajslova, J., Ambient mass spectrometry employing direct analysis in real time (DART) ion source for olive oil quality and authenticity assessment. *Anal Chim Acta* **2009**, 645, (1-2), 56-63.
144. Kawamura, M.; Kikura-Hanajiri, R.; Goda, Y., [Simple and rapid screening for psychotropic natural products using Direct Analysis in Real Time (DART)-TOFMS]. *Yakugaku Zasshi* **2009**, 129, (6), 719-25.
145. Vaclavik, L.; Zachariasova, M.; Hrbek, V.; Hajslova, J., Analysis of multiple mycotoxins in cereals under ambient conditions using direct analysis in real time (DART) ionization coupled to high resolution mass spectrometry. *Talanta* 82, (5), 1950-57.
146. Curtis, M.; Minier, M. A.; Chitranshi, P.; Sparkman, O. D.; Jones, P. R.; Xue, L., Direct analysis in real time (DART) mass spectrometry of nucleotides and nucleosides: elucidation of a novel fragment [C₅H₅O]⁺ and its in-source adducts. *J Am Soc Mass Spectrom* **2010**, 21, (8), 1371-81.
147. Domin, M. A.; Steinberg, B. D.; Quimby, J. M.; Smith, N. J.; Greene, A. K.; Scott, L. T., Routine analysis and characterization of highly insoluble polycyclic aromatic compounds by direct analysis in real time mass spectrometry (DART). *Analyst* **2010**, 135, (4), 700-04.

148. Bajpai, V.; Sharma, D.; Kumar, B.; Madhusudanan, K. P., Profiling of Piper betle Linn. cultivars by direct analysis in real time mass spectrometric technique. *Biomed Chromatogr* **2010**, 24, (12), 1283-86.
149. Fukuda, E.; Baba, M.; Iwasaki, N.; Uesawa, Y.; Arifuku, K.; Kamoe, O.; Tsubono, K.; Okada, Y., Identification of Glycyrrhiza species by direct analysis in real time mass spectrometry. *Nat Prod Commun* **2010**, 5, (11), 1755-58.
150. Vaclavik, L.; Zachariasova, M.; Hrbek, V.; Hajslova, J., Analysis of multiple mycotoxins in cereals under ambient conditions using direct analysis in real time (DART) ionization coupled to high resolution mass spectrometry. *Talanta* **2010**, 82, (5), 1950-57.
151. Banerjee, S.; Madhusudanan, K. P.; Khanuja, S. P.; Chattopadhyay, S. K., Analysis of cell cultures of *Taxus wallichiana* using direct analysis in real-time mass spectrometric technique. *Biomed Chromatogr* **2008**, 22, (3), 250-53.
152. Madhusudanan, K. P.; Banerjee, S.; Khanuja, S. P.; Chattopadhyay, S. K., Analysis of hairy root culture of *Rauvolfia serpentina* using direct analysis in real time mass spectrometric technique. *Biomed Chromatogr* **2008**, 22, (6), 596-600.
153. Zhou, M.; McDonald, J. F.; Fernandez, F. M., Optimization of a direct analysis in real time/time-of-flight mass spectrometry method for rapid serum metabolomic fingerprinting. *J Am Soc Mass Spectrom* **2009**, 21, (1), 68-75.
154. Nyadong, L. Ambient Ionization Mass Spectrometry for the Forensic Screening of Pharmaceuticals and the Determination of Potential Drug Candidates. Georgia Institute of Technology, Atlanta, 2009.
155. Bevilacqua, V. L.; Nilles, J. M.; Rice, J. S.; Connell, T. R.; Schenning, A. M.; Reilly, L. M.; Durst, H. D., Ricin activity assay by direct analysis in real time mass spectrometry detection of adenine release. *Anal Chem* **2010**, 82, (3), 798-800.
156. Chapman, S., Carrier mobility spectra of spray electrified liquids. *Phys Rev* **1937**, 52, (3), 0184-90.
157. Chapman, S., Interpretation of carrier mobility spectra of liquids electrified by bubbling and spraying. *Phys Rev* **1938**, 54, (7), 528-33.
158. Dole, M.; Mack, L. L.; Hines, R. L., Molecular Beams of Macroions. *J Chem Phys* **1968**, 49, (5), 2240.
159. Horning, E. C.; Carroll, D. I.; Dzidic, I.; Haegele, K. D.; Horning, M. G.; Stillwell, R. N., Atmospheric pressure ionization (API) mass spectrometry. Solvent-mediated ionization of samples introduced in solution and in a liquid chromatograph effluent stream. *J Chromatogr Sci* **1974**, 12, (11), 725-29.
160. Horning, M. G.; Stillwell, W. G.; Nowlin, J.; Lertratanangkoon, K.; Carroll, D.; Dzidic, I.; Stillwell, R. N.; Horning, E. C.; Hill, R. M., The use of stable isotopes in gas

chromatography-mass spectrometric studies of drug metabolism. *J Chromatogr* **1974**, 91, 413-23.

161. Whitehouse, C. M.; Dreyer, R. N.; Yamashita, M.; Fenn, J. B., Electrospray Interface for Liquid Chromatographs and Mass Spectrometers. *Anal Chem* **1985**, 57, (3), 675-79.

162. Fenn, J. B.; Mann, M.; Meng, C. K.; Wong, S. F.; Whitehouse, C. M., Electrospray Ionization for Mass-Spectrometry of Large Biomolecules. *Science* **1989**, 246, (4926), 64-71.

163. Fenn, J. B.; Mann, M.; Meng, C. K.; Wong, S. F.; Whitehouse, C. M., Electrospray Ionization-Principles and Practice. *Mass Spectrometry Reviews* **1990**, 9, (1), 37-70.

164. Aleksandrov, M. L.; Gall, L. N.; Krasnov, N. V.; Nikolaev, V. I.; Pavlenko, V. A.; Shkurov, V. A.; Baram, G. I.; Grachev, M. A.; Knorre, V. D.; Kusner, Y. S., Direct Coupling of a Microcolumn Liquid Chromatograph and a Mass-Spectrometer. *Bioorganicheskaya Khimiya* **1984**, 10, (5), 710-12.

165. Aleksandrov, M. L.; Gall, L. N.; Krasnov, N. V.; Nikolaev, V. I.; Pavlenko, V. A.; Shkurov, V. A., Mechanism of Ion Formation during the Electrohydrodynamic Sputtering of a Liquid into a Vacuum. *J Anal Chem USSR* **1984**, 39, (9), 1268-74.

166. Aleksandrov, M. L.; Gall, L. N.; Krasnov, N. V.; Nikolaev, V. I.; Shkurov, V. A., Mass-Spectrometric Analysis of Thermally Unstable Compounds of Low Volatility by the Extraction of Ions from Solution at Atmospheric-Pressure. *J Anal Chem USSR* **1985**, 40, (9), 1227-36.

167. Meng, C.; Mann, M.; Fenn, J. In Proceedings of the 36th ASMS Conference on Mass Spectrometry and Allied Topics, San Francisco, CA, June 5-10, 1988; San Francisco, CA, 1988; pp 771.

168. Taylor, G., Disintegration of Water Drops in an Electric Field. *Proceedings of the Royal Society of London. Series A, Mathematical and Physical Sciences* **1964**, 280, 383-97

169. Kwasnik, M. Development and Fundamental Characterization of a Nanoelectrospray Ionization Atmospheric Pressure Drift Time Ion Mobility Spectrometer. Georgia Institute of Technology, Atlanta, 2010.

170. Karas, M.; Bahr, U.; Dulcks, T., Nano-electrospray ionization mass spectrometry: addressing analytical problems beyond routine. *Fresenius J Anal Chem* **2000**, 366, (6-7), 669-76.

171. Graham, T. T. G.; Samuel, M. M.; Richard, D. O., Nanoelectrospray emitters: Trends and perspective. *Mass Spectrom Rev* **2009**, 28, (6), 918-36.

172. Vaidyanathan, S.; Goodacre, R., High-throughput Microbial Characterizations using Electrospray Ionization Mass Spectrometry and its Role in Functional Genomics. In *Identification of Microorganisms by Mass Spectrometry*, Wilkins, C.; Lay, J., Eds. John Wiley & Sons, Inc.: Hoboken, NJ, 2006; Vol. 169, p 352.
173. Williams, T. L.; Leopold, P.; Musser, S., Automated postprocessing of electrospray LC/MS data for profiling protein expression in bacteria. *Anal Chem* **2002**, 74, (22), 5807-13.
174. Domon, B.; Aebersold, R., Mass spectrometry and protein analysis. *Science* **2006**, 312, (5771), 212-17.
175. Bateman, R. J.; Munsell, L. Y.; Chen, X.; Holtzman, D. M.; Yarasheski, K. E., Stable isotope labeling tandem mass spectrometry (SILT) to quantify protein production and clearance rates. *J Am Soc Mass Spectrom* **2007**, 18, (6), 997-1006.
176. Voisin, S.; Watson, D. C.; Tessier, L.; Ding, W.; Foote, S.; Bhatia, S.; Kelly, J. F.; Young, N. M., The cytoplasmic phosphoproteome of the Gram-negative bacterium *Campylobacter jejuni*: evidence for modification by unidentified protein kinases. *Proteomics* **2007**, 7, (23), 4338-48.
177. Bauersachs, T.; Hopmans, E. C.; Compaore, J.; Stal, L. J.; Schouten, S.; Damste, J. S., Rapid analysis of long-chain glycolipids in heterocystous cyanobacteria using high-performance liquid chromatography coupled to electrospray ionization tandem mass spectrometry. *Rapid Commun Mass Spectrom* **2009**, 23, (9), 1387-94.
178. Wunschel, D.; Fox, K. F.; Fox, A.; Nagpal, M. L.; Kim, K.; Stewart, G. C.; Shahgholi, M., Quantitative analysis of neutral and acidic sugars in whole bacterial cell hydrolysates using high-performance anion-exchange liquid chromatography-electrospray ionization tandem mass spectrometry. *J Chromatogr A* **1997**, 776, (2), 205-19.
179. Ishihama, Y.; Schmidt, T.; Rappsilber, J.; Mann, M.; Hartl, F. U.; Kerner, M. J.; Frishman, D., Protein abundance profiling of the *Escherichia coli* cytosol. *BMC Genomics* **2008**, 9, 102.
180. He, T.; Roelofsen, H.; Alvarez-Llamas, G.; de Vries, M.; Venema, K.; Welling, G. W.; Vonk, R. J., Differential analysis of protein expression of *Bifidobacterium* grown on different carbohydrates. *J Microbiol Methods* **2007**, 69, (2), 364-70.
181. Nie, L.; Wu, G.; Zhang, W., Correlation between mRNA and protein abundance in *Desulfovibrio vulgaris*: a multiple regression to identify sources of variations. *Biochem Biophys Res Commun* **2006**, 339, (2), 603-10.
182. Williamson, Y. M.; Moura, H.; Schieltz, D.; Rees, J.; Woolfitt, A. R.; Pirkle, J. L.; Sampson, J. S.; Tondella, M. L.; Ades, E.; Carlone, G.; Barr, J. R., Mass spectrometric analysis of multiple pertussis toxins and toxoids. *J Biomed Biotechnol* **2010**, 2010, 942365.

183. Devreese, B.; Vanrobaeys, F.; Van Beeumen, J., Automated nanoflow liquid chromatography/tandem mass spectrometric identification of proteins from *Shewanella putrefaciens* separated by two-dimensional polyacrylamide gel electrophoresis. *Rapid Commun Mass Spectrom* **2001**, 15, (1), 50-56.
184. Hanna, S. L.; Sherman, N. E.; Kinter, M. T.; Goldberg, J. B., Comparison of proteins expressed by *Pseudomonas aeruginosa* strains representing initial and chronic isolates from a cystic fibrosis patient: an analysis by 2-D gel electrophoresis and capillary column liquid chromatography-tandem mass spectrometry. *Microbiol* **2000**, 146 (Pt 10), 2495-508.
185. Williams, T.; Monday, S.; Musser, S., Bacterial Protein Biomarker Discovery: A Focused Approach to Developing Molecular-Based Identification Systems. In *Identification of Microorganisms by Mass Spectrometry*, Wilkins, C.; Lay, J., Eds. John Wiley and Sons: Hoboken, NJ, USA, 2006; Vol. 169, p 352.
186. Schulze, W. X.; Usadel, B., Quantitation in mass-spectrometry-based proteomics. *Annu Rev Plant Biol* **2010**, 61, 491-516.
187. Browne, T. R.; Van Langenhove, A.; Costello, C. E.; Biemann, K.; Greenblatt, D. J., Kinetic equivalence of stable-isotope-labeled and unlabeled phenytoin. *Clin Pharmacol Ther* **1981**, 29, (4), 511-15.
188. Oda, Y.; Huang, K.; Cross, F.; Cowburn, D.; Chait, B., Accurate quantitation of protein expression and site-specific phosphorylation. *Proc Natl Acad Sci* **1999**, 96, 6591-96.
189. Gruhler, A.; Kratchmarova, I., Stable isotope labeling by amino acids in cell culture (SILAC). *Methods Mol Biol* **2008**, 424, 101-11.
190. Ong, S. E.; Blagoev, B.; Kratchmarova, I.; Kristensen, D. B.; Steen, H.; Pandey, A.; Mann, M., Stable isotope labeling by amino acids in cell culture, SILAC, as a simple and accurate approach to expression proteomics. *Mol Cell Proteomics* **2002**, 1, (5), 376-86.
191. Conrads, T. P.; Alving, K.; Veenstra, T. D.; Belov, M. E.; Anderson, G. A.; Anderson, D. J.; Lipton, M. S.; Pasa-Tolic, L.; Udseth, H. R.; Chrisler, W. B.; Thrall, B. D.; Smith, R. D., Quantitative analysis of bacterial and mammalian proteomes using a combination of cysteine affinity tags and ¹⁵N-metabolic labeling. *Anal Chem* **2001**, 73, (9), 2132-39.
192. Pandhal, J.; Snijders, A. P.; Wright, P. C.; Biggs, C. A., A cross-species quantitative proteomic study of salt adaptation in a halotolerant environmental isolate using ¹⁵N metabolic labeling. *Proteomics* **2008**, 8, (11), 2266-84.
193. Kremer, A.; Schneider, R.; Terstappen, G. C., A bioinformatics perspective on proteomics: data storage, analysis, and integration. *Biosci Rep* **2005**, 25, (1-2), 95-106.

194. Jarman, K. H.; Daly, D. S.; Petersen, C. E.; Saenz, A. J.; Valentine, N. B.; Wahl, K. L., Extracting and visualizing matrix-assisted laser desorption/ionization time-of-flight mass spectral fingerprints. *Rapid Commun Mass Spectrom* **1999**, 13, (15), 1586-94.
195. Walker, J.; Fox, A. J.; Edwards-Jones, V.; Gordon, D. B., Intact cell mass spectrometry (ICMS) used to type methicillin-resistant *Staphylococcus aureus*: media effects and inter-laboratory reproducibility. *J Microbiol Methods* **2002**, 48, (2-3), 117-26.
196. Barker, M.; Rayens, W., *J. Chemom.* **2003**, 17, 166-73.
197. ENTREZ Genome Project; National Center for Biotechnology Information <http://www.ncbi.nlm.nih.gov/genomes/lproks.cgi>; <http://www.ncbi.nlm.nih.gov/genomes/lproks.cgi> (February 24, 2011),
198. Wilkins, C.; Lay, J. O., *Identification of Microorganisms by Mass Spectrometry*. John Wiley and Sons: Hoboken, NJ, 2006.
199. Cooks, R. G.; Ouyang, Z.; Takats, Z.; Wiseman, J. M., Detection Technologies. Ambient mass spectrometry. *Science* **2006**, 311, (5767), 1566-70.
200. Takats, Z.; Wiseman, J. M.; Cooks, R. G., Ambient mass spectrometry using desorption electrospray ionization (DESI): instrumentation, mechanisms and applications in forensics, chemistry, and biology. *J Mass Spectrom* **2005**, 40, (10), 1261-75.
201. Jones, R. W.; Cody, R. B.; McClelland, J. F., Differentiating writing inks using direct analysis in real time mass spectrometry. *J Forensic Sci* **2006**, 51, (4), 915-18.
202. Fernandez, F. M.; Cody, R. B.; Green, M. D.; Hampton, C. Y.; McGready, R.; Sengaloundeth, S.; White, N. J.; Newton, P. N., Characterization of solid counterfeit drug samples by desorption electrospray ionization and direct-analysis-in-real-time coupled to time-of-flight mass spectrometry. *Chem Med Chem* **2006**, 1, (7), 702-05.
203. Xu, M.; Basile, F.; Voorhees, K. J., Differentiation and classification of user-specified bacterial groups by in situ thermal hydrolysis and methylation of whole bacterial cells with tert-butyl bromide chemical ionization ion trap mass spectrometry. *Anal Chim Acta* **2000**, 418, (2), 119-28.
204. Smilde, A.; Bro, R.; Geladi, P., *Multi-Way Analysis*. John Wiley & Sons: New York, 2004.
205. Maurin, M.; Raoult, D., Q fever. *Clin. Microbiol. Rev.* **1999**, 12, (4), 518-53.
206. Madariaga, M. G.; Rezai, K.; Trenholme, G. M.; Weinstein, R. A., Q fever: a biological weapon in your backyard. *Lancet Infect Dis* **2003**, 3, (11), 709-21.
207. Hackstadt, T., Antigenic variation in the phase I lipopolysaccharide of *Coxiella burnetii* isolates. *Infect Immun* **1986**, 52, (1), 337-40.

208. To, H.; Hotta, A.; Zhang, G. Q.; Nguyen, S. V.; Ogawa, M.; Yamaguchi, T.; Fukushima, H.; Amano, K.; Hirai, K., Antigenic characteristics of polypeptides of *Coxiella burnetii* isolates. *Microbiol Immunol* **1998**, 42, (2), 81-85.
209. Hackstadt, T.; Peacock, M. G.; Hitchcock, P. J.; Cole, R. L., Lipopolysaccharide variation in *Coxiella burnetii*: intrastain heterogeneity in structure and antigenicity. *Infect Immun* **1985**, 48, (2), 359-65.
210. Honstetter, A.; Ghigo, E.; Moynault, A.; Capo, C.; Toman, R.; Akira, S.; Takeuchi, O.; Lepidi, H.; Raoult, D.; Mege, J. L., Lipopolysaccharide from *Coxiella burnetii* is involved in bacterial phagocytosis, filamentous actin reorganization, and inflammatory responses through Toll-like receptor 4. *J Immunol* **2004**, 172, (6), 3695-703.
211. Fournier, P. E.; Marrie, T. J.; Raoult, D., Diagnosis of Q fever. *J Clin Microbiol* **1998**, 36, (7), 1823-34.
212. Field, P. R.; Santiago, A.; Chan, S. W.; Patel, D. B.; Dickeson, D.; Mitchell, J. L.; Devine, P. L.; Murphy, A. M., Evaluation of a novel commercial enzyme-linked immunosorbent assay detecting *Coxiella burnetii*-specific immunoglobulin G for Q fever prevaccination screening and diagnosis. *J Clin Microbiol* **2002**, 40, (9), 3526-29.
213. Brouqui, P.; Dumler, J. S.; Raoult, D., Immunohistologic Demonstration of *Coxiella-Burnetii* in the Valves of Patients with Q-Fever Endocarditis. *Amer J Med* **1994**, 97, (5), 451-58.
214. McCaul, T. F.; Williams, J. C., Localization of DNA in *Coxiella-Burnetii* by Postembedding Immunoelectron Microscopy. *Annl NY Acad Sci* **1990**, 590, 136-47.
215. Muhlemann, K.; Matter, L.; Meyer, B.; Schopfer, K., Isolation of *Coxiella-Burnetii* from Heart-Valves of Patients Treated for Q-Fever Endocarditis. *J Clin Microbiol* **1995**, 33, (2), 428-31.
216. Thiele, D.; Karo, M.; Krauss, H., Monoclonal-Antibody Based Capture Elisa/Elifa for Detection of *Coxiella-Burnetii* in Clinical Specimens. *Euro J Epidemiol* **1992**, 8, (4), 568-74.
217. Budowle, B.; Schutzer, S. E.; Einseln, A.; Kelley, L. C.; Walsh, A. C.; Smith, J. A. L.; Marrone, B. L.; Robertson, J.; Campos, J., Building microbial forensics as a response to bioterrorism. *Science* **2003**, 301, (5641), 1852-53.
218. Krishnamurthy, T.; Rajamani, U.; Ross, P.; Jabhour, R.; Nair, H.; Eng, J.; Yates, J.; Davis, M.; Stahl, D.; Lee, T., Mass spectral investigations on microorganisms. *J Toxicol-Toxin Rev* **2000**, 19, (1), 95-117.
219. Lay, J. O., MALDI-TOF mass spectrometry of bacteria. *Mass Spectrom. Rev* **2001**, 20, (4), 172-94.

220. Cottingham, K., MS on the Bioterror Front Lines. *Anal Chem* **2006**, 78, 19-23.
221. Warscheid, B.; Fenselau, C., A targeted proteomics approach to the rapid identification of bacterial cell mixtures by matrix-assisted laser desorption/ionization mass spectrometry. *Proteomics* **2004**, 4, (10), 2877-92.
222. Whiteaker, J.; Warscheid, B.; Pribil, P.; Hathout, Y.; Fenselau, C., Complete sequences of small acid-soluble proteins from *Bacillus globigii*. *J Mass Spectrom* **2004**, 39, (10), 1113-21.
223. Dworzanski, J.; Snyder, A.; Chen, R.; Zhang, H.; Wishart, D.; Li, L., Identification of bacteria using tandem mass spectrometry combined with a proteome database and statistical scoring. *Anal Chem* **2004**, 76, (8), 2355-66.
224. Pribil, P.; Fenselau, C., Characterization of Enterobacteria using MALDI-TOF mass spectrometry. *Anal Chem* **2005**, 77, (18), 6092-95.
225. Demirev, P. A.; Feldman, A. B.; Kowalski, P.; Lin, J. S., Top-down proteomics for rapid identification of intact microorganisms. *Anal Chem* **2005**, 77, (22), 7455-61.
226. Jones, J.; Stump, M.; Fleming, R.; Lay, J.; Wilkins, C., Investigation of MALDI-TOF and FT-MS techniques for analysis of *Escherichia coli* whole cells. *Anal Chem* **2003**, 75, (6), 1340-47.
227. Pineda, F.; Antoine, M.; Demirev, P.; Feldman, A.; Jackman, J.; Longenecker, M.; Lin, J., Microorganism identification by matrix-assisted laser/desorption ionization mass spectrometry and model-derived ribosomal protein biomarkers. *Anal Chem* **2003**, 75, (15), 3817-22.
228. Tao, L. D.; Yu, X. L.; Snyder, A. P.; Li, L., Bacterial identification by protein mass mapping combined with an experimentally derived protein mass database. *Anal Chem* **2004**, 76, (22), 6609-17.
229. Hofstadler, S.; Sampath, R.; Blyn, L.; Eshoo, M.; Hall, T.; Jiang, Y.; Drader, J.; Hannis, J.; Sannes-Lowery, K.; Cummins, L.; Libby, B.; Walcott, D.; Schink, A.; Massire, C.; Ranken, R.; Gutierrez, J.; Manalili, S.; Ivy, C.; Melton, R.; Levene, H.; Barrett-Wilt, G.; Li, F.; Zapp, V.; White, N.; Samant, V.; McNeil, J.; Knize, D.; Robbins, D.; Rudnick, K.; Desai, A.; Moradi, E.; Ecker, D., TIGER: the universal biosensor. *Internl J Mass Spectrom* **2005**, 242, (1), 23-41.
230. Jarman, K.; Cebula, S.; Saenz, A.; Petersen, C.; Valentine, N.; Kingsley, M.; Wahl, K., An algorithm for automated bacterial identification using matrix-assisted laser desorption/ionization mass spectrometry. *Anal Chem* **2000**, 72, (6), 1217-23.
231. Xu, M.; Voorhees, K.; Hadfield, T., Repeatability and pattern recognition of bacterial fatty acid profiles generated by direct mass spectrometric analysis of in situ thermal hydrolysis/methylation of whole cells. *Talanta* **2003**, 59, (3), 577-89.

232. Ochoa, M. L.; Harrington, P. B., Chemometric studies for the characterization and differentiation of microorganisms using in situ derivatization and thermal desorption ion mobility spectrometry. *Anal Chem* **2005**, 77, (3), 854-63.
233. Shnayderman, M.; Mansfield, B.; Yip, P.; Clark, H. A.; Krebs, M. D.; Cohen, S. J.; Zeskind, J. E.; Ryan, E. T.; Dorkin, H. L.; Callahan, M. V.; Stair, T. O.; Gelfand, J. A.; Gill, C. J.; Hitt, B.; Davis, C. E., Species-specific bacteria identification using differential mobility spectrometry and bioinformatics pattern recognition. *Anal Chem* **2005**, 77, (18), 5930-37.
234. Jungnickel, H.; Jones, E. A.; Lockyer, N. P.; Oliver, S. G.; Stephens, G. M.; Vickerman, J. C., Application of TOF-SIMS with chemometrics to discriminate between four different yeast strains from the species *Candida glabrata* and *Saccharomyces cerevisiae*. *Anal Chem* **2005**, 77, (6), 1740-45.
235. Jarman, K.; Daly, D.; Petersen, C.; Saenz, A.; Valentine, N.; Wahl, K., Extracting and visualizing matrix-assisted laser desorption/ionization time-of-flight mass spectral fingerprints. *Rapid Comm Mass Spectrom* **1999**, 13, (15), 1586-94.
236. Wahl, K.; Wunschel, S.; Jarman, K.; Valentine, N.; Petersen, C.; Kingsley, M.; Zartolas, K.; Saenz, A., Analysis of microbial mixtures by matrix-assisted laser desorption/ionization time-of-flight mass spectrometry. *Anal Chem* **2002**, 74, (24), 6191-99.
237. Dickinson, D. N.; La Duc, M. T.; Satomi, M.; Winefordner, J. D.; Powell, D. H.; Venkateswaran, K., MALDI-TOFMS compared with other polyphasic taxonomy approaches for the identification and classification of *Bacillus pumilus* spores. *J Microbiol Methods* **2004**, 58, (1), 1-12.
238. Verhoeckx, K. C.; Bijlsma, S.; de Groene, E. M.; Witkamp, R. F.; van der Greef, J.; Rodenburg, R. J., A combination of proteomics, principal component analysis and transcriptomics is a powerful tool for the identification of biomarkers for macrophage maturation in the U937 cell line. *Proteomics* **2004**, 4, (4), 1014-28.
239. Zhang, Z.; Wang, D.; Harrington, P.; Voorhees, K.; Rees, J., Forward selection radial basis function networks applied to bacterial classification based on MALDI-TOF-MS. *Talanta* **2004**, 63, (3), 527-32.
240. Saenz, A.; Petersen, C.; Valentine, N.; Gantt, S.; Jarman, K.; Kingsley, M.; Wahl, K., Reproducibility of matrix-assisted laser desorption/ionization time-of-flight mass spectrometry for replicate bacterial culture analysis. *Rapid Comm Mass Spectrom* **1999**, 13, (15), 1580-85.
241. Valentine, N.; Wunschel, S.; Wunschel, D.; Petersen, C.; Wahl, K., Effect of culture conditions on microorganism identification by matrix-assisted laser desorption ionization mass spectrometry. *Appl Environ Microbiol* **2005**, 71, (1), 58-64.

242. Wilkes, J. G.; Glover, K. L.; Holcomb, M.; Rafii, F.; Cao, X. X.; Sutherland, J. B.; McCarthy, S. A.; Letarte, S.; Bertrand, M. J., Defining and using microbial spectral databases. *J Amer Soc Mass Spectrom* **2002**, 13, (7), 875-87.
243. Ruelle, V.; El Moualij, B.; Zorzi, W.; Ledent, P.; De Pauw, E., Rapid identification of environmental bacterial strains by matrix-assisted laser desorption/ionization time-of-flight mass spectrometry. *Rapid Comm Mass Spectrom* **2004**, 18, (18), 2013-19.
244. Williams, T. L.; Andrzejewski, D.; Lay, J. O.; Musser, S. M., Experimental factors affecting the quality and reproducibility of MALDI TOF mass spectra obtained from whole bacteria cells. *J Am Soc Mass Spectrom* **2003**, 14, (4), 342-51.
245. Wunschel, S. C.; Jarman, K. H.; Petersen, C. E.; Valentine, N. B.; Wahl, K. L.; Schauki, D.; Jackman, J.; Nelson, C. P.; White, E., Bacterial analysis by MALDI-TOF mass spectrometry: An inter-laboratory comparison. *J Amer Soc Mass Spectrom* **2005**, 16, (4), 456-62.
246. Wold, S.; Sjostrom, M.; Eriksson, L., PLS-regression: a basic tool of chemometrics. *Chemom Intell Lab Sys* **2001**, 58, (2), 109-30.
247. Giraffa, G.; Paris, A.; Valcavi, L.; Gatti, M.; Neviani, E., Genotypic and phenotypic heterogeneity of *Streptococcus thermophilus* strains isolated from dairy products. *J Appl Microbiol* **2001**, 91, (5), 937-43.
248. Barker, M.; Rayens, W., Partial least squares for discrimination. *J Chemom* **2003**, 17, (3), 166-73.
249. Lundquist, M.; Caspersen, M. B.; Wikstrom, P.; Forsman, M., Discrimination of *Francisella tularensis* subspecies using surface enhanced laser desorption ionization mass spectrometry and multivariate data analysis. *Fems Microbiol Lett* **2005**, 243, (1), 303-310.
250. Massart, D. L.; Vandeginste, B. G. M.; Buydens, L. M. C.; De Jong, S.; Lewi, P. J.; Smeyers-Verbeke, J., *Handbook of Chemometrics and Qualimetrics*. Elsevier: Amsterdam, 1997.
251. Seshadri, R.; Paulsen, I. T.; Eisen, J. A.; Read, T. D.; Nelson, K. E.; Nelson, W. C.; Ward, N. L.; Tettelin, H.; Davidsen, T. M.; Beanan, M. J.; Deboy, R. T.; Daugherty, S. C.; Brinkac, L. M.; Madupu, R.; Dodson, R. J.; Khouri, H. M.; Lee, K. H.; Carty, H. A.; Scanlan, D.; Heinzen, R. A.; Thompson, H. A.; Samuel, J. E.; Fraser, C. M.; Heidelberg, J. F., Complete genome sequence of the Q-fever pathogen *Coxiella burnetii*. *Proc Nat Acad Sci USA* **2003**, 100, (9), 5455-60.
252. Miller, J. D.; Thompson, H. A., Permeability of *Coxiella burnetii* to ribonucleosides. *Microbiol* **2002**, 148, (Pt 8), 2393-403.

253. Williams, J. C.; Peacock, M. G.; McCaul, T. F., Immunological and biological characterization of *Coxiella burnetii*, phases I and II, separated from host components. *Infect Immun* **1981**, 32, (2), 840-51.
254. Waag, D. M.; Kende, M.; Damrow, T. A.; Wood, O. L.; Williams, J. C., Injection of inactivated phase I *Coxiella burnetii* increases non-specific resistance to infection and stimulates lymphokine production in mice. *Ann N Y Acad Sci* **1990**, 590, 203-14.
255. Scott, G. H.; McCaul, T. F.; Williams, J. C., Inactivation of *Coxiella burnetii* by gamma irradiation. *J Gen Microbiol* **1989**, 135, (12), 3263-70.
256. Satten, G. A.; Datta, S.; Moura, H.; Woolfitt, A. R.; Carvalho Mda, G.; Carlone, G. M.; De, B. K.; Pavlopoulos, A.; Barr, J. R., Standardization and denoising algorithms for mass spectra to classify whole-organism bacterial specimens. *Bioinformatics* **2004**, 20, (17), 3128-36.
257. Francois, P.; Schrenzel, J., Rapid Diagnosis and Typing of *Staphylococcus aureus*. In *Staphylococcus: Molecular Genetics*, Lindsay, J., Ed. Caister Academic Press: London, UK, May 2008.
258. Annane, D.; Bellissant, E.; Cavaillon, J. M., Septic shock. *Lancet* **2005**, 365, (9453), 63-78.
259. Tacconelli, E.; De Angelis, G.; de Waure, C.; Cataldo, M. A.; La Torre, G.; Cauda, R., Rapid screening tests for methicillin-resistant *Staphylococcus aureus* at hospital admission: systematic review and meta-analysis. *Lancet Infect Dis* **2009**, 9, (9), 546-54.
260. Carroll, K. C., Rapid diagnostics for methicillin-resistant *Staphylococcus aureus*: current status. *Mol Diagn Ther* **2008**, 12, (1), 15-24.
261. Wellinghausen, N.; Siegel, D.; Gebert, S.; Winter, J., Rapid detection of *Staphylococcus aureus* bacteremia and methicillin resistance by real-time PCR in whole blood samples. *Eur J Clin Microbiol Infect Dis* **2009**, 28, (8), 1001-05.
262. Huletsky, A.; Giroux, R.; Rossbach, V.; Gagnon, M.; Vaillancourt, M.; Bernier, M.; Gagnon, F.; Truchon, K.; Bastien, M.; Picard, F. J.; van Belkum, A.; Ouellette, M.; Roy, P. H.; Bergeron, M. G., New real-time PCR assay for rapid detection of methicillin-resistant *Staphylococcus aureus* directly from specimens containing a mixture of staphylococci. *J Clin Microbiol* **2004**, 42, (5), 1875-84.
263. Jeyaratnam, D.; Gottlieb, A.; Ajoku, U.; French, G. L., Validation of the IDI-MRSA system for use on pooled nose, axilla, and groin swabs and single swabs from other screening sites. *Diagn Microbiol Infect Dis* **2008**, 61, (1), 1-5.
264. Gonzalez, V.; Padilla, E.; Gimenez, M.; Vilaplana, C.; Perez, A.; Fernandez, G.; Quesada, M. D.; Pallares, M. A.; Ausina, V., Rapid diagnosis of *Staphylococcus aureus* bacteremia using *S. aureus* PNA FISH. *Eur J Clin Microbiol Infect Dis* **2004**, 23, (5), 396-98.

265. Wolk, D. M.; Struelens, M. J.; Pancholi, P.; Davis, T.; Della-Latta, P.; Fuller, D.; Picton, E.; Dickenson, R.; Denis, O.; Johnson, D.; Chapin, K., Rapid detection of *Staphylococcus aureus* and methicillin-resistant *S. aureus* (MRSA) in wound specimens and blood cultures: multicenter preclinical evaluation of the Cepheid Xpert MRSA/SA skin and soft tissue and blood culture assays. *J Clin Microbiol* **2009**, 47, (3), 823-26.
266. Cohen, D.; Almeida, M.; Bagoole, B. In *Evaluation of the 3M BacLite Rapid MRSA test for the direct detection of MRSA*. , Abstracts of the Institute of Biomedical Science International Congress, Birmingham, UK, 2007; Birmingham, UK, 2007.
267. Schofield, D. A.; Molineux, I. J.; Westwater, C., Diagnostic bioluminescent phage for detection of *Yersinia pestis*. *J Clin Microbiol* **2009**, 47, (12), 3887-94.
268. Shabani, A.; Zourob, M.; Allain, B.; Marquette, C. A.; Lawrence, M. F.; Mandeville, R., Bacteriophage-modified microarrays for the direct impedimetric detection of bacteria. *Anal Chem* **2008**, 80, (24), 9475-82.
269. Ripp, S.; Jegier, P.; Johnson, C. M.; Brigati, J. R.; Sayler, G. S., Bacteriophage-amplified bioluminescent sensing of *Escherichia coli* O157:H7. *Anal Bioanal Chem* **2008**, 391, (2), 507-14.
270. Madonna, A. J.; Van Cuyk, S.; Voorhees, K. J., Detection of *Escherichia coli* using immunomagnetic separation and bacteriophage amplification coupled with matrix-assisted laser desorption/ionization time-of-flight mass spectrometry. *Rapid Commun Mass Spectrom* **2003**, 17, (3), 257-63.
271. Reiman, R. W.; Atchley, D. H.; Voorhees, K. J., Indirect detection of *Bacillus anthracis* using real-time PCR to detect amplified gamma phage DNA. *J Microbiol Methods* **2007**, 68, (3), 651-53.
272. Rajakaruna, L.; Hallas, G.; Molenaar, L.; Dare, D.; Sutton, H.; Encheva, V.; Culak, R.; Innes, I.; Ball, G.; Sefton, A. M.; Eydmann, M.; Kearns, A. M.; Shah, H. N., High throughput identification of clinical isolates of *Staphylococcus aureus* using MALDI-TOF-MS of intact cells. *Infect Genet Evol* **2009**, 9, (4), 507-13.
273. Niu, Q.; Huang, Z.; Shi, Y.; Wang, L.; Pan, X.; Hu, C., Specific serum protein biomarkers of rheumatoid arthritis detected by MALDI-TOF-MS combined with magnetic beads. *Int Immunol* **2010**, 22, (7), 611-18.
274. Franco, C. F.; Mellado, M. C.; Alves, P. M.; Coelho, A. V., Monitoring virus-like particle and viral protein production by intact cell MALDI-TOF mass spectrometry. *Talanta* **2010**, 80, (4), 1561-68.
275. Bohme, K.; Fernandez-No, I. C.; Barros-Velazquez, J.; Gallardo, J. M.; Calomata, P.; Canas, B., Species Differentiation of Seafood Spoilage and Pathogenic Gram-Negative Bacteria by MALDI-TOF Mass Fingerprinting. *J Proteome Res* **2010**, 9, (6), 3169-83.

276. Edgar, R.; McKinstry, M.; Hwang, J.; Oppenheim, A. B.; Fekete, R. A.; Giulian, G.; Merril, C.; Nagashima, K.; Adhya, S., High-sensitivity bacterial detection using biotin-tagged phage and quantum-dot nanocomplexes. *Proc Natl Acad Sci U S A* **2006**, 103, (13), 4841-45.
277. Adams, M., *Bacteriophages*. Interscience Publishers New York, 1959.
278. Keller, A.; Nesvizhskii, A. I.; Kolker, E.; Aebersold, R., Empirical statistical model to estimate the accuracy of peptide identifications made by MS/MS and database search. *Anal Chem* **2002**, 74, (20), 5383-92.
279. Nesvizhskii, A. I.; Keller, A.; Kolker, E.; Aebersold, R., A statistical model for identifying proteins by tandem mass spectrometry. *Anal Chem* **2003**, 75, (17), 4646-58.
280. Ralston, D. J.; Baer, B. S.; Lieberman, M.; Krueger, A. P., Lysis from without of *S. aureus* K1 by the combined action of phage and virolysin. *J Gen Physiol* **1957**, 41, (2), 343-58.
281. Wada, M.; Lkhagvadorj, E.; Bian, L.; Wang, C.; Chiba, Y.; Nagata, S.; Shimizu, T.; Yamashiro, Y.; Asahara, T.; Nomoto, K., Quantitative reverse transcription-PCR assay for the rapid detection of methicillin-resistant *Staphylococcus aureus*. *J Appl Microbiol* **2010**, 108, (3), 779-88.
282. Fuchs, B.; Suss, R.; Schiller, J., An update of MALDI-TOF mass spectrometry in lipid research. *Prog Lipid Res* **2010**, 49, (4), 450-75.
283. Monagas, M.; Quintanilla-Lopez, J. E.; Gomez-Cordoves, C.; Bartolome, B.; Lebron-Aguilar, R., MALDI-TOF MS analysis of plant proanthocyanidins. *J Pharm Biomed Anal* **2010**, 51, (2), 358-72.
284. Giebel, R.; Worden, C.; Rust, S. M.; Kleinheinz, G. T.; Robbins, M.; Sandrin, T. R., Microbial fingerprinting using matrix-assisted laser desorption ionization time-of-flight mass spectrometry (MALDI-TOF MS) applications and challenges. *Adv Appl Microbiol* **2010**, 71, 149-84.
285. Zhang, H.; Li, X. J.; Martin, D. B.; Aebersold, R., Identification and quantification of N-linked glycoproteins using hydrazide chemistry, stable isotope labeling and mass spectrometry. *Nat Biotechnol* **2003**, 21, (6), 660-66.
286. Cravatt, B. F.; Simon, G. M.; Yates, J. R., 3rd, The biological impact of mass-spectrometry-based proteomics. *Nature* **2007**, 450, (7172), 991-1000.
287. Kristjansdottir, K.; S.J., K., Stable-Isotope Labeling for Protein Quantitation by Mass Spectrometry. *Current Proteomics* **2010**, 7, 144-55.
288. Gingras, A. C.; Gstaiger, M.; Raught, B.; Aebersold, R., Analysis of protein complexes using mass spectrometry. *Nat Rev Mol Cell Biol* **2007**, 8, (8), 645-54.

289. Trinkle-Mulcahy, L.; Boulon, S.; Lam, Y. W.; Urcia, R.; Boisvert, F. M.; Vandermoere, F.; Morrice, N. A.; Swift, S.; Rothbauer, U.; Leonhardt, H.; Lamond, A., Identifying specific protein interaction partners using quantitative mass spectrometry and bead proteomes. *J Cell Biol* **2008**, 183, (2), 223-39.
290. Gygi, S. P.; Rist, B.; Gerber, S. A.; Turecek, F.; Gelb, M. H.; Aebersold, R., Quantitative analysis of complex protein mixtures using isotope-coded affinity tags. *Nat Biotechnol* **1999**, 17, (10), 994-9.
291. Zhou, H.; Ranish, J. A.; Watts, J. D.; Aebersold, R., Quantitative proteome analysis by solid-phase isotope tagging and mass spectrometry. *Nat Biotechnol* **2002**, 20, (5), 512-15.
292. Cagney, G.; Emili, A., De novo peptide sequencing and quantitative profiling of complex protein mixtures using mass-coded abundance tagging. *Nat Biotechnol* **2002**, 20, (2), 163-70.
293. Chakraborty, A.; Regnier, F. E., Global internal standard technology for comparative proteomics. *J Chromatogr A* **2002**, 949, (1-2), 173-84.
294. Veenstra, T. D.; Martinovic, S.; Anderson, G. A.; Pasa-Tolic, L.; Smith, R. D., Proteome analysis using selective incorporation of isotopically labeled amino acids. *J Am Soc Mass Spectrom* **2000**, 11, (1), 78-82.
295. Foster, L. J.; De Hoog, C. L.; Mann, M., Unbiased quantitative proteomics of lipid rafts reveals high specificity for signaling factors. *Proc Natl Acad Sci U S A* **2003**, 100, (10), 5813-18.
296. Blagoev, B.; Kratchmarova, I.; Ong, S. E.; Nielsen, M.; Foster, L. J.; Mann, M., A proteomics strategy to elucidate functional protein-protein interactions applied to EGF signaling. *Nat Biotechnol* **2003**, 21, (3), 315-18.
297. Ibarrola, N.; Kalume, D. E.; Gronborg, M.; Iwahori, A.; Pandey, A., A proteomic approach for quantitation of phosphorylation using stable isotope labeling in cell culture. *Anal Chem* **2003**, 75, (22), 6043-49.
298. Mirgorodskaya, O. A.; Kozmin, Y. P.; Titov, M. I.; Korner, R.; Sonksen, C. P.; Roepstorff, P., Quantitation of peptides and proteins by matrix-assisted laser desorption/ionization mass spectrometry using (18)O-labeled internal standards. *Rapid Commun Mass Spectrom* **2000**, 14, (14), 1226-32.
299. Yao, X.; Freas, A.; Ramirez, J.; Demirev, P. A.; Fenselau, C., Proteolytic 18O labeling for comparative proteomics: model studies with two serotypes of adenovirus. *Anal Chem* **2001**, 73, (13), 2836-42.
300. Pan, S.; Aebersold, R., Quantitative Proteomics by Stable Isotope Labeling and Mass Spectrometry. In *Methods in Molecular Biology*, Matthiesen, R., Ed. Totowa, NJ, 2007; Vol. 367, pp 209-218.

301. Gouw, J. W.; Krijgsveld, J.; Heck, A. J., Quantitative proteomics by metabolic labeling of model organisms. *Mol Cell Proteomics* **2010**, 9, (1), 11-24.
302. Walther, T. C.; Mann, M., Mass spectrometry-based proteomics in cell biology. *J Cell Biol* **2010**, 190, (4), 491-500.
303. Nelson, C. J.; Huttlin, E. L.; Hegeman, A. D.; Harms, A. C.; Sussman, M. R., Implications of ¹⁵N-metabolic labeling for automated peptide identification in *Arabidopsis thaliana*. *Proteomics* **2007**, 7, (8), 1279-92.
304. Pierce, C.; Rees, J.; Fernandez, F.; Barr, J., Rapid Detection of *Staphylococcus aureus* Using ¹⁵N-labeled Bacteriophage Amplification Coupled with Matrix-Assisted Laser Desorption/Ionization Time-of-Flight Mass Spectrometry *Anal Chem* **2011**, 83, (6), 2286-93.
305. Yu, Y. Q.; Gilar, M.; Lee, P. J.; Bouvier, E. S.; Gebler, J. C., Enzyme-friendly, mass spectrometry-compatible surfactant for in-solution enzymatic digestion of proteins. *Anal Chem* **2003**, 75, (21), 6023-28.
306. Suder, P.; Bierczynska, A.; Konig, S.; Silberring, J., Acid-labile surfactant assists in-solution digestion of proteins resistant to enzymatic attack. *Rapid Commun Mass Spectrom* **2004**, 18, (7), 822-24.
307. Mo, W.; Ma, Y.; Takao, T.; Neubert, T. A., Sequencing of oxidized methionine-containing peptides for protein identification. *Rapid Commun Mass Spectrom* **2000**, 14, (21), 2080-81.
308. Taylor, S. W.; Fahy, E.; Murray, J.; Capaldi, R. A.; Ghosh, S. S., Oxidative post-translational modification of tryptophan residues in cardiac mitochondrial proteins. *J Biol Chem* **2003**, 278, (22), 19587-90.
309. Atrih, A.; Turnock, D.; Sellar, G.; Thompson, A.; Feuerstein, G.; Ferguson, M. A.; Huang, J. T., Stoichiometric quantification of Akt phosphorylation using LC-MS/MS. *J Proteome Res* **2010**, 9, (2), 743-51.
310. Payne, R. J.; Jansen, V. A., Understanding bacteriophage therapy as a density-dependent kinetic process. *J Theor Biol* **2001**, 208, (1), 37-48.
311. Kasman, L. M.; Kasman, A.; Westwater, C.; Dolan, J.; Schmidt, M. G.; Norris, J. S., Overcoming the phage replication threshold: a mathematical model with implications for phage therapy. *J Virol* **2002**, 76, (11), 5557-64.
312. Counting Colonies. In *The Microbiology Network*, 2011; Vol. 2011.
313. Norrgran, J.; Williams, T. L.; Woolfitt, A. R.; Solano, M. I.; Pirkle, J. L.; Barr, J. R., Optimization of digestion parameters for protein quantification. *Anal Biochem* **2009**, 393, (1), 48-55.

314. Andrew, E. R., Nuclear magnetic resonance and the brain. *Brain Topogr* **1992**, 5, (2), 129-33.
315. Damadian, R., Tumor detection by nuclear magnetic resonance. *Science* **1971**, 171, (976), 1151-53.
316. Damadian, R.; Goldsmith, M.; Minkoff, L., NMR in cancer: XVI. FONAR image of the live human body. *Physiol Chem Phys* **1977**, 9, (1), 97-100, 108.
317. Hinshaw, W. S.; Bottomley, P. A.; Holland, G. N., Radiographic thin-section image of the human wrist by nuclear magnetic resonance. *Nature* **1977**, 270, (5639), 722-23.
318. Newnham, D., This week we explain the history of the MRI scanner. *Nurs Stand* **2004**, 18, (26), 23.
319. Goh, R. H.; Somers, S.; Jurriaans, E.; Yu, J., Magnetic resonance imaging. Application to family practice. *Can Fam Physician* **1999**, 45, 2118-28, 2131-32.
320. Gross, J., *Mass spectrometry - a textbook*. Springer-Verlag: Berlin, 2006.
321. Fuchs, B.; Suss, R.; Schiller, J., An update of MALDI-TOF mass spectrometry in lipid research. *Prog Lipid Res* 50, (1), 132.
322. *Mass Spectrometry*; Strategic Directions International, Inc. : Los Angeles, 2010; pp 59-75.
323. Atzori, L.; Antonucci, R.; Barberini, L.; Griffin, J. L.; Fanos, V., Metabolomics: a new tool for the neonatologist. *J Matern Fetal Neonatal Med* **2009**, 22 Suppl 3, 50-53.
324. Flad, T.; Tolson, J., Mass spectrometry meets medical sciences: making headway in molecular disease diagnostics. *Anal Bioanal Chem* **2005**, 381, (1), 24-27.
325. Constanzer, M.; Chavez, C.; Matuszewski, B., Development and comparison of high-performance liquid chromatographic methods with tandem mass spectrometric and ultraviolet absorbance detection for the determination of cyclobenzaprine in human plasma and urine. *J Chromatogr B Biomed Appl* **1995**, 666, (1), 117-26.
326. Lennard, L., Therapeutic drug monitoring of cytotoxic drugs. *Br J Clin Pharmacol* **2001**, 52 Suppl 1, 75S-87S.
327. Gu, J.; Soldin, S. J., Modification of tandem mass spectrometric method to permit simultaneous quantification of 17 anti-HIV drugs which include atazanavir and tipranavir. *Clin Chim Acta* **2007**, 378, (1-2), 222-24.
328. Maurer, H. H., Current role of liquid chromatography-mass spectrometry in clinical and forensic toxicology. *Anal Bioanal Chem* **2007**, 388, (7), 1315-25.

329. Holst, J. P.; Soldin, S. J.; Tractenberg, R. E.; Guo, T.; Kundra, P.; Verbalis, J. G.; Jonklaas, J., Use of steroid profiles in determining the cause of adrenal insufficiency. *Steroids* **2007**, 72, (1), 71-84.
330. Rosner, W.; Auchus, R. J.; Azziz, R.; Sluss, P. M.; Raff, H., Position statement: Utility, limitations, and pitfalls in measuring testosterone: an Endocrine Society position statement. *J Clin Endocrinol Metab* **2007**, 92, (2), 405-13.
331. Rodriguez, H.; Tezak, Z.; Mesri, M.; Carr, S. A.; Liebler, D. C.; Fisher, S. J.; Tempst, P.; Hiltke, T.; Kessler, L. G.; Kinsinger, C. R.; Philip, R.; Ransohoff, D. F.; Skates, S. J.; Regnier, F. E.; Anderson, N. L.; Mansfield, E., Analytical validation of protein-based multiplex assays: a workshop report by the NCI-FDA interagency oncology task force on molecular diagnostics. *Clin Chem* **2010**, 56, (2), 237-43.
332. Sparbier, K.; Wenzel, T.; Dihazi, H.; Blaschke, S.; Muller, G. A.; Deelder, A.; Flad, T.; Kostrzewa, M., Immuno-MALDI-TOF MS: new perspectives for clinical applications of mass spectrometry. *Proteomics* **2009**, 9, (6), 1442-50.
333. Gowda, G. A.; Zhang, S.; Gu, H.; Asiago, V.; Shanaiah, N.; Raftery, D., Metabolomics-based methods for early disease diagnostics. *Expert Rev Mol Diagn* **2008**, 8, (5), 617-33.
334. Palmblad, M.; Tiss, A.; Cramer, R., Mass spectrometry in clinical proteomics - from the present to the future. *Proteomics Clin Appl* **2009**, 3, (1), 6-17.
335. Shushan, B., A Review of Clinical Diagnostic Applications of Liquid Chromatography-Tandem Mass Spectrometry *Mass Spectrom Rev* **2009**, 29, 930-44.
336. Weile, J.; Knabbe, C., Current applications and future trends of molecular diagnostics in clinical bacteriology. *Anal Bioanal Chem* **2009**, 394, (3), 731-42.
337. Fox, A., Mass spectrometry: Identification and biodetection, lessons learned and future developments In *Identification of Microorganisms by Mass Spectrometry*, Wilkins, C.; Lay, J., Eds. John Wiley & Sons, Inc.: Hoboken, NJ, 2006; Vol. 169, pp 23-38.
338. Xu, Y.; Cheung, W.; Winder, C. L.; Dunn, W. B.; Goodacre, R., Metabolic profiling of meat: assessment of pork hygiene and contamination with *Salmonella typhimurium*. *Analyst* **2011**, 136, (3), 508-14.
339. Bizzini, A.; Durussel, C.; Bille, J.; Greub, G.; Prod'homme, G., Performance of matrix-assisted laser desorption ionization-time of flight mass spectrometry for identification of bacterial strains routinely isolated in a clinical microbiology laboratory. *J Clin Microbiol* **2010**, 48, (5), 1549-54.
340. Ferroni, A.; Suarez, S.; Beretti, J. L.; Dauphin, B.; Bille, E.; Meyer, J.; Bougnoux, M. E.; Alanio, A.; Berche, P.; Nassif, X., Real-time identification of bacteria and *Candida*

species in positive blood culture broths by matrix-assisted laser desorption ionization-time of flight mass spectrometry. *J Clin Microbiol* **2010**, 48, (5), 1542-48.

341. Marklein, G.; Josten, M.; Klanke, U.; Muller, E.; Horre, R.; Maier, T.; Wenzel, T.; Kostrzewa, M.; Bierbaum, G.; Hoerauf, A.; Sahl, H. G., Matrix-assisted laser desorption ionization-time of flight mass spectrometry for fast and reliable identification of clinical yeast isolates. *J Clin Microbiol* **2009**, 47, (9), 2912-17.

342. Rueping, M. J.; Vehreschild, J. J.; Cornely, O. A., Invasive candidiasis and candidemia: from current opinions to future perspectives. *Expert Opin Investig Drugs* **2009**, 18, (6), 735-48.

343. Stevenson, L. G.; Drake, S. K.; Shea, Y. R.; Zelazny, A. M.; Murray, P. R., Evaluation of matrix-assisted laser desorption ionization-time of flight mass spectrometry for identification of clinically important yeast species. *J Clin Microbiol* **2010**, 48, (10), 3482-86.

344. van Veen, S. Q.; Claas, E. C.; Kuijper, E. J., High-throughput identification of bacteria and yeast by matrix-assisted laser desorption ionization-time of flight mass spectrometry in conventional medical microbiology laboratories. *J Clin Microbiol* **2010**, 48, (3), 900-07.

345. Maier, T.; Klepel, S.; Renner, U.; Kostrzewa, M., Fast and Reliable MALDI-TOF MS based microorganism identification. *Nature Methods* **2006**, 3.

346. Bruker, MALDI Biotyper: Microorganism Identification and Classification. In *Brochure MALDI Biotyper*, 2008.

347. ARUP Laboratories Selects Bruker's MALDI Biotyper Solution for Rapid Microbial Identification by Proteomic Fingerprinting. In *Business Wire*, 2010.

348. Bruker In *Expert Opinion: Bruker Daltonics MALDI Biotyper*, 18th European Congress of Clinical Microbiology and Infectious Disease (ECCMID), Barcelona, Spain, 2008; Barcelona, Spain, 2008.

349. Lakham, K., Will Bruker's MALDI-TOF Mass Spec Lead the Way for Clinical Use in US? In *The Sample; Molecular Tools in the Clinical Lab*, Genomeweb 2010.

350. Salomon, J.; Dunk, T.; Yu, C.; Pollitt, J.; Reuben, J. In *Rapid Automated Identification of Gram-Positive and Gram-Negative Bacteria in the Phoenix System*, 99th General Meeting of the American Society for Microbiology, Chicago, IL, 1999; BD Biosciences: Chicago, IL, 1999.

351. Saffert, R. T.; Cunningham, S. A.; Ihde, S. M.; Monson Jobe, K. E.; Mandrekar, J.; Patel, R., Comparison of Bruker Biotyper Matrix-Assisted Laser Desorption Ionization-Time of Flight Mass Spectrometer to BD Phoenix Automated Microbiology

System for Identification of Gram-Negative Bacilli. *J Clin Microbiol* **2011**, 49, (3), 887-92.

352. Thomas, P.; Wenger, C.; Parks, B.; Robinson, D.; Fellers, R.; Kim, Y.; Zamborg, L.; LeDuc, R.; Forbes, A.; Kelleher, N. In 54th ASMS Conf. Mass Spectrometry and Allied Topics, Seattle, WA, 2006; Seattle, WA, 2006.

353. Lowe, C. A.; Diggle, M. A.; Clarke, S. C., A single nucleotide polymorphism identification assay for the genotypic characterisation of *Neisseria meningitidis* using MALDI-TOF mass spectrometry. *Br J Biomed Sci* **2004**, 61, (1), 8-10.

354. Ecker, D.; Drader, J.; Guitierrez, J.; Guitierrez, A.; Hannis, J.; Schink, A.; Sampath, R.; Blyn, L.; Eshoo, M.; Hall, T.; Tobarmosquera, M.; Jiang, Y.; Sannes-Lowery, K.; Cummins, L.; Libby, B.; Walcott, D.; Massire, C.; Ranken, R.; Manalili, S.; Ivy, C.; Melton, R.; Levene, H.; Harpin, V.; Li, F.; White, N.; Pear, M.; Ecker, J.; Samant, V.; Knize, D.; Robbins, D.; Rudnick, K.; Hajjar, F.; Hofstadler, S. A., The Ibis T5000 Universal Biosensor: An Automated Platform for Pathogen Identification and Strain Typing. *J Assoc Lab Automat* **2006**, 11, (6), 341-51.

355. Ecker, D. J.; Sampath, R.; Massire, C.; Blyn, L. B.; Hall, T. A.; Eshoo, M. W.; Hofstadler, S. A., Ibis T5000: a universal biosensor approach for microbiology. *Nat Rev Microbiol* **2008**, 6, (7), 553-58.

356. Abbott, L.; Ibis, B. PLEX-ID The next generation of the T5000: Technical FAQs. <http://www.ibisbiosciences.com/support/faq.html> (March 10, 2011),

357. Arnold, R.; Karty, J.; Reilly, J., Bacterial Strain Differentiation by Mass Spectrometry. In *Identification of Microorganisms by Mass Spectrometry*, Wilkins, C. L.; Lay, J. O., Eds. John Wiley & Sons: Hoboken, 2006; Vol. 169, p 352.

358. Madonna, A.; Basile, F.; Furlong, E.; Voorhees, K., Detection of bacteria from biological mixtures using immunomagnetic separation combined with matrix-assisted laser desorption/ionization time-of-flight mass spectrometry. *Rapid Commun Mass Spectrom* **2001**, 15, (13), 1068-74.

359. Sampath, R.; Hall, T. A.; Massire, C.; Li, F.; Blyn, L. B.; Eshoo, M. W.; Hofstadler, S. A.; Ecker, D. J., Rapid identification of emerging infectious agents using PCR and electrospray ionization mass spectrometry. *Ann N Y Acad Sci* **2007**, 1102, 109-20.

360. Honisch, C.; Chen, Y.; Mortimer, C.; Arnold, C.; Schmidt, O.; van den Boom, D.; Cantor, C. R.; Shah, H. N.; Gharbia, S. E., Automated comparative sequence analysis by base-specific cleavage and mass spectrometry for nucleic acid-based microbial typing. *Proc Natl Acad Sci U S A* **2007**, 104, (25), 10649-54.

LIST OF PUBLICATIONS

CHAPTER 2

Pierce CY, Barr, JR, Cody RB, Massung RF, Woolfitt AR, Moura H, Fernández FM, “Ambient Generation of Fatty Acid Methyl Ester Profiles From Bacterial Whole Cells by Direct Analysis in Real Time (DART) Mass Spectrometry”, *Chemical Communications* **2007** 8, 807-809.

CHAPTER 3

Pierce CY, Barr JR, Woolfitt AR, Moura H, Shaw EI, Thompson HA, Fernández FM, “Strain and phase identification of the U.S. Category B agent *Coxiella burnetii* by matrix assisted laser desorption/ionization time-of-flight mass spectrometry and multivariate pattern recognition”, *Analytica Chimica Acta* **2007** 583(1) 23-31.

CHAPTER 4

Pierce CL, Rees, JC, Fernández FM, Barr JR, “Detection of *Staphylococcus aureus* Using ¹⁵N-labeled Bacteriophage Amplification Coupled with Matrix-Assisted Laser Desorption/Ionization Time-of-Flight Mass Spectrometry”, *Analytical Chemistry* **2011** 83, 2286-2293.

CHAPTER 5

Pierce CL, Rees, JC, Fernández FM, Barr JR, “Viable *Staphylococcus aureus* Quantification using ¹⁵N Metabolically-Labeled Bacteriophage Amplification Coupled with a Multiple Reaction Monitoring Proteomic Workflow”, in CDC clearance. To be submitted to *Molecular and Cellular Proteomics* **2011**.

VITA

CARRIE LEIGH PIERCE

Carrie Leigh Pierce (maiden: Carrie Leigh Young) was born in West Palm Beach, Florida. She attended public schools in both Florida and Georgia and received her high school diploma from McIntosh High School in Peachtree City, Georgia. She earned her B.S. in Chemistry at the Georgia Institute of Technology in 2000 and immediately began her present career at the Centers for Disease Control and Prevention (CDC). In 2004, while working at the CDC, she earned a Master's in Public Health and began pursuing a doctorate in analytical chemistry from the Georgia Institute of Technology. When she is not working on her research, Mrs. Pierce enjoys spending time with her husband and two children.